

TOWARDS A METHODOLOGICAL APPROACH TO BUILDER SPECIFIC, PRECONSTRUCTION
AIRTIGHTNESS ESTIMATES FOR LIGHT-FRAMED, DETACHED, LOW-RISE RESIDENTIAL BUILDINGS
IN CANADA

by
BOMANI KHEMET

Bachelor of Applied Science in Mechanical Engineering, University of Ottawa, 2001

Master of Engineering in Mechanical, Howard University, 2003

Master of Building Science, Ryerson University, 2012

A dissertation

presented to Ryerson University

in partial fulfillment of the

requirements for the degree of

Doctor of Philosophy

in the program of

Civil Engineering

Toronto, Ontario, Canada, 2019

© BOMANI KHEMET, 2019

Author's Declaration

AUTHOR'S DECLARATION FOR ELECTRONIC SUBMISSION OF A DISSERTATION

I hereby declare that I am the sole author of this dissertation. This is a true copy of the dissertation, including any required final revisions, as accepted by my examiners.

I authorize Ryerson University to lend this dissertation to other institutions or individuals for the purpose of scholarly research.

I further authorize Ryerson University to reproduce this dissertation by photocopying or by other means, in total or in part, at the request of other institutions or individuals for the purpose of scholarly research. I understand that my dissertation may be made electronically available to the public.

Abstract

Towards A Methodological Approach to Builder Specific, Preconstruction Airtightness Estimates for Light-Framed, Detached, Low-Rise Residential Buildings in Canada

Bomani Khemet, Doctor of Philosophy in Civil Engineering, Ryerson University, 2019

This research is an investigation into residential building airtightness. Its purpose is to establish a methodology to predict preconstruction airtightness in Canadian homes.

The dissertation presented an analysis of a large, national blower door testing population, numbering over 900,000 low-rise detached homes. The relationship between airtightness and various building factors, such as; insulation levels, building size, and year of construction, is explored. Regression-based models were found to be highly significant ($p < 0.01$) and explained up to 48% ($R = 0.69$, $p < 0.01$) of whole building airtightness. The national models' scope was confined to predicting airtightness in existing homes with heterogeneous wall construction.

In order to estimate preconstruction airtightness in conventionally constructed homes, a local blower door testing population of nearly 3000 homes was examined. Three builder-specific, geometric-based, temporally independent, multiple linear regression models were developed. Some of these builder-specific models were found to be strong, and explained over 58% ($R = 0.79$, $p < 0.001$) of whole building airtightness. A five variable, geometrically based model which controlled for handicraft was found to be very strong, explaining up to 73% ($R = 0.87$, $p < 0.001$) of the whole building airtightness. The regression-based analyses on the local population suggests that air leakage is prominent through two building details: the floor-to-wall details, and at the window-to-wall assemblies.

An empirically based design of experiments was devised to quantify the impact of air leakage through a floor-to-wall detail. A very strong laboratory-based model explained up to 88% of the air leakage through the floor-to-wall joint ($R = 0.95$, $p < 0.001$). A builder-specific, temporally-independent model was combined with the empirically-based, floor-to-wall model to illustrate the applicability of the approach residential building designers. The synthesis of the two models resulted in a novel, whole building, preconstruction airtightness forecasting model.

The dissertation demonstrated that airtightness in homes could be estimated with temporally independent, builder-specific, and geometrically-based preconstruction models. The estimation approach spurred models that were stronger in explanatory power, and industrial applicability as compared to previous airtightness models.

Acknowledgements

I would like to express my gratitude to my advisors Dr. Russell Richman and Dr. Medhat Shehata. Russell, your critical eye, vast knowledge, and enthusiasm were foundational in my progress. Medhat, I'm indebted to you for your council and continuous support. Thank you to Greg Labbé for providing me with access to a wealth of field experience, and hours of dedication to see this project to the end. Thank you to Julia Purdy, Michael Lio, and John Godden for your expertise and valuable inputs to this endeavour. I would also like to thank my fellow graduate students in Civil Engineering and the Sustainable Building Group members in Architectural Science, for lively conversations, great insights, and good cheer. And finally, I would like to give the deepest thanks to my family for your perspective, inspiration, and support throughout this journey.

Dedication

For Kaleb Diata and Keira Sizani.

Table of Contents

Author's Declaration	ii
Abstract	iii
Acknowledgements	iv
Dedication	v
List of Figures	ix
List of Tables	x
List of Abbreviations	xii
1 Introduction	1
1.1 Research Context	1
1.2 Research Motivation	2
1.3 Dissertation Structure	4
2 Theoretical Background and Conceptual Framework	7
2.1 Theoretical Background	7
2.1.1 Impact of Air Leakage	7
2.1.2 Air Leakage Control	14
2.1.3 Methods to Control Air Leakage	18
2.1.4 Technologies available for Post Construction Measurements	23
2.2 Modeling Whole Building Air leakage	25
2.2.1 Whole Building Parameters	25
2.2.2 Whole Building Model Types	27
2.2.3 Selected Whole Building Airtightness Studies	28
2.3 Research Objectives	33
2.4 Research Questions	34
2.5 Conceptual Framework	34
3 Methodology	37
3.1 Mathematical Models	37
3.2 Phase I: National Level Airtightness Predictions	40
3.2.1 National Sample of 900,000 homes	40
3.2.2 National Sample of 330,000 homes	41
3.2.3 Analysis Methodology	42
3.3 Phase II: Predicting Airtightness in Regional Populations	43
3.3.1 Analysis Methodology	43

3.3.2	Selection of Predictive Variables.....	45
3.4	Phase III: Predicting Airtightness with Laboratory Tests	50
3.4.1	Analysis Methodology.....	51
3.4.2	Synthesis of Predictive and Reactive Predictions	54
4	National Level Airtightness Predictions	57
4.1	Introduction	57
4.1.1	Data, Results & Discussion.....	57
4.2	Summary	75
5	Local Airtightness Predictions.....	77
5.1	Introduction	77
5.1.1	Univariate Exploratory Analyses	78
5.1.2	Builder Specific, Geometry Based Multiple Linear Regression Analyses	86
5.1.3	Handicraft & Geometry based Multiple Linear Regression Analyses	94
5.1.4	Phase II Models - Comparison to Previous Literature and Current Contributions	103
5.2	Summary	108
6	Transition Detail Airtightness Predictions.....	109
6.1	Laboratory Testing Design & Calibration	109
6.1.1	Sample and Test Chamber Construction	109
6.1.2	Instrumentation	114
6.1.3	Calibration.....	116
6.2	Data, Results & Discussion	121
6.2.1	Regression Models for Rim Joist Detail.....	124
6.2.2	Results and Integration into Whole House Prediction Models.....	127
6.3	Summary	130
7	Conclusions	132
7.1	Significance of Work	132
7.2	Resolved Research Questions	134
7.2.1	Chapter 5 Summary: National Level Airtightness Predictions.....	134
7.2.2	Chapter 5 Summary: Predicting Airtightness in Local Populations.....	134
7.2.3	Chapter 6 Summary: Predicting Airtightness with Laboratory Tests.....	136
7.3	Strengths and Limitations	137
7.4	Recommendations and Future Work.....	139

Appendix	141
Works Cited.....	148

List of Figures

Figure 1 Sources of Air Leakage in Low Rise Residential Homes	15
Figure 2 Representation of the Conceptual Framework.....	34
Figure 3 Airtightness Estimation Approach for Builder Specific Time Independent Populations	45
Figure 4 Fenestration Perimeter to Height Ratio.....	48
Figure 5 Rim Joist Ratio	48
Figure 6 Cube Plot Visualisation.....	53
Figure 7 Representation of the Conceptual Framework	56
Figure 8 Air Leakage Frequency	58
Figure 9 Alternate Mean Air Leakage Rate Frequency	60
Figure 10 Frequency plot of Building Year of Construction Table	62
Figure 11 Airtightness Frequency Plot of a Local Blower Door Sample Population	79
Figure 12 Representation of Population Samples	79
Figure 13 ACH50 Frequency Distribution for 272 Modeled Homes	81
Figure 14 Mean ACH50 by Builder (N=272)	82
Figure 15 Builder A Standardised Residual Frequency Plot.....	87
Figure 16 Builder A Standardised Residuals Probability-Probability Plot	88
Figure 17 Builder B Standardised Residual Probability-Probability Plot	89
Figure 18 Builder B Standardised Residual Frequency Plot	90
Figure 19 Builder C Standardised Residual Probability-Probability Plot.....	92
Figure 20 Builder C Standardised Residual Frequency Plot	92
Figure 21 NL II Standardised Residual Frequency Plot.....	96
Figure 22 NL II Standardised Residual Probability-Probability.....	96
Figure 23 ACH50 IIa Standardised Residual Frequency Plot	98
Figure 24 ACH IIa Standardised Residual Probability-Probability Plot.....	99
Figure 25 ACH50 IIb Standardised Residual Frequency Plot.....	100
Figure 26 ACH IIb Standardised Residual Probability-Probability Plot	101
Figure 27 Proportion of Air Leakage in Low Rise Residential Homes (ASHRAE – Fundamentals)	105
Figure 28 Elevation View Showing Sheathing Board Joints	110
Figure 29 Horizontal Cross-Section Showing Framing Joints	110
Figure 30 Empty Test Chamber	112
Figure 31 Membranes Applied to Samples	112
Figure 32 Chamber with Sample Under Test	113
Figure 33 Prototype sample.....	114
Figure 34 Digital Manometer	114
Figure 35 Microleakage Meter.....	114
Figure 36 Microleakage Orifice Disks.....	115
Figure 37 Variable Speed Depressurisation Fan	115
Figure 38 Micro Leakage Meter Calibration Curves.....	116
Figure 39 Flow Characterisation of Apparatus via Tare Background Leakage Log (L/s)	118
Figure 40 Flow Characterisation of With Crack Length (Qx) Log (L/s)	118
Figure 41 Comparison of Equivalent Leakage Area to Crack Area.....	120
Figure 42 Log-Log Plot of Air Flow Regime by Sample Configuration.....	123
Figure 43 Summary of Approach to Preconstruction Airtightness Prediction.....	133

List of Tables

Table 1 GHG Emissions & Energy Intensity by Housing Typology	13
Table 2 Summary of Relevant Multiple Regression Based Studies.....	29
Table 3 Provisional Predictor Variables by Class.....	50
Table 4 Mean Air Leakage by Jurisdiction.....	59
Table 5 Mean Air Leakage by Building Height	59
Table 6 Alternate Mean Air Leakage by Jurisdiction.....	59
Table 7 Alternate Mean Air Leakage by Province	61
Table 8 Mean Building Year by Province.....	63
Table 9 Mean Building Year by Building Height	63
Table 10 Mean Air Leakage Compared to Mean Building Year	64
Table 11 Mean Air Leakage Compared to Mean Building Volume	64
Table 12 Mean House Volume by Province	65
Table 13 Regression Variables for Varying Leakage Metrics	65
Table 14 Comparison of Pearson's Correlation and Coefficient of Determination N=900,000.....	66
Table 15 Comparison of Pearson's Correlation and Coefficient of Determination N=330,000.....	66
Table 16 Regression Model Strength by R and R ² per Province N=900,000.....	66
Table 17 Regression Model Strength by R and R ² per Province N=330,000.....	67
Table 18 Comparison of R & R ² with respect to building code issuance dates N=900,000	68
Table 19 Comparison of R & R ² with respect to building code issuance dates N=330,000	69
Table 20 Linear Regression Coefficients 95% CI, N=900,000.....	70
Table 21 Linear Regression Coefficients 95% CI, N=330,000.....	70
Table 22 Comparison of Phase I Model with Existing Literature	75
Table 23 Descriptive Statistics for Population Types	80
Table 24 Effect Size Interpretation (Cohen's d)	81
Table 25 ACH50 Descriptive Statistics per Builder (N=272).....	82
Table 26 ANOVA, ACH between and Within Builders (N=272)	83
Table 27 Difference of Means Bonferroni Method (N=272).....	83
Table 28 Difference of Means Least Significant Difference (LSD) (N=272).....	83
Table 29 Effect Sizes Between Builders (Cohen's d Method)	84
Table 30 Univariate Analysis of ACH Compared to Predictor Variables	85
Table 31 Builder A Regression Model	86
Table 32 ANOVA Builder A	86
Table 33 Builder A Regression Model Parameters.....	86
Table 34 Builder B Regression Model	88
Table 35 for Builder B ANOVA.....	89
Table 36 Builder B Regression Model Parameters.....	89
Table 37 Builder C Regression Model	90
Table 38 Builder C ANOVA	90
Table 39 Builder C Regression Model Parameters.....	91
Table 40 Builder D Multiple Linear Regression Model	93
Table 41 Builder D ANOVA.....	93
Table 42 Builder D Regression Model Parameters	93

Table 43 NL II Multiple Linear Regression.....	94
Table 44 NL II ANOVA.....	94
Table 45 NL II Regression Model Parameters	95
Table 46 ACH IIa Multiple Linear Regression	97
Table 47 ACH IIa ANOVA	97
Table 48 ACH IIa Regression Model Parameter	98
Table 49 ACH IIb Multiple Linear Regression.....	99
Table 50 ACH IIb ANOVA.....	99
Table 51 ACH IIb Regression Model Parameters	100
Table 52 Phase II Airtightness Model Summary Table.....	102
Table 53 Comparative Phase I Regression Model.....	103
Table 54 Airtightness Model Comparison to Preceding Studies.....	104
Table 55: Quadruplicate Measures Ideal ABS at 4 Pressures	116
Table 56 ELA compared to Crack Area & Pressure	119
Table 57 Equivalent Leakage Area compared to Sample Crack Area	120
Table 58 Air leakage Output in Standard Order	122
Table 59 Regression Summary for Floor to Wall Detail Air Leakage Models.....	125
Table 60 Multiple Linear Regression for Empirical Models	126
Table 61 Regression Strength for Empirical Models of Floor to Wall Detail via ANOVA	126
Table 62 Regression Strength for Empirical Models of Floor to Wall Details	127
Table 63 Output for Model #4 for Rim Joist Details	127
Table 64 Weighting Factor for Model #4's Floor to Wall Detail	128

List of Abbreviations

A.Mean	Arithmetic Mean
ABS	Air Barrier System
ACH	Air Changes Per Hour
ACH50	Air Changes Per Hour at 50 Pa
Adj. R2	Adjusted R2
AGradeH	Above Grade Height
ANOVA	Analysis of Variance
ASHRAE	American Society of Heating Refrigeration Air Conditioning Engineers
ASTM	American Society for Testing & Materials
B	Beta Parameter
BuilderID	Builder Identification
C	Air flow Coefficient
CeilingA	Ceiling Area
CFD	Computational Fluid Dynamics
CGSB	Canadian General Standards Board
CeilingRSI	Ceiling Insulation Level
CI	Confidence Interval
CO2e	Carbon Dioxide Equivalent
CWR	Ceiling to Wall Ratio
DF	Degrees of Freedom
DoorA	Door Area
DoorP	Door Perimeter
ELA	Equivalent Leakage Area
ExCondFA	Exposed Area to Condition Floor Area
ExFloorA	Exterior Floor Area
F	F - statistic
FenPerimR	Fenestration Perimeter to Height Ratio
FoundationRSI	Foundation Insulation Level
G.Mean	Geometric Mean
GHG	Green House Gas
HDD	Heating Degree Days
HVAC-R	Heating Ventilation and Air Conditioning - Refrigeration
IAQ	Indoor Air Quality
JoistR	Joist Ratio
L	Detail Length
LB	Lower Bound
M	Sheathing Membrane Type
Mt	Metric tonnes
m	Fluid Mass
MS	Mean Square

n	Flow Exponent
N	Population
NL	Normalised Leakage Rate
NWT	North West Territories
OBC	Ontario Building Code
OEE	Office of Energy Efficiency
PJ	Peta Joules
P	Depressurisation Pressure
PEI	Prince Edward Island
PerimR	Perimeter Ratio
p-value	Significance
R	Pearson's Correlation Coefficient
R ²	Coefficient of Determination
RJoistL	Rim Joist Length
RJoistR	Rim Joist Ratio
SD	Standard Deviation
SE	Standard Error
ShellA	Shell Area
Sig	Significance
Sig.	Significance
t	t- statistic
TotalH	Total Height
UB	Upper Bound
V	Volume
v	Fluid velocity
VIF	Variance Inflation Factor
WallRSI	Above Grade Wall Insulation Level
Wi	Weighting Factor
WindowA	Window Area
WindowP	Window Perimeter
WindowRSI	Nominal Window Unit Insulation Level
Z	Fluid Height
μ	residual mean

1 Introduction

1.1 Research Context

The construction industry requires the capability to reasonably predict air leakage in buildings in order to build economical, comfortable, and durable spaces for people who use them. Forecasting air leakage also allows builders to proactively design and construct homes, as opposed to reacting ineffectively to post-construction airtightness tests. Quantifying an accurate air leakage rate at the preconstruction phase is vital for:

- Controlling Energy Consumption
- Minimising GHG Emissions
- Improving Building Enclosure Durability
- Enhancing Human Comfort
- Optimising HVAC design

Furthermore, the degree at which we can enclose and control indoor conditioned air is a fundamental component directly related to environmental stewardship.

Predicting preconstruction airtightness in residential buildings represents an important step in designing and constructing healthy and durable homes, especially in cold climates. The rate of air leakage across exterior walls is also a primary driver in establishing human comfort within an enclosed space. Both high and low interior relative humidity levels are known to have adverse physiological actions on building occupants. Conversely, the optimum amount humidity levels inside a space maximise occupant well-being. When all other parameters are held constant, ideal indoor humidity levels are best designed when air leakage is properly quantified and minimized.

Similarly, uncontrolled air leakage is also directly related to seasonal energy consumption in two important ways. Conditioned air, whether it be cooled, heated, humidified, or

dehumidified, requires a commensurate energy expenditure. Uncontrolled air leakage through the building enclosure represents an additional amount of energy consumed to condition the leaking air.

Furthermore, underestimating or overestimating air leakage across a building enclosure may result in the oversizing or under sizing of a buildings' heating, ventilation, cooling, air conditioning and refrigeration (HVAC-R). Both undersized and oversized HVAC-R systems consume excess energy. Undersized HVAC-R systems duty cycles can be too frequent and operate for longer than optimal durations, contributing to wasteful energy use patterns and shortened equipment lifecycles. In contrast, oversized systems using ventilation safety factors or rules of thumb can result in energy wasteful overventilation, increased on/off cycling and poor air mixing resulting in localised pollutant and stale air accumulation.

Finally, accurate airtightness estimation may affect durability of exterior walls. Condensation of moist exfiltrating air in wall assemblies can cause structural degradation. Enclosure damage due to air infiltration is of growing importance in both contemporary, and high performing, low-energy buildings, which have wall assemblies with a lower thermal transmittance, and low drying potentials in the face of interstitial moisture accumulation.

Therefore, accurately estimating preconstruction airtightness is essential to aspects of building design, construction, and operation.

1.2 Research Motivation

Airtightness has long been understood as an important building performance factor to be quantified since the discovery of thermal bypass in the late 1970s (Beyea, Dutt, & Woteki, 1977).

These early researchers noted a marked discrepancy on heat loss estimates and measured heat

loss in insulated dwellings amounting to a total of 35%. The major source of the detected difference was uncontrolled air movement from the basement to the attic spaces. Ever since, air leakage targets have taken an increasingly prominent role in the building sector. Canadian Federal, Provincial and municipal jurisdictions have implemented airtightness design targets due to energy consumption concerns. For instance, the Ontario Building Code (OBC) has a voluntary target airtightness standard of 2.5 Air Changes at 50 pascals (Government of Ontario, 2018). Future OBC updates are in consultation with stakeholders to make airtightness measurements mandatory by 2020 (Government of Ontario, 2016). While the measurements may be mandatory, the targets will not take force until the Ontario building industry has the capability to achieve a 2.5 ACH50 mandate. Similarly, other jurisdictions such as the province of Alberta only require a blower door test if a particular house energy consumption compliance path is taken which assumes an air leakage rate less than 2.5ACH50 (Alberta Municipal Affairs, 2014). The R2000 Standard, with a goal to improve building performance and environmental stewardship without jeopardising indoor and outdoor environments, has a national voluntary standard with a mandatory airtightness limit of 1.5 ACH50 (Natural Resources Canada, 2012). Perhaps the most aggressive target within Canada is the contained as a voluntary option in British Columbia with an Air tightness of 1.0 ACH50(BC Housing, 2017). While the city of Vancouver's building code allows certain zoning relaxations for homes adhering to the German based Passive House standard which mandates 0.6 ACH50 (City of Vancouver, 2015; Vancouver, 2018).

As evidenced by the preceding paragraphs, legislation at all three levels of government throughout many parts of Canada are interested in responding to international and nationally set climate change targets. The 2016 *“Pan-Canadian Framework on Clean Growth and Climate*

Change” discusses a framework for Canada’s various governments to proactively respond to a national challenge to reduce the amount of energy consumption of fuels high in green house gas emissions. The building industry is an important component of this set of solutions and can proactively address issues of resource efficiency, comfort, carbon emissions, and energy security. Detached residential homes have been shown to have a disproportionate role in absolute and relative energy consumption. Therefore, addressing airtightness in detached homes represents an opportunity to significantly reduce their environmental impact. This research proposes a methodology to estimate preconstruction air leakage in detached, low-rise, residential buildings so that builders can forecast building airtightness at the design stage. The methodology bases airtightness predictions on the performance builder’s current construction portfolio and on its’ next generation design details. The approach to preconstruction airtightness prediction will allow builders to meet current and impending airtightness requirements targeted toward reduce energy consumption and GHG emissions. The approach will also allow designers opportunities to correct for HVAC-R equipment sizing, HVAC-R operation, increase IAQ, extend building enclosure durability as well as improve occupant human comfort.

1.3 Dissertation Structure

This dissertation is divided into 7 Chapters. Chapter 2 describes the impact of uncontrolled air leakage on the building, it’s occupants and the environmental resources. How human comfort can be improved or degraded is explored. The various mechanisms responsible for energy consumption and energy efficiency are discussed. Lastly, building durability and its connection to airtightness is outlined. Air leakage prediction methods are discussed for both pre-construction and post construction methods. The state of the current research is summarised and unexplored

research opportunities are highlighted. A framework and research questions for this paper is then elaborated upon.

Chapter 3 describes a three-phased methodology used to develop this approach to airtightness estimation - national prediction, local prediction and detail level prediction. A description of National, Local, and Wall Detail explorations are discussed at length. Model strength and validation methods are considered. The integration of the three phases of research are synthesised into a global airtightness estimation methodology.

Chapters 4, 5, and 6, contain the results, discussion and analysis of each phase of the work. Chapter 4 considers the univariate and multiple linear regression analyses of a temporal based large national dataset numbering upwards to 12% of the total housing stock of detached homes across Canada. The chapter considers whether a national database can be used as a lower bound for airtightness predictions in existing homes. Multiple linear regression models are used to select and discard predictor variables. The validity of these predictor variables are then compared to existing literature. Chapter 5 considers a set of local builders in southern Ontario with higher resolution information on the building enclosure geometry. Builder-specific airtightness models are developed based on novel and conventional predictor variables. The chapter further explores if the builder-specific models can be time independent, climate independent and volume independent. The models are then calibrated against the large temporal based national airtightness housing population from chapter 4. Chapter 6 focusses on laboratory based factorial design of experiments on a building detail shown to contribute substantially to air leakage based on results presented in Chapter 5. Chapter 6 further explores

whether the factorial designs results can be used to iterate a next generation airtightness prediction model.

Chapter 7 revisits the research questions and provides conclusions in light of the results presented in the previous three chapters. Some further discussion is reserved to discuss the study's strengths and limitation. The chapter further highlights the significance of the work and the applicability to the building industry. Chapter 7 also considers current ongoing research to strengthen the predictive approach to air tightness estimation. Lastly, the chapter explores possible avenues for future work.

2 Theoretical Background and Conceptual Framework

A detailed review of the impact of air leakage on building performance will be discussed from various vantage points in the literature, including; human comfort, energy consumption, building durability, and green house gas emissions. Secondly, a cursory look at airtightness controls will be discussed including; identifying the sources of air leakage, exploring common air barrier systems, and summarising airtightness measurement techniques. Thirdly, a review of contemporary studies and airtightness methods will be highlighted. Finally, research objectives and a conceptual framework will be presented.

2.1 Theoretical Background

2.1.1 Impact of Air Leakage

Air infiltration is an important factor in establishing human comfort. Infiltration affects the rate at which outdoor pollutants are brought through the building enclosure. Depending on environmental conditions, air leakage also directly influences the amount of moisture deposition inside wall cavities and often increases the risk of interstitial condensation. Sustained condensation can cause mould or decay in moisture sensitive organic materials, such as exterior wood sheathing, which in addition to deteriorating the building enclosure, increases the risks associated with indoor air quality (IAQ) concerns. A continued wetting of wood based structural members may also lead to structurally compromised exterior walls. Energy consumption, and general operation of heating and cooling equipment may also be directly affected by uncontrolled air infiltration.

2.1.1.1 Human Comfort, IAQ & Airtightness

Human thermal comfort is an active field of research where parameters are governed by several independent and interrelated phenomena. A number of these phenomena are related to air movement within and across the building enclosure. Examples of these are: gaseous pollutants, particulate matter concentrations, bio-aerosols, odours, spores, moulds, water vapour, and the effects of enclosure draughts (J. F. Straube, 2002). Unacceptably high levels of these can originate from the indoor environment or from the outdoor environment. Their persistence in the indoor environment can be exacerbated with poor uncontrolled air leakage through the building enclosure. Poor indoor air quality can also originate with an imbalance between natural and mechanical ventilation rates across the building enclosure.

As uncontrolled air leakage may lead to significant moisture deposition due to condensation within exterior walls, the possibility of mould growth within those walls is a significant concern (Lazure & Lavoie, n.d.)(Lstiburek, 2005). Uncontrolled air leakage can also contribute to the reduction of thermal performance of the building enclosure by acting as a thermal bypass (e.g. 'wind washing' of air-permeable insulation). Increased heat loss (both localized and global) from the interior to the exterior reduces interior surface temperatures, thus lowering the mean radiative temperature of a space, causing occupants to feel colder during the heating season.

Air leakage can also deposit indoor pollutants into wall stud cavities during infiltration. For instance, Muise et al have indicated that fungal and mould spores can enter electrical wall services as a result of air leakage (Muise, Seo, Blair, & Applegate, 2010). It has also been demonstrated that building enclosures that increase the level of air tightness can reduce the

number of contaminants in an occupied space when coupled with low flow continuous ventilation. The increase high air flow ventilation rates such as ASHRAE 62.1 did not reduce the indoor contaminant levels. In fact, continuous low flow 24 hour ventilation decreased both air contaminant levels and energy consumption (Ng, Persily, & Emmerich, 2015). Increasing airtightness with naturally ventilated buildings that rely on enclosure-based ventilation sources can worsen Indoor Air Quality (IAQ). This was observed with the increase of window sealing quality in homes built during the 20th century in the southern European coast of the Mediterranean (d'Ambrosio Alfano, Dell'Isola, Ficco, Palella, & Riccio, 2016). Thus, to increase indoor air quality, high performance buildings have used the approach of very airtight enclosures below 1.0 ACH50 with continuous low flow ventilation rates.

2.1.1.2 HVAC, Energy Consumption & Airtightness

Air leakage affects energy consumption in a variety of direct or indirect ways. Since the amount of energy consumed by HVAC-R systems is directly proportional to the amount of air that is to be conditioned, unconditioned infiltrating air requires surplus energy to re-establish indoor air conditions. Energy losses due to infiltration can account for up to 37% of based on simulation and calibration with a set of detached Australia homes(Ren & Chen, 2015). Modern Spanish residential homes are reported to lose approximately 11-27% of their energy due to air leakage(Meiss & Feijó-Muñoz, 2015). In detached Finnish homes, between 15% -30% of energy can be wasted due to air infiltration(Jokisalo, Kurnitski, Korpi, Kalamees, & Vinha, 2009). Furthermore, the Finnish study showed that each unit increase of 1 ACH50 contributed to an increase in 7% of space heating and an increase of 4% of total energy loss.

A significant amount of energy can be lost during building operation due to improper assumptions poorly estimating enclosure airtightness. Building enclosure airtightness is a direct input for HVAC-R designers. It informs designers on the proper ventilation rate as well as the maximum heating loads which help size HVAC-R systems. Improper airtightness estimates may cause serious energy penalties resulting from oversized furnaces and fans.

As a precautionary measure to extreme environmental conditions, design engineers for both residential and commercial buildings may oversized HVAC-R systems (Djunaedy, den Wymelenberg, Acker, & Thimmana, 2011). Instead of using limit states design methodology, a combination of experience, rules of thumbs or safety factors encourage HVAC-R designer to use these conservative estimates on enclosure performance, at peak load conditions. In practice commercial roof top units are oversized by applying a 15-25% addition load to accommodate unforeseen peak loads (Ruya & Augenbroe, 2016). Oversizing HVAC-R systems allow designers to achieve their primary objective which is to ensure that the air conditioning system provides the appropriate space cooling and heating for all extreme conditions. However, oversizing does not translate to the best energy efficient operation. In addition, oversizing of HVAC-R equipment may lead to higher humidity levels which can cause mould and other occupant health issues in addition to higher operational energy costs, and shortened equipment lifespans due to compressor short cycling. The scale of buildings that are oversized should not be underestimated. In one study 40% of small commercial roof top units surveyed were oversized by 25% while another 10% of units were oversized by 50% (Felts & Bailey, 2000). In a study of over 350 Florida residential homes, it was found that over 50% of the homes were oversized by 20%. The study also confirmed that these residential homes had increased energy consumption (James, Cummings,

Sonne, Vieira, & Klongerbo, 1997). We are reminded that air conditioning load calculations and ventilation rates are heavily dependant on accurate knowledge of airtightness levels and enclosure thermal resistance. Hence HVAC-R oversizing and undersizing are largely due to a poor estimate of preconstruction airtightness.

2.1.1.3 Building Durability

The building enclosure is also susceptible to reduced durability as a result of uncontrolled air leakage. When moisture in the air is carried through building cavities due to poor airtightness, it will condense when moist air touches surfaces below the dew point of that air. Sustained or substantial condensation over time may corrode fasteners, steel studs, or deteriorate other moisture sensitive materials such as organic based sheathing (Canada Mortgage Housing Corporation, 2007). Condensation may equally rot wood framed walls that have surpassed their hygric buffer capacity, leaving load bearing walls compromised in strength and stability. Although vapour diffusion can carry moisture into an interior wall, moisture transport and deposition due to air movement is orders of magnitude more effective, and in greater quantities via air leakage. This is illustrated by an example by Quirouette who showed that a small electrical service opening of 625 mm^2 under 10 Pa air pressure difference would allow 14 kg of water vapour to pass through the opening over a month's time, as compared to just 6 grams of water vapour diffusing through the same wall (Quirouette, 1985). Hence air leakage via infiltration and exfiltration has a greater potential for interstitial water damage as compared to vapour diffusion.

2.1.1.4 Green House Gas Emissions & Housing Typology

Canadian Green House Gas emissions are affected profoundly by building operation. Inefficient building operations can be a result of poor building envelope design, or inaccurate envelope performance estimation. The impact of buildings on the built environment cannot be overstated. Buildings account for 13% of yearly energy related GHG emissions in Canada, with 7.3% for residential buildings (39Mt CO₂e) and 5.3% (30Mt CO₂e) for institutional and commercial buildings. When combined, residential and industrial buildings are the third highest contributor to GHG, only surpassed by emission by Road Transportation (143 Mt CO₂e) or Oil & Gas Refining industries (100 Mt CO₂e)(Pollutant Inventories and Reporting Division, 2018). The largest share of Canadian home energy use belongs to space heating. Space heating fuel was found to be a primary driver of green house gas emissions in the building sector. As such, in 2016 Canada's space heating needs require 885.1PJ representing 61% of the home energy use (Office of Energy Efficiency, 2018a).

Although some provinces are using low greenhouse gas emitting fuels such as hydropower and nuclear power, other provinces use a different home heating profile that include important amounts of fossil fuels as a main source of heating. For instance, hydro-nuclear electricity is the dominant heating source in Quebec numbering 85% of all heating power. In contrast, Ontario and Alberta's primary home heating fuels are originating from GHG intensive natural gas representing 76% and 91% of home heating fuels respectively. Nationally, 64% of space heating is derived from GHG intense combustion of natural gas, wood, oil and propane(Environment Accounts and Statistics Division, 2015).

Table 1 GHG Emissions & Energy Intensity by Housing Typology

House Typology	Space Heating				Floor Space m ² x10 ⁶
	GHG Mt CO ₂ eq	Heating PJ	GHG Intensity kg CO ₂ eq /m ²	Energy Intensity GJ/m ²	
Detached	27.3	645	20.8 ^a	0.49 ^a	1310.5
Attached	3.5	81.2	15.0 ^a	0.35 ^a	233.3
Apartment/Condo	5.8	138.6	12.7 ^a	0.30 ^a	458.2
(a) Derived values					

Building typology has one of the largest influences on total energy consumption and GHG emissions. Within the Canadian landscape, detached single family homes consume the most energy in both relative and in absolute terms. Detached homes also tend to be the largest in floor space and volume per dwelling. Detached homes also represent the largest share in absolute floor space. The total housing stock in 2016 was 15.2 million in which detached single family homes represented 54%. For comparison, apartments and attached homes represented 32% and 12%, of floor space respectively. Since single detached homes are the largest housing type in floor area, they tend to be, by extension, larger in enclosure area as compared to other housing types. Single family homes averaged 158m² of floor space per home, while attached homes and apartment/condo were 128m² and 92 m², respectively(Office of Energy Efficiency, 2018b). Larger houses typically demand more energy, and by extension a greater energy loss via air leakage. Detached homes consume more energy per square meter of living space as compared to other typologies. Energy intensity for detached, attached and apartment dwellings was 0.49GJ/m²(Office of Energy Efficiency, 2018c), 0.35GJ/m²(Office of Energy Efficiency, 2018d) , and 0.30 GJ/m²(Office of Energy Efficiency, 2018e), respectively(Office of Energy Efficiency, 2018b). The larger energy demands per floor area also align with GHG emission where Detached,

Attached, and Apartment housing were 20.8kg CO₂e/m²(Office of Energy Efficiency, 2018f), 15.0kgCO₂e/m²(Office of Energy Efficiency, 2018g) and 12.7kg CO₂e/m²(Office of Energy Efficiency, 2018) respectively(Office of Energy Efficiency, 2018b). Thus, single detached homes have the largest absolute and relative GHG emission profile as compared to attached homes and apartment type homes. A summary of the GHG and energy consumption per unit floor area and housing type is summarised in Table 1.

In summary, airtightness levels in homes are tightly allied with several important impacts both on occupants, and the environment. Human comfort, as experienced as indoor air quality, and thermal comfort can be meaningfully improved with appropriate and predictable airtightness levels. Estimated and actual airtightness levels directly affect the design, operation and longevity of HVAC systems. Building enclosure durability can be adversely affected when moist air infiltration is combined with interstitial condensation. Lastly, building typology has important environmental influences. Canadian detached low-rise single-family homes represent the greatest share of the housing stock. Detached homes also disproportionately emit larger quantities of green house gases in annual space heating, 39% more GHG's than attached homes, and 46% GHG's than apartments. Thus, predicting and reducing air leakage levels in detached low-rise homes could foster the largest impact housing GHG and energy consumption.

2.1.2 Air Leakage Control

The following discusses the multiple sources of air leakage, the different methods available to control air leakage and the measurement techniques available to quantify air leakage.

2.1.2.1 Air leakage Paths and Sources

The amount of air leakage associated with transitions and penetrations located at exterior walls can vary considerably. The quantity of air leakage has been estimated to be a result of a complex combination of the components or assemblies of interest themselves, the installations or assembly design or method utilised, and the installation quality as represented by handicraft. Each building component, whether it be walls, windows, ceilings, or HVAC-R systems, have their own influence on whole building airtightness. The following explores the contributions of each major building component.

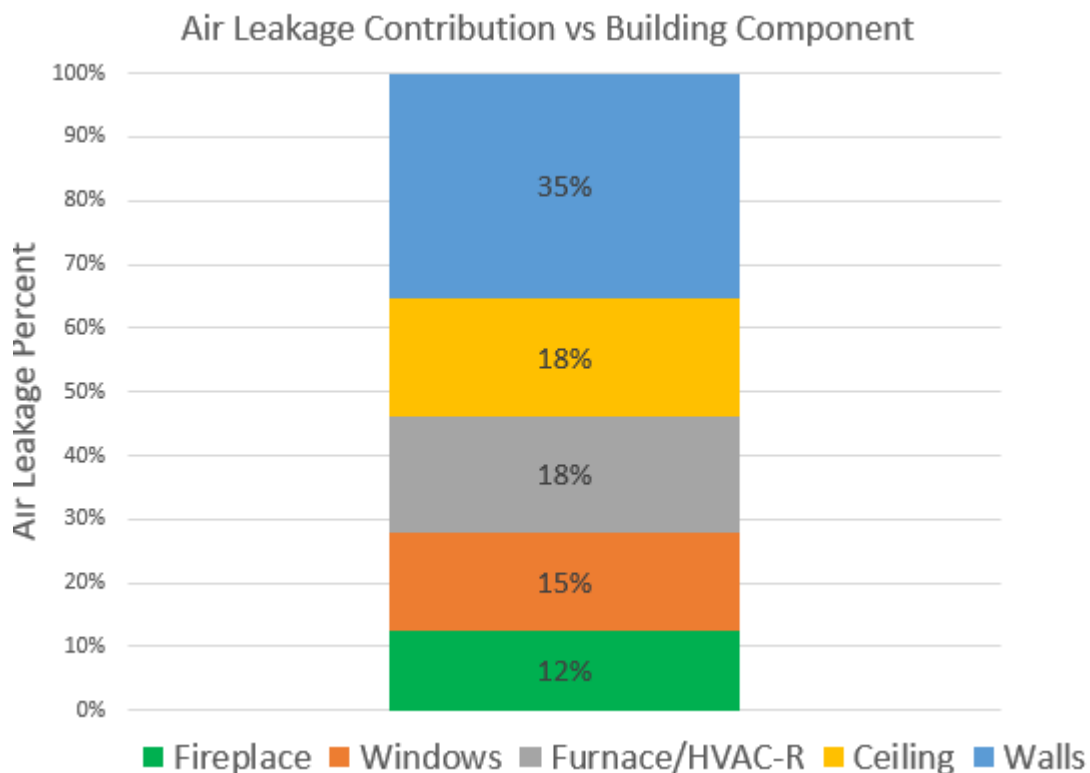


Figure 1 Sources of Air Leakage in Low Rise Residential Homes (Adapted from ASHRAE Handbook)

Walls contributed approximately 35% of the air leakage at sites including foundation walls to above grade wall connections at cracks at the bottom of gypsum wallboards located at the

floor to exterior wall joints and ceiling to attic space connections. There is however a considerable variation within the category of wall airtightness. The total attributable air leakage in a buildings can range from 18% to 50% of (ASHRAE, 2009).

The effective thermal resistance can be severely compromised at ceiling locations due to building service penetrations. The contribution of ceiling air leakage was found to have a mean air leakage contribution of 18%, varying from 30% to as little as 3% (ASHRAE, 2009)(Harrje & Born, 1982).

The contribution of fenestration to airtightness is estimated to be 15%. The range of air leakage at windows could vary from 6% to 22% of whole building levels. The window type had a significant effect on air leakage rate. For instance, casement windows had improved airtightness over sliding windows, and double hung windows, as a result of the casement window sealing method. Furthermore, the air leakage was not uniform around the frame, with increased air leakage meeting rails, window corners and sills(Weidt, 1979).

All-air residential heating and cooling systems have an important contribution to total air leakage. The mean air leakage was found to be 18% of whole building air leakage in residential homes. The furnace or air-conditioner type and ducting arrangements were found to be important contributors to the resultant air leakage. The range in air conditioning type and configuration varied the airtightness contribution from as small as 3% to 28%(ASHRAE, 2009) (Dickerhoff, Grimsrud, & Lipschutz, 1982). The influence of individual HVAC-R components such as ducting, fireplaces vents, bathrooms ducting, and kitchens vents can also vary. For instance, vents in condition spaces, contributed to approximately 5% of the overall air leakage. Fireplaces

can contribute to 12% of whole building air leakage, however this amount has been shown to vary widely, from 0%-30%(ASHRAE, 2009).

Air diffusion through walls is negligible as compared to leakage at wall transitions and exterior wall openings and represented a mean of less than 1% of the total air leakage.

Therefore, the sum of the major building enclosure components comprising of walls details (35%), ceilings details(18%), and windows details(15%), accounted for approximately 68% of whole building air tightness. Depending of the house configuration, the air leakage contribution can range between $\frac{1}{2}$ or $\frac{3}{4}$ of the total attributable share of building air tightness (ie. 53% to 74%).

The consensus that air leakage predominates at exterior wall transitions has motivated considerable research on subassembly air leakage contribution to building airtightness. For instance, the focus on window to wall interfaces, floor to wall transitions, roof penetrations, foundation walls transitions, and prefabricated panel joints air leakage has advanced our understanding of air leakage.

Representative samples of standard Norwegian construction comprising the floor beam to wall details were tested with insulation, weather barrier and combinations of air barriers constituting gypsum or a vapour barrier. The full-scale detail included both insulation and semi finished interior gypsum cladding. The relative influence of different air tightness strategies on airtightness were explored and discussed. In this case, the house wrap air barrier system was found to be the most airtight (Relander, Bauwens, Roels, Thue, & Uvsløkk, 2011).

Other building details, such as window to wall interfaces in residential buildings, can also have a significant impact on: effective heat loss, total energy consumption and total uncontrolled

air leakage(Van Den Bossche, Huyghe, Moens, Janssens, & Depaepe, 2012) (Almeida, Ramos, & Pereira, 2017). Air tight window framing can reduce total building energy use by 33% based on a study of attached low rise test houses with conventional double-glazed windows(Cuce, 2017).

Air leakage through other wall transitions have been individually tested and quantified as well. For instance, the air leakage through roof and chimney penetrations in wood frame wall has also been studied for low rise wood framed houses(Relander, Kvande, & Thue, 2010). In addition, the effect of sealing method on the sill plate to foundation wall interface was isolated, tested and quantified in laboratory testing as well (Relander, Heiskel, & Tyssedal, 2011).

More recently, researchers have examined air leakage of wall penetrations and transitions for modern low energy wall construction. Joints connecting three envelope elements were found to have more leakage than joints connecting two elements in panelised enclosure systems. Although leakage in these types of joints highly influenced by sealants, joint seam design was found to be an important criterion affecting air leakage at panel joints. The researchers also determined that quantifying the amount of joint air leakage was not always easily calculated experimentally or by way of simulation (Kayello, Ge, Athienitis, & Rao, 2017).

2.1.3 Methods to Control Air Leakage

The four of the most common approaches to air barrier system construction are discussed below. Their relative merit as compared to the four requirements of an air barrier system are explored.

2.1.3.1 Air Barrier Requirements

An “air barrier” or “air control layer” may be a single material or material system with overall reduced air permeability as compared to other construction materials. The design and application of an air barrier typically follow three broad strategies(J. Straube, 2009):

- Exterior Air Control Layer
- Interior Air Control Layer
- Hybrid/Dual Air Control Layers

The first strategy provides an air resistive control layer to the exterior building enclosure. The exterior approach typically relies on a material combination applied onto the exterior sheathing and transition joints (Langmans, Klein, De Paepe, & Roels, 2010). The second strategy applies an air resistive barrier towards the interior of the framed wall. The interior air barrier is typically applied just behind the interior sheathing, or utilise the sheathing itself as the major component of the exterior air barrier(Proskiw & Eng, 1997)(Rousseau, 2004). The third strategy applies both and exterior and interior air resistive layer where practical and cost effective. All three strategies rely on one or more planes of air tightness. Regardless of which strategy is utilised, it is generally accepted that the requirements of an air barrier system should satisfy four basic requirements (J. F. Straube, 2002):

- Impermeability
- Continuity
- Strength & Rigidity`
- Serviceability or Durability

Individual materials that form part of the air barrier system should be relatively air impermeable. In practice, this means that single air barrier materials should not exceed $0.02\text{L/m}^2/\text{s}$ at 75Pa of differential air pressure according to Canada’s National Building Code. Secondly, the air control layer should be continuous and act an air barrier system. This means that the various air barrier

materials should be joined together or sealed tight to provide a monolithic plane of air tightness which would encase the whole building envelope. Third, all materials comprising the air control layer should be durable enough to withstand differential air pressures caused by wind gusts and retain impermeability if punctured. In practice this may mean that the air barrier is sandwiched or adhered to a rigid material, or that the air barrier materials themselves are rigid enough to withstand such loading. Lastly, the air control layer should either be durable or serviceable. A durable air barrier system will be able to maintain the other three requirements for the expected service life of the building. Therefore, an unserviceable air barrier system may be placed in a relatively inaccessible space inside the framed wall. By contrast, a serviceable air barrier should be placed in a location where it can be repaired or replaced in whole or in part during the expected service life of the building(Lstiburek, 2005).

2.1.3.2 Sealed Polyethylene ABS

In the sealed polyethylene approach, the air barrier is mainly composed of thin and flexible polyethylene film typically 0.15mm in thickness. The main air barrier material can be sealed to other pieces of polyethylene, plywood subfloors, rim joists, concrete foundation walls, and window flanges to form the air barrier system. In cold climates, the polyethylene film is placed on the warm side of the framed wall assembly between the interior face of the studs and interior face of the stud cavity insulation to act additionally as the vapour control layer (Proskiw & Eng, 1997). Unsupported polyethylene can tear under a pressure differential. Thus, polyethylene sheets need to be supported due to its' poor structural strength. Polyethylene is typically located behind the interior gypsum board which provides for a modest amount of rigidity. The location

of the air barrier also allows most of this air barrier system to be serviceable. However, the polyethylene sheet is also susceptible to rupture and pin hole damage during construction phase from staples, screws and nailing to the stud frame and occupant activities following construction. It is important to note that polyethylene sheet was originally developed and still is used primarily as a vapour retarder. As such, imperfection such as tears, or pin holes originating from the installation process are tolerable from a vapour transport point of view. The same cannot be said about the holes, tears or discontinuities through an air barrier system. Tears and holes supply a leakage path and reduce air permeability of air barrier systems. Ideally, holes produced in polyethylene-based air barrier materials by fasteners should be sealed, self-sealing or avoided altogether when possible.

2.1.3.3 Air Tight Drywall ABS

The air tight drywall approach utilises the interior finishes as the name implies. The interior gypsum sheathing board joints are taped and sealed (Lischkoff & Lstiburek, 1980). The other drywall edges are sealed to exterior walls, ceilings and wooden subfloors as the primary components. This approach provides for an impermeable, rigid, serviceable air barrier. However, the continuity of the air control strategy may be compromised post occupancy when contractors or homeowners make openings in the gypsum board without sealing the renovated components to the gypsum board.

2.1.3.4 House Wrap ABS

The house wrap approach involves installing the plane of air tightness to the exterior of the framed wall. The wrapping material is often a thin sheet of vapour permeable but air impermeable polyethylene or polypropylene. The sheets of house wrap are typically either taped,

stapled, or adhered to the rigid exterior sheathing(Langmans et al., 2010). The wrapping material is eventually protected from the exterior by cladding. The house wrap material is inherently structurally weak and must be supported by the sheathing to provide resistance to differential pressure across the building enclosure. The ends of the wrapping sheet are typically overlapping and placed shingle style. Taping the ends of the house wrap helps provide continuity to the air barrier. Serviceability of the air barrier is difficult by virtue of the wraps' location behind the cladding. There is also a risk that the wrap will be penetrated due punctures by tacks, staples, or wear during the installation process. In this regard, taped sheeting joints would be more air tight than tacked methods of adhesion. Liquid applied housing wraps and adhesive backed sheets can also be used as an alternative to the standard housing wraps. These liquid-applied and self-adhesive sheet applied air control layers better satisfy the strength, stiffness and continuity requirements of an air barrier when compared to standard house wraps.

2.1.3.5 Exterior Sheathing System

Finally, a fourth class of air barrier is the use of rigid exterior sheathing as the primary plane of airtightness(Langmans et al., 2010). Plywood, exterior grade gypsum board, or insulated sheathing could be used as the primary material. The board joints and penetrating fasteners are typically taped or sealed to provide air barrier continuity.

Each air barrier system method described above; whether it be sealed polyethylene, airtight drywall, house wrap, or exterior sheathing, all attempt to reduce air leakage that can occur at multiple locations throughout the building enclosure. The primary methods available to estimating air leakage through the air barrier system occur at the post-construction phase. The

post-construction phase measurements are robust and repeatable. However post-construction airtightness evaluations are reactive in nature, since buildings are either complete or substantially complete at this stage. The access to the air barrier system is either limited or out of reach without considerable deconstruction. Correcting leakage sources identified in post-construction evaluations can be technically challenging, resource intensive, or both. The most common methods to air leakage measurement are described below.

2.1.4 Technologies available for Post Construction Measurements

The three common methods used to empirically estimate airtightness of homes are Acoustic, Tracer Gas, and Fan Depressurisation.

The Acoustic method has been proposed and applied on large buildings (Iordache & Catalina, 2012). The principle behind the method is to emit known sound profiles within the building, while detecting any changes to the sound profile with receivers on the exterior of the building. Sound waves, which are regular density fluctuation in air, require a path from the emitter to the receiver. The degree of sound attenuation between the emitter and receivers is proportional to the homes' level of airtightness. Airtight homes have less holes in the air barrier system than leaky homes. In addition, airtight homes may also have sound absorbing, or sound reflecting materials in their enclosures. The acoustic method however, seems to have been more adequate for large buildings which are typically made of high-density materials. The acoustic model was not validated on a large number of light weight buildings, which are typical of North American homes. Various two dimensional and three dimensional software modeling methods have been created and validated on wall sections(Saber, Maref, Elmahdy, Swinton, & Glazer,

2012) using the acoustic method. These models are geared towards determining the added effect on air leakage as a vehicle for hygrothermal performance of wall assemblies.

The Tracer Gas Concentration Decay Method has also been employed on existing buildings and in theoretical computational models to estimate airtightness(Wang, Beausoleil-Morrison, & Reardon, 2009). The principal behind this method is based on concentration decay measurement. The air change rate or air tightness of a building can be determined by releasing a small amount of inert gas within the building enclosure at a known concentration. The gas concentration decreases due to the slow process of diffusion and by the air leakage points throughout the building enclosure. The decrease of inert gas concentration is then measured within the building enclosure. An algorithm is then used to correlate the tracer gas decay to the resultant air leakage. This method is more properly suited for the investigation of Indoor Air Quality and the migration of contaminants throughout the building enclosure(ASTM, 2017a).

The most common method to estimate building airtightness is through the use of a pressurisation or depressurisation fan to induce air leakage through holes in the fabric of the building enclosure. The so-called blower door method operates on the principle of orifice flow. Input fan pressure and output air leakage rates are recorded to provide an estimated volumetric air leakage per unit time, surface area or other normalisation metrics. The method also allows for the estimation of the equivalent hole size in the building enclosure. The method is discussed in detail in ASTM E1827(ASTM, 2017c).

2.2 Modeling Whole Building Air leakage

The ability to accurately predict airtightness can have a strong effect on building energy consumption. In some instances, the difference between estimated and actual airtightness was found to be more than 130%. This large difference between estimated and actually air leakage levels were responsible for an additional 30% in whole building heat loss (Bell, Wingfield, Miles-Shenton, & Seavers, 2010). Clearly, proper air leakage estimates can have large impact on various aspects of building practice. The following section will expand upon past approaches to modeling whole building airtightness. A discussion on the types of parameters used as well as their impact on the model will be elaborated upon. The overall airtightness model strengths and their respective applicability will be considered. And, lastly the implication of sampling population sizes will be discussed.

2.2.1 Whole Building Parameters

There are several approaches that can be used to model airtightness. Each modeling approach may result in specific outcomes. Furthermore, each modeling approach is typically dependent on a set of parameters. There are however four broad classes of parameters types which can be used:

- Materials & Technology,
- Supervision/Handicraft,
- Geometry, and
- Others(Prignon & Van Moeseke, 2017)

Materials and Technology can be reflected in the buildings' wall type. Walls types can vary from; prefabricated walls, heavy construction (masonry or poured concrete) to light framing (wood or steel stud). Roofing and below grade construction may also vary independently from

above grade walls. Hence roofing and below grade construction are sometimes captured as independent parameters. For instance, various roof configurations such as: pitched, flat, shed, or combination roof, were represented by a single parameter in a study by Bramiana et al (Bramiana, Entrop, & Halman, 2016). Supervision and Handicraft have been used as measures of quality of construction. Controlling for handicraft with the use of a parameter could be used to quantify its contribution to building air leakage rates. For instance, Kalamees (Jokisalo et al., 2009) in a study of Estonian single-family homes, tracked whether or not the construction of the homes were completed with or without professional supervision. Moreover, Chan et al (Chan, Joh, & Sherman, 2013) tracked whether or not homes were conventional or part of weatherisation programs in the United States.

Geometry is also an important parameter class. Building geometry defines the length enclosure discontinuities characterised at exterior wall interfaces, transitions, roof articulations, and service penetrations. Geometry also describes overall building size in the form of building height, building volume, floor area, and perimeter. However, not all modeling approaches have included geometry as explicit variables. Pan's United Kingdom analysis developed three predictive equations that did not require geometric parameters (Pan, 2010).

External based parameter classes can also have an important contributory effect to air tightness. Many models (Antretter, Karagiozis, TenWolde, & Holm, 2007; Bramiana et al., 2016; Chan et al., 2013; Khemet & Richman, 2018; Montoya, Pastor, Carrie, Guyot, & Planas, 2010) have used the buildings year of construction, or building age, as a predictor. Building age may be a proxy of both construction quality, joint or material deterioration and even building size. Relative humidity at time of test may influence air tightness in wood framed dwellings based on test hut

experiments. During the moistening phase airtightness has been shown to increase by 40% over the first few days. During the drying phase airtightness has been shown to decrease by 38% from 0.74 l/s m² to 0.98 l/s m². This change is attributed to the wood shrinkage and sealing condition due to increase in crack openings during drying of the wall assemblies(Domhagen & Wahlgren, 2017).

Parameter types such as Material, Geometry and Handicraft have been shown through experimentation and modeling to be influential to whole building air leakage rates. The author had used various combinations of these parameters in different phases of the research.

2.2.2 Whole Building Model Types

Prignon *et al* summarised four major predictive model types used in air tightness estimation. They include the Single Component Model, the Building Characteristic Model, The Theoretical Model, and the Empirical model. The single component modeling approach isolates a particular building feature such as a floor to wall details(Prignon & Van Moeseke, 2017), prefabricated panel joints, or a window detail (Cuce, 2017)(Almeida et al., 2017). This approach is helpful in directing designers on how to improve specific detailing qualities to improve airtightness characteristics.

The Building Characteristic Model type utilises simplified spread sheet calculations or mathematical equations that essentially multiply a series of parameters coefficients with an input variable level. Although is the most user-friendly model for designers, it is considered outdated. Building Characteristic Models rely on air leakage rates based on construction that may be obsolete and is thus not ideal for estimating preconstruction airtightness in newer buildings.

The third modeling type is the Theoretical Model. The Theoretical Model is based on highly localised leakage cracks using fundamental fluid flow analyses. This approach is important to understand complex flow through details. Theoretical Models often requires the use of Computational Fluid Dynamics(CFD) to manage the complex two or three dimensional flow thorough wall details (Younes & Shdid, 2013). The models are typically validated with scale model laboratory tests. These models can also be used in conjunction with heat transfer and moisture mass transfer analysis. For instance, a standard framed wall was tested with, and without a standard electrical wall penetration. One of the goals for the wall penetration study was to understand the impact on whole wall thermal resistance as a result of air leakage.(Saber et al., 2012).

Lastly there are Empirical Models. Empirical models are typically reliant on large data sets of whole building pressurisation data. The data sets are often analysed utilising statistical methods (Khemet & Richman, 2018), (Almeida et al., 2017), (Bramiana et al., 2016; Chan et al., 2013; Montoya et al., 2010),(Antretter et al., 2007; Cuce, 2017) . This approach to airtightness forecasting is typically accurate for buildings that are close to the data set used. Thus, the prediction accuracy is highly dependent on whether the geometry, materials, handicraft, and external parameters substantially match the original data set.

2.2.3 Selected Whole Building Airtightness Studies

A summary of select airtightness studies are reviewed below. Their relative strengths, parameters, and population characteristics are discussed throughout.

Table 2 shows a summary of significant multiple linear regression models based post-construction airtightness measurements in chronological order.

Chan et al analysed 70,000 houses in the United States which varied in both typology and in wall construction (Chan, Nazaroff, Price, Sohn, & Gadgil, 2005). The study found that construction year and floor area were the most important predictor variables. The study strength was also derived from a global airtightness category defined as “house type” which was a highly significant variable. The airtightness category had three levels: low income, conventional, and energy efficient homes. Thus, this level of airtightness through this stratification was known and controlled for in the modeling. The overall model strength was $R^2=0.56$.

Table 2 Summary of Relevant Multiple Regression Based Studies

Jurisdiction	R2	Parameters	N	Description
United States (2005)	0.56 ^{a,b}	4	70 000	Heterogeneous Typology Heterogeneous Wall
Greece (2006)	0.56 ^a , 0.93 ^a	1	20	Homogeneous Typology
Spain & France (2009)	0.94 ^{a,b}	2	483	Homogeneous Typology Heterogeneous Wall
United Kingdom (2010)	0.49 ^a	7 – 6	287	Heterogeneous Typology Heterogeneous Wall
United States (2013)	0.68 ^{a,b}	12	134 000	Homogeneous Typology Heterogeneous Wall
Netherlands (2016)	0.43 ^{ab}	5	320	Heterogeneous Typology Heterogeneous Wall
Notes: a. airtightness level known <i>a priori</i> b. year of construction used as predictor				

Sfakianaki et al performed blower door testing and tracer gas decay analysis on 20 homes in Greece (Sfakianaki et al., 2008). They developed and utilised a unique variable called the Frame Length Factor for their univariate regression analysis. The housing type was homogeneous and when all 20 homes were analysed as a set, the coefficient of determination was $R^2=0.56$. However, when the data set was further stratified into three categories of airtightness corresponding to low, medium and highly airtight, R^2 varied significantly. The 6 low airtightness

homes had a coefficient of determination of 0.32. The 11 homes that were grouped into medium airtightness had $R^2=0.40$, while the remaining three highly airtight homes has an $R^2=0.93$. This study demonstrated that a new, single predictor variable, comprising of a ratio of primary predictors could be used as a better predictor than when taken independently. However, the study was limited by relatively small sample size utilised for predictive power.

Montoya et al studied a set of 483 homes of homogeneous typology in France and Spain's Catalonia region (Montoya et al., 2010). Using only two parameters (building age and construction technique) the researchers were able to develop a model with $R^2=0.94$. However, the Construction Technique parameters represented three level airtightness stratification of discrete values of 1=airtight, 2=average, 3=leaky. The pre-categorisation of buildings according to airtightness acts as a feed forward control loop. The feed forward control allows for a partial modification and refinement of the airtightness prediction based on the houses existing air leakage class. Hence the high degree of model strength was not only dependant on building year, but by the ranked level of airtightness.

Pan analysed 287 houses and apartments in the United Kingdom that ranged in build method, typology, and construction company for up to 7 parameters (Pan, 2010). None of the parameters were geometric. However, one parameter controlled for airtightness level via a discrete five scale air leakage design target (range: $5\text{m}^3/\text{hm}^2$ - $10\text{m}^3/\text{hm}^2@50\text{Pa}$). The study did not however find the design target to be significant. The model considered heterogeneous walls such as masonry, reinforced concrete, wood framing, and prefabricated panels. The sample population's housing typology was also heterogeneous. The model considered apartment and terraced homes in their analysis. The model also controlled for the construction company

utilised. The coefficient of determination for the strongest model was found to be 0.49 explaining 49% of the data.

Eight years from their previous study, Chan et al analysed an even larger data set numbering 134, 000 homes ranging in wall construction, foundation, climatic region and HVAC component location(Chan et al., 2013). The model also stratified the airtightness level of the homes using occupant income level as an indicator to the level of airtightness. The 12 variable model was able to explain 68% of the airtightness variation using the developed regression equation. The study demonstrated that strong airtightness predictions were possible with few geometric variables provided that large samples sizes were available to study.

Bramiana *et al* examined combined a literature review and empirical study of 320 homes in the Netherlands. The empirical portion of the study included parameters for: housing typology, period of construction, wall typology, construction management, and target airtightness standard (Bramiana et al., 2016). The authors also created a novel parameter called sighted leakage. Sighted air leakage, identified and ranked the building's airtightness level. The sighted leakage parameter was defined as an algebraic function that describing the actual level of leakage in the house using thermographic scanning or using a smoke pencil inspection. The build year period was found to be an extremely significant predictor of airtightness based on their regression analysis. The models' coefficient of determination was found to be $R^2=0.43$.

Wolf et al conducted a rigorous quantification of air leakage of individual paths at rim joists, inside corners, outside corners, and various mechanical and electrical wall penetrations. The quantification resulted in assigning a leakage value per leakage path in air changes per hour at 50Pa or in volume leakage rate per linear dimension or per unit. The leakage rates were then

tested in-situ with a test house. This methodology helped prioritise the most important air leakage contributor for this housing typology (Wolf & Tyler, 2013a)(Wolf & Tyler, 2013b). In addition to the isolation of air leakage paths through the building enclosure. Investigation into parameter estimation has been studied. The air tightness coefficient C , and pressure exponent n were estimated using an iterative computational statistical approach(Okuyama & Onishi, 2012).

The regression-based prediction models discussed above showed a range of strengths. Many of the models needed to be representative of the area of study. Therefore, typology heterogeneity, and wall construction heterogeneity were logical conditions to impose for these kinds of investigation. These models were additionally dependant on knowing the degree of airtightness *a priori*. As a result, the model strength represented by Pearson's correlation coefficient were often moderate to strong. Moreover, the explanatory power of these models as expressed by the coefficient of determination was commensurately high. The high degree of variation based on housing typology provided an extra degree of modeling strength. Furthermore, the regression-based models used variables to control for the level of airtightness. The usage *a priori* airtightness levels increased the model strength by using this feed-forward control loop on air leakage predictions. Lastly it is difficult and impractical to attempt to make preconstruction airtightness estimates with models that are strongly dependent parameters associated with year of construction and the airtightness category. What if we were to combine the strengths of subassembly component testing with the rigors of population level statistical analysis? Could a viable airtightness models be constructed with increased specificity of housing, and wall typology? Can a non-temporal, climate independent airtightness model have more explanatory power than the current literature suggests?

2.3 Research Objectives

The central objective of this thesis is to provide an approach to estimating preconstruction airtightness levels in new single family, detached, light framed homes. Based on this objective, the work explores if a national airtightness database can be used to predict airtightness in single family detached homes. Additionally, the research will examine whether a builder specific model can be created to reflect the particularities of design detailing, and handicraft associated with individual home builders. Finally, the work aims to discover if a new approach applied to influential air leakage details can be utilised to re-weight prediction equation parameters for builder specific models – allowing for the implementation of next generation designs with predictable air leakage range per housing configuration.

This research provides a bridge between the reactive and predictive methods of airtightness estimation by merging high resolution data sets with the specificity of controlled, laboratory-based leakage testing. A schematic depiction of the framework governing the approach to this research is depicted in Figure 2.

2.4 Research Questions

To fulfill the objectives stated above, this research aims to answer the following questions:

1. *Can a linear regression model estimate building airtightness in conventionally constructed, low-rise, residential buildings in a Canadian cold climate?*
2. *Can a builder-specific blower door testing population be used to estimate airtightness in conventional construction based on geometric details associated with air barrier leakage, in low rise, residential, light framed buildings, in a Canadian cold climate?*
3. *Can an experimentally based methodology be used to modify estimates of whole building airtightness in new construction at pre-construction phases of development, for low rise, detached, residential, light framed buildings, in a Canadian cold climate?*

2.5 Conceptual Framework

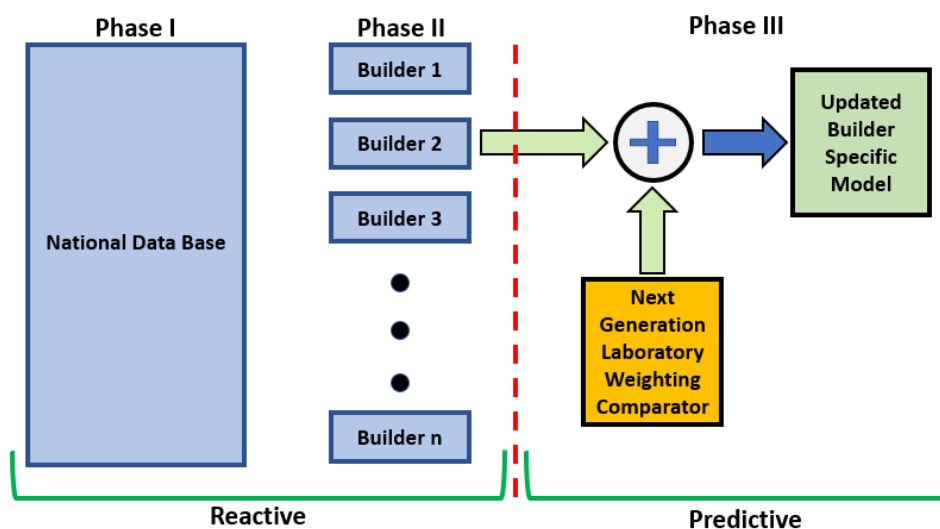


Figure 2 Representation of the Conceptual Framework

This research investigates airtightness prediction of single family, detached, light framed homes using both reactive (i.e. post construction) and predictive (i.e. pre-construction) novel methods. Phase I utilises a univariate analysis in conjunction with a multiple linear regression method on a national database of a blower door testing population numbering over 900,000 detached Canadian homes. Three and eight parameter regression models predicting air tightness were developed. These Phase I models identified important predictor variables related to estimating airtightness. The modeling also allowed for the establishment of a lower bound for airtightness predictions for Canadian low-rise buildings.

Phase II of this research developed several builder specific models, utilising fined grained design information comprising building geometry and envelope details, paired with a tested air leakage rate for a population of 272 detached houses. Through an iterative approach, unique models were developed for different builders. A larger model was also designed such that the effects of assembly quality or handicraft could be taken into account.

The transition between reactive and predictive approaches is completed between Phase II and Phase III of the research. A building detail identified as significant to total air leakage in Phase II was then isolated, and tested in a controlled laboratory setting for Phase III. A full factorial design of experiments was developed to ascertain the relative air leakage through the detail of interest. The iterative model linking both Phase II and Phase III into a next-generation, multiple linear regression model was then used to estimate builder specific whole building air leakage. Using both a combination of reactive and predictive approaches to airtightness estimation, for the purposes of builder-specific air leakage forecasting of residential Canada, has not been achieved

before. The following will establish a global framework whereby preconstruction airtightness could be estimated in detached, light-framed, residential buildings.

3 Methodology

The primary objective of this research was to develop a preconstruction estimate for whole building airtightness in detached low rise, light framed, residential buildings for a Canadian cold climate. The method to answer the research questions stemming from this objective was by first performing a macro analysis on a national blower door testing population. The purpose of the macro level analysis was to quantify the lower bound of multiple linear regression airtightness models for existing homes. The second phase of the approach comprised developing time independent, builder specific predictive models with equal or higher strength than those of the national level models. The third phase of the approach was to use laboratory-based component air leakage measurements for building details that contributed the most to total building air leakage. These details were constructed and tested in a factorial based experimental design. The relative airtightness performance of the details was then integrated with builder-specific models. Such updated next generation builder specific model would then be able to provide builders with an approach to estimate preconstruction whole building airtightness in detached low rise, light framed, residential buildings with novel construction details.

3.1 Mathematical Models

The physics of airflow through building enclosures can be estimated using both an analytical solution and an empirical approximation. The analytical solution originates from analysing the momentum of a particle flowing along a streamline, as in Bernoulli's equation. Since momentum is conserved (Van Wylen & Sonntag, 1985), integrating momentum yields an expression of the conservation of energy for a fluid moving over a stream line shown in Equations (1) and (2). The

relationships in these equations hold true with the assumptions of steady flow, no friction, and incompressible flow(Pritchard, Mitchell, & Leylegian, 2016).

$$\text{Pressure Work} + \text{Kinetic Energy} + \text{Potential Energy} = \text{Constant} \quad (1)$$

$$P_1V_1 + 1/2m_1v_1^2 + m_1gZ_1 = P_2V_2 + 1/2m_2v_2^2 + m_2gZ_2 \quad (2)$$

Air leakage through building enclosures have been modeled based on orifice flow. The assumption of orifice flow through the side of a large reservoir implies net zero change in potential energy, and an initial fluid velocity of zero. This model yields the important “Power Law”(Hutcheon & Handegord, 1983) in Equation (3):

$$Q=C_oA\Delta P^n \quad (3)$$

Where Q is the output volumetric flow rate, C_o is the flow coefficient, A is the leakage area, ΔP input pressure difference across the building enclosure, and n is the flow exponent typically ranging from 0.5 to 1.0. Turbulent flow is indicated by n = 0.5 and laminar flow is indicated by n = 1.0(Hutcheon & Handegord, 1983). An airflow exponent of n=0.65 has been taken as a good approximation for typical enclosure air leakage when no other data has been available. The power law for airflow can be linearised into Equation (4 and transformed to Equation (5) such that Y = log Q, C = log C_oA and the input X=ΔP.

$$\text{Log}(Q)=\text{Log}(C_oA)+ n\cdot\text{Log}(\Delta P) \quad (4)$$

$$Y = C + nX \quad (5)$$

The expression for air leakage, Y , is then simplified to a single input X , which is the transformed change in pressure when the flow coefficient of “ C ”, and flow exponent “ n ” are known. However, we can also model the air flow empirically using multiple linear regression such that the airflow through the building enclosure is the linear combination of a series of independent inputs. The air leakage output metric can be expressed in air changes per hour at 50 Pascals (ACH50) as shown in Equation (6). The alternate output air leakage metric, normalized leakage (NL), can be expressed as in Equation (7).

$$ACH50 = B_0 + B_1X_1 + B_2X_2 + \dots + \epsilon \quad (6)$$

$$NL = B_0 + B_1X_1 + B_2X_2 + \dots + \epsilon \quad (7)$$

Normalized air leakage is a non dimensional number comprised of the ratio of equivalent leakage over total enclosure area and building height ratio (Sherman, 1995) as shown in Equation (8):

$$NL = 1000 \left(\frac{ELA}{Area} \right) \left(\frac{Height}{2.5m} \right)^{0.3} \quad (8)$$

The software used to run the univariate and multiple linear regression analyses was IBM’s SPSS 10; a predictive analytics software package that allows for data analysis and model building. All three phases of the research will apply the results from the analytic and the empirical expressions of air leakage through the building enclosure.

The following elaborates on the methodology used at each of the three phases of research. Care is taken to discuss both the mathematical and theoretical underpinnings relevant to each phase.

3.2 Phase I: National Level Airtightness Predictions

The first phase of the research used a univariate exploration to identify important regional and national trends in the data set. Multiple linear regression was utilised to predict airtightness levels for conventionally constructed, detached, low-rise residential homes for two large national population levels. The selection and derivation of the input variables are discussed. The analysis procedure for each population was also formalised.

3.2.1 National Sample of 900,000 homes

A national blower door testing population of over 900,000 homes from the Office of Energy Efficiency at Natural Resources Canada was analysed (Office of Energy Efficiency, n.d.). The data collection originated from the voluntary ecoEnergy Retrofit program which required homeowners' participants to have their dwellings undergo a pre-retrofit energy evaluation. Part of this pre-retrofit evaluation included an airtightness test via fan (de)pressurization. The method procedure was performed in general accordance to testing standards such as the CAN/CGSB 149. The relationship between the pressure imposed on the building enclosure and air leakage rate fits the power law as stated in Equations (3),(4) and (5). The age of the detached homes in the same population ranged from the 1700's through to 2016. Canada's housing stock in 2016 was approximately 14 million according to Statistics Canada. Nearly 53.6% of these residential homes were detached. Thus, the national sample analysed represented upwards of 12% of the national housing stock, and hence a sizable contribution Canada's housing profile.

The following variables were chosen for univariate and multiple linear regression analyses based on previous international post-construction models: air changes per hour, equivalent leakage area, building volume, building height, and year of construction. Additional variables could have been chosen; however, this would have reduced the sample size due to incomplete entries in the data set (e.g. number of corners on the exterior walls). Previous studies have shown that the age of the building was of primary importance in airtightness modeling [53], (Montoya et al., 2010), [56], [57]. Therefore, building *Age* was selected as predictor variable in an attempt to produce the strongest model possible. Building *Volume* was selected as a secondary predictor variable due to the direct mathematical relationship between volume and volumetric air changes per hour. Using volume as a predictor also allows for verification of this research's model with historical airtightness results which have also used a volume-based predictor variable. Lastly, building *Height* was used as a third predictor variable to represent a missing identifier.

3.2.2 National Sample of 330,000 homes

The total number of airtightness data points was reduced from approximately 900,000 to 330,000 records. This reduction was completed to enhance the models' granularity by increasing the number independent predictor variables from 3 to 8. Incomplete data records were removed which ensured that every airtightness value had a corresponding full set of predictor variable values. The 330,000 sample sub-set remained nationally representative since it included airtightness data from both major and minor cities throughout most provinces and territories. The expanded 8 predictor variable list included building enclosure insulation levels such as: *CeilingRSI*, *FoundationRSI*, *WallRSI*, and *WindowRSI*. The additional climate variable for Heating

Degree Days (*HDD*), was derived using the buildings municipal geographical location and ASHRAE Climate Data (ASHRAE, 2013, 2009) utilising 18°C as the datum.

3.2.3 Analysis Methodology

The analysis considered any possible correlation between a dwellings *Age*, *Volume*, and *Height* as it related to both air leakage measures, *ACH50* and *NL*. By focussing on jurisdiction, a measure of air barrier workmanship as it related to *ACH50* and Normalised Leakage was investigated. The question of the usefulness of a multiple linear regression model as a predictor for the existing NRCan data set was investigated. Regression was used in order to connect every airtightness test and its respective predictor variables to a compact prediction equation. From the outset, it was assumed that the predictor variables were insignificant unless otherwise shown to be important through the null hypothesis test on the regression parameters, as established by a conventional significance level of $\alpha = 0.05$. The regression analysis determined whether each predictor variable was significant. The analysis also determined how significant each parameter may have been. The significance of each term was evaluated by the p-value. The convention used in this study is that p-values above 0.10 showed no significance, p-values between 0.10 and 0.05 showed weak significance, p-values between 0.05 and 0.025 showed strong significance, p-values less than 0.01 show very strong evidence of significance, and p-values below 0.001 indicated extremely significant results.

Furthermore, the use of linear regression as opposed to non-linear methods allows this study to be more readily compared to other previous studies using its relative strength. Although the Pearson Correlation coefficient was reported to determine the strength of the model, its' square, the coefficient of determination, R^2 , is a more useful metric when comparing between

studies. The convention used was that R below 0.3 showed weak model strength, R values between 0.3 and 0.7 showed moderate model strength and R values above 0.7 showed strong explanatory power. When R^2 was multiplied by 100%, the explanatory power of the models could then be compared within this study, and between prior studies. It is believed that a single, compact, predictive airtightness equation built upon a large national data set could form a lower bound for future regression based linear models.

3.3 Phase II: Predicting Airtightness in Regional Populations

A regional blower door testing population of 2297 light framed, low-rise, detached homes from southern Ontario homes was analysed. A Toronto Ontario consulting firm in conjunction with four building developers provided detailed airtightness testing data and access to building plans for examination. These light framed homes code compliant, were built within the same decade and comprised of two storeys, a garage, and a basement. A modeling sample of 272 homes represented 54 discrete layouts. Blower door pressurisation testing results were coupled with high resolution building take-offs. Builder specific, non-temporal airtightness models were developed along side a model that considered the effects of handicraft on airtightness results. A five-step post regression airtightness modeling verification procedure was used to evaluate model strength. The iterative process is illustrated in Figure 3.

3.3.1 Analysis Methodology

The first step to modeling airtightness was to provide a first estimate of important air leakage sources. This was done by assigning geometry-based parameters that represented locations of

potential air leakage. Next, a multiple linear regression analysis was performed. The strength of the overall model was first assessed using Pearson's correlation coefficient. If $R > 0.6$, the predictor variable parameters was examined for significance. If $R < 0.6$ then the model may have been too weak, and would have required a larger sample size before moving to the next iteration. Secondly, the designer would need to have verified if the parameters B have p-values > 0.1 . If the associated predictor had variables have Beta's with significance values above 0.1 then the respective predictor should have been provisionally discarded. An ANOVA would have been performed on the model where the p-value would have been checked against $\alpha = 0.05$. The ANOVA is a method that determines whether or not there is significance between two sample means. The null hypothesis is that two groups have the same mean, and are indistinguishable from each other. The ANOVA employs the F-test to make the determination of significance. If the ANOVA is found to be significant (i.e. $p < 0.05$) then the two sets of data are considered to be distinct. If the ANOVA is found to be insignificant, then one fails to reject the null hypothesis. The confidence in the airtightness if the calculated p-value is found to be below the specified level of significance, $\alpha = 0.05$. In the third step, the designer analyses the residuals to verify if the normality assumption was satisfied. If the standardised residuals have a mean $\mu = 0.0$, the standardised standard deviation that is nearly $\sigma = 1.0$, and a randomly dispersed plot of standardised residuals about the horizontal axis, then the confidence in the model is increased. The designers' fifth verification step was to verify that there was little multicollinearity between the predictor variables. The multiple collinearity would be verified through the Variance Inflation Factor (VIF) for each parameter in the model. VIF values larger than 10 would indicate high correlation with other existing predictors. Variables with VIF's above the threshold would be removed. If the

mathematical airtightness model satisfied a sensible R, significant Beta parameters, satisfactory ANOVA, residual analysis, and an acceptable VIF then the mathematical predictive model could be accepted. The model would then take the form of Equation(6) or Equation(7).

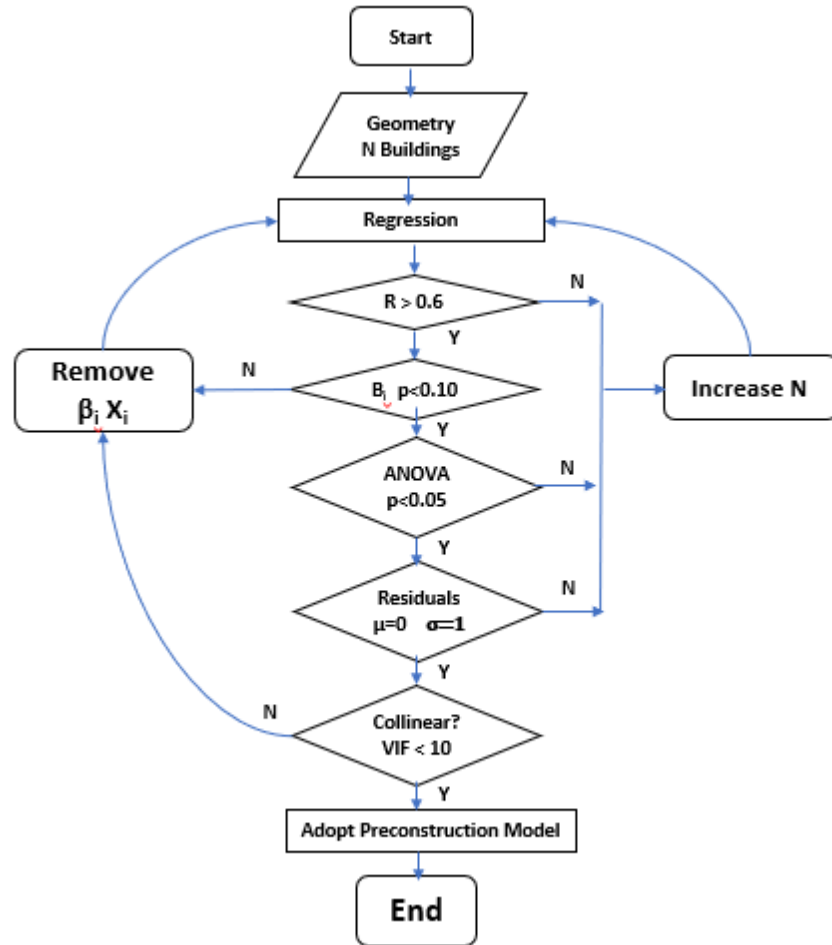


Figure 3 Airtightness Estimation Approach for Builder Specific Time Independent Populations

3.3.2 Selection of Predictive Variables

A total of twenty predictor variables were used to model air leakage across 272 detached homes. Nineteen of the twenty predictor variables were geometric in nature. These continuous variables belonged to five broad classes;

- length variables,
- length ratio variables,
- area variables,
- area ratio variables,
- and capacity variables

Previous studies have shown that building size as measured by building height had a strong influence on overall building airtightness estimation (Chan et al., 2013, 2005). Thus, both the above grade building height (*AGradeH*) and the total building height (*TotalH*) were selected. These height-based variables likely have higher impact on the measurement of ACH50 as opposed to NL. Larger homes, on average, may be more airtight as compared to smaller homes, if other factors can be kept constant. Secondly, normalised leakage controls for building size as shown in Equation (8). Other length variables describing Window perimeter (*WindowP*) and door perimeter (*DoorP*) were defined as predictor variables to account for air leakage gaps at window to wall openings in the building enclosure. As discussed in Chapter 2, fenestration had been shown to negatively affect airtightness in homes. Wall transitions, such as wall interior floor to exterior walls were also important to capture. The houses total rim joist length (*RJoistL*) was used to track possible air leakage through the building enclosure.

Air leakage is complex and comprises multiple dimensions. Thus, five area-based variables with the potential to impact air leakage. The total enclosure area (*ShellA*) was used to account for bulk air leakage that may occur at joints and penetrations through the field of the wall. Air leakage at the wall to ceiling as well as the penetrations through the ceiling air barrier were monitored using a ceiling area (*CeilingA*) predictor variable. The possible air leakage between exposed floors was logged by using an exposed floor area variable (*ExFloorA*). Exposed floor area may cover bay window or cantilevered floors but are mainly applicable to second floor rooms

located above garages. Finally, door area (*DoorA*) and window area (*WindowA*) were used as a second set of predictor variables to identify fenestration size as a source of air leakage.

Three length ratios were created to monitor airtightness. A variable called the fenestration perimeter to height ratio (*FenPerimHR*) was developed. The variable represents the total crack length for all doors and windows normalised to the building height. In addition, the rim joist ratio (*RJoistR*) which is actual rim joist length, normalised by the optimum (ie minimized) building perimeter, based on floor area. The joist ratio thus normalised actual joist length, to an idealised rim joist length. The idealised joist length is based on a minimum interior floor area. Thus, every home in the data base would have an idealised joist length particular to its individual geometry. Similarly, the perimeter ratio (*PerimR*) is the actual rim joist length for a single floor, based on an idealised joist length. However, *PerimR* idealised joist length is the minimum joist length achievable based on the houses' actual volume. These three area ratios *FPerimR*, *JoistR* and *PerimR*, were devised to be non dimensional predictor variables that are scaled to its building size. This approach is akin to *NL* where two of its variables (see Equation (8)) *ELA* and building *Height* are normalised by total enclosure area and standard floor height respectively.

This approach is also similar to what Sfakianaki et al devised to monitor airtightness in homes in Athens(Sfakianaki et al., 2008). That study utilised a frame length factor which was the sum of total window frame lengths divided by the net volume of the buildings in question. This variable hence normalised crack length to building massing. However, that factor was dimensional. In contrast; *FPerimR*, *JoistR* and *PerimR* are non dimensional ratios normalised by height, idealised area-based perimeter, and idealised volume-base perimeter respectively. It will be possible to compare the significance of the ratio-based predictor variables against the absolute length's

predictor variables when regression models are built. The significant predictor variables will appear as significant (p-value < 0.05) Beta parameters.

Fenestration Perimeter to Height Ratio

$$\text{FenPerimHR} = \sum (L_i) / L_o$$

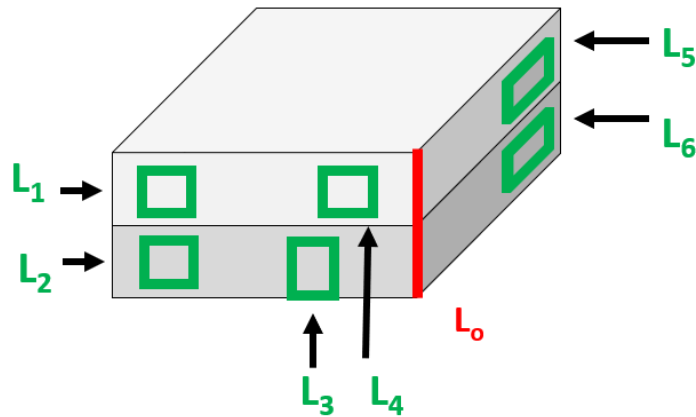


Figure 4 Fenestration Perimeter to Height Ratio

$$\text{Rim Joist Ratio} = L_o / L \cdot 100$$

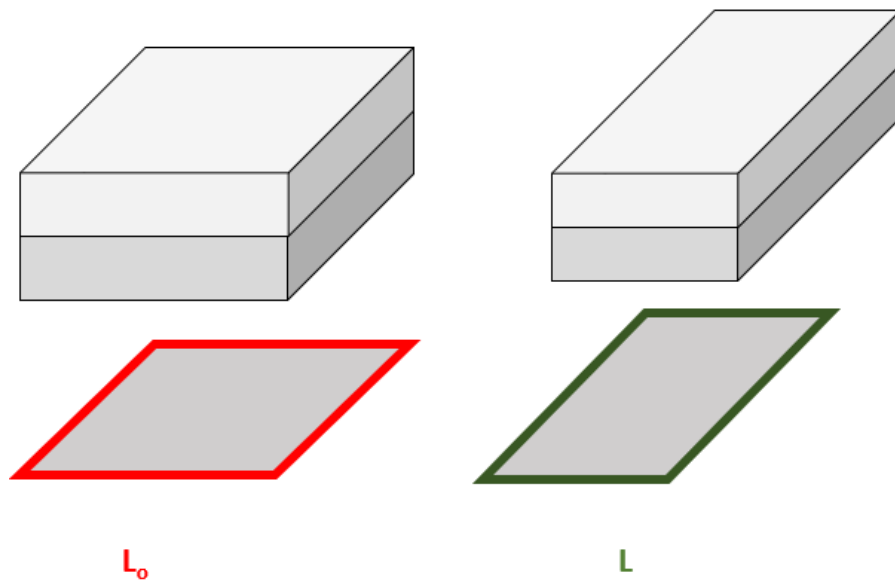


Figure 5 Rim Joist Ratio

Three area-based ratios were also included into the initial airtightness model. Fenestration to wall ratio (*FWR*), a variable typically used in problems dealing with thermal transmittance was

included. The use of this same metric might have been useful in predicting air leakage since it adds a size dimension not available in total fenestration perimeters. *FWR* would help add distinguishing element to a building with several small windows as opposed to those with large windows but same equivalent window area. More enclosure penetration cracks may increase the amount of framing required for support. The increase in the number of framing supports may also increase the number of sites for air leakage due increasing framing complexity.

In addition, ceiling to wall ratio (*CWR*) was used to track air leakage at ceiling to exterior wall interfaces as well as air leakage in the field of the ceiling due to air-barrier penetration in the field of the ceiling due to electrical services for lighting, plumbing and ventilation risers. An exposed floor area to conditioned floor area ratio (*ExCondFA*) was also devised to monitor the impact of the exposed floors at the garage relative to the overall floor area.

The only capacity based geometric predictor used in this study was house volume (*Volume*). Building volume is directly proportional to the air changes per hour metric. Hence larger buildings tend to be less air permeable if a non normalised volumetric air change per hour metric is used.

Finally, handicraft and build quality effects on whole building air leakage was tracked using builder identification (*BuilderID*). *BuilderID* represented the only discrete variable the twenty predictor variables discussed.

In summary (Table 3), twenty predictor variables were selected or created to track potential sources of air leakage. These variables were used in an exploratory univariate analysis as well as in multiple linear regression-based airtightness models. The 5-step modeling calibration

criterium was also discussed. The following phase will incorporate a builder specific model with weighting factors devised by research in Phase III.

<u>Length Variables</u>	<u>Area Variables</u>
Above Grade Height	Shell Area
Total Height	Exposed Floor Area
Rim Joist Length	Floor Area
Door Perimeter	Ceiling Area
Window Perimeter	Door Area
<u>Length Ratio Variables</u>	Window Area
Perimeter Ratio	Rim Joist Area
Joist Ratio	<u>Area Ratios Variables</u>
Fenestration Perimeter to Height Ratio	Fenestration to Wall Ratio
Other Variables	Exposed Floor Conditioned Floor Area
Volume	Ceiling to Wall Ratio
Builder ID	

Table 3 Provisional Predictor Variables by Class

3.4 Phase III: Predicting Airtightness with Laboratory Tests

Estimating preconstruction airtightness requires knowledge of how air leakage behaves in both conventional and next generation building details. The following proposes an approach on how to account for the differences in air leakage due to differing transition detail joints. The modeling results from the local blower door testing population in Phase II can show that certain construction details had a strong relationship with whole building airtightness. Thus, a builder

can triage high impact building details on order of importance. The most important details would be the most suited to be modeled in a controlled laboratory environment. Furthermore, next generation details could be evaluated in tandem with the important leakage details to be improved.

3.4.1 Analysis Methodology

A factorial analysis was used to evaluate the important effects related to specific building enclosure details known to impact airtightness. Factorial analyses have been used as an effective approach in both investigatory and optimisation problems (Box, Hunter, & Hunter, 2005). It is a beneficial approach partly because the analysis procedure evaluates multiple factors simultaneously rather than one factor at a time. The factorial analysis allows the investigator to isolate influential parameters while eliminating low impact parameters of lower significance. The factorial approach also allows the investigator to discover the effects of complex interaction that are otherwise difficult to identify or test (Montgomery, 2017). The method employs a multiple linear regression approach that can be used to create predictive equations for the phenomena under study.

The analysis in Phase II will show that the rim joist was the most important air leakage parameter (see Chapter 5). Hence, the laboratory-based testing Phase III was focused on isolating air leakage in through the rim joist. An improved next-generation detail was to be tested alongside the conventional rim joist detail.

3.4.1.1 *2³ Factorial Design*

A 2 level, 3 Factorial designs with 2 replicates was selected as an analysis approach. The factorial approach has the advantage of analysing the behaviour of multiple air leakage factors to be evaluated simultaneously. This experimental design gave 8 possible test configurations which form the basis of the analysis. The ordinal relationship between these test configurations can be visualised in the cube plot shown in Figure 6. The three factors selected were:

- Sheathing Membrane Type (M),
- Detail Length (L), and
- Depressurisation Pressure (P)

There were two sheathing membranes corresponding to the two levels in M. The high level was a retail available, weather resistive barrier sheet product. The low-level sheathing membrane was a commercially available self adhering weather resistant barrier. The high level represented the advanced, high performing joint detail. The low-level material was representative of the conventional, code compliant material application in current use. The factor M thus varied from -1 to +1 where -1 was assigned to the self adhering weather resistant barrier and +1 was assigned the taped and stapled sheet.

The length of the floor to wall detail was selected to be between lengths of 2380 +/- 10 mm and 1340 +/- 10 mm. These detail lengths corresponded to a test area of 1.225m² and 0.690m² respectively. The longer samples were assigned "+1" while the shorter samples were assigned a "-1" level.

The high and low depressurisation pressures for factor P were chosen to be of 75 Pa and 50 Pa. The high-pressure level +1 was assigned to 75Pa, while a low-level of -1 was assigned to 50 Pa pressure. The two pressures were chosen in order to represent the pressure range used in for

enclosure testing and window testing (ASTM, 2017b)(ASTM, 2017c). Future test protocols (outside the scope of this research) could use a low-level pressure between 5Pa and 10Pa to replicate measurements for natural air exchange rates.

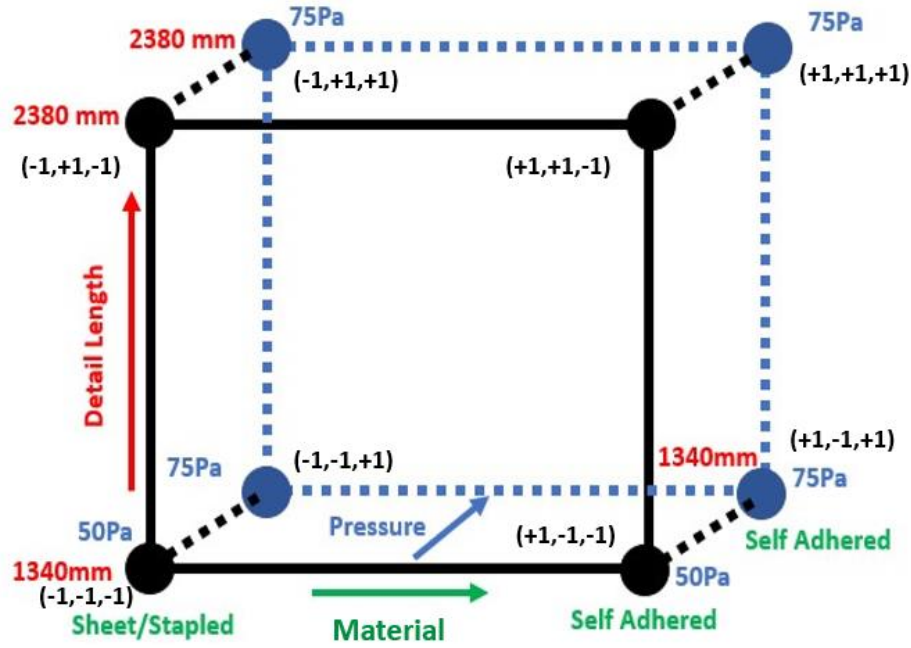


Figure 6 Cube Plot Visualisation

The general form of the equation describing air leakage through any configuration will take the form of Equation (9). The significance of the model is determined by using the t-test on the B's, R and Adj.R², ANOVA, Residual Analysis. The predictive chamber airtightness equation has B's parameters for three main effects which are B₁, B₂, B₃.

$$ACHc = B_0 + B_1 \cdot M + B_2 \cdot P + B_3 \cdot L + B_4 \cdot M \cdot P + B_5 \cdot M \cdot L + B_6 \cdot P \cdot L + B_7 \cdot M \cdot P \cdot L \quad (9)$$

There are four beta parameters that account for the interactions between the main effects. The parameters associated with interactions are B₄, B₅, B₆, and B₇. The generalised

chamber air change rate in Equation (9) reduces to Equation (10) based on significant parameters determined by the t-test. X_i represents the significant factors and interactions that influence the airtightness of the laboratory specimens.

$$ACH^C = B_0 + B_i \cdot X_i + \dots \quad (10)$$

3.4.2 Synthesis of Predictive and Reactive Predictions

The results obtained from both Phase II and Phase III could be synthesised into a single model. A predictive airtightness equation could be developed for detached, low-rise, light framed, residential homes with next generation enclosure details. The builder specific, non-temporal models shown generalised in Equation (6) could be reweighted with a factor W_i described in results from Phase III's Equation's (11) or (12). Evidently, Equation's (11) or (12) represent upper and lower bounds of the weighting factor W_i . The weighting factor W_i is ratio between the existing building detail as compared to the new detail.

$$W_i = (ACH^C_{\text{existing}} - ACH^C_{\text{proposed}}) / (ACH^C_{\text{existing}}) \quad (11)$$

$$W_i = (ACH^C_{\text{proposed}}) / (ACH^C_{\text{existing}}) \quad (12)$$

$$B^* = W_i \cdot B_i \quad (13)$$

Where ACH^C_{existing} is the test chamber air change rate for existing or conventional joint details, ACH^C_{proposed} is the test chamber air change rate for new, or proposed joint details, and B^*

is the modified parameter. One should note that the weighting factor may cause the other Beta parameters to have suboptimal values. However, the validity of the whole building airtightness model vis-à-vis in-situ construction can be assessed using the recommendation discussed in upcoming chapters. The combined reactive and predictive parts of the airtightness estimation equation would take the form of Equation (14).

$$ACH = B_{0i} + [B^*] \cdot X_1 + B_{2i}X_2 + B_{3i}X_3 + \dots \quad (14)$$

Preconstruction airtightness could be estimated using a combination of reactive (Phase II) and predictive (Phase III) approaches based on builder-specific, local, blower door testing populations in combination with laboratory-based factorial design of experiments (Figure 7).

In Summary, the design of experiments would be used to create a weighting factor W_i for the relevant wall detail under test. Existing building enclosure details could be empirically checked against novel construction based on the procedure described above. details. The variation in the performance of the two exterior wall details configurations could be captured in a weighting function. The weighting function could then be applied directly to Phase II's builder specific, whole building airtightness model.

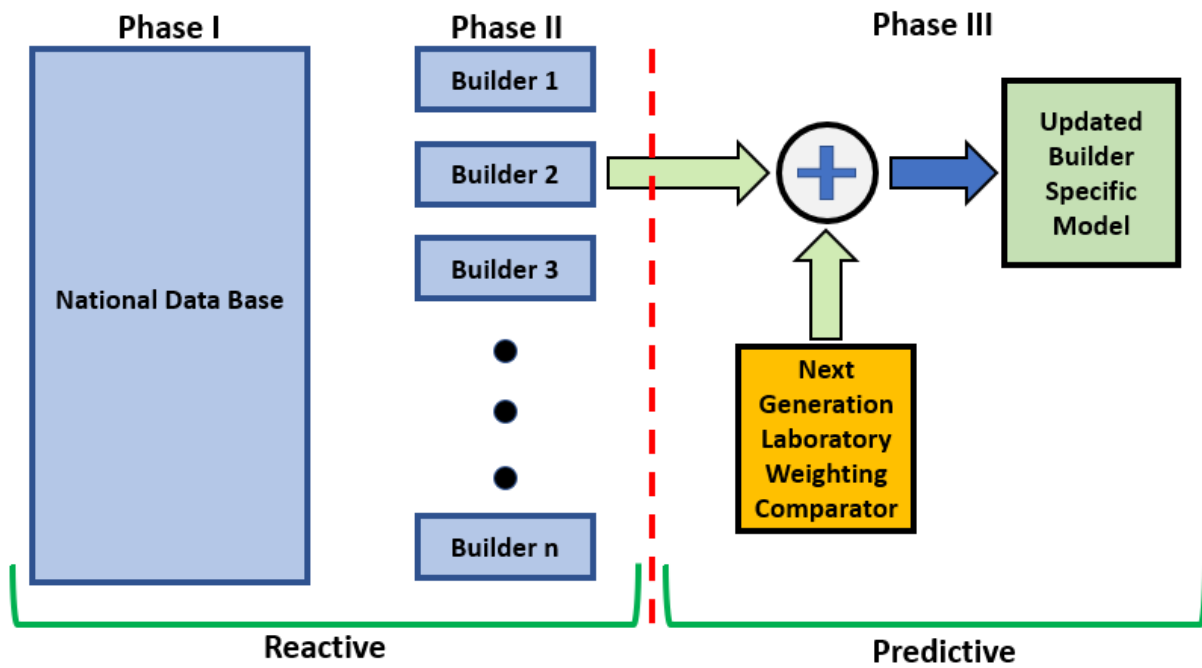


Figure 7 Representation of the Conceptual Framework

4 National Level Airtightness Predictions

4.1 Introduction

This chapter presents the development and analysis of predictive models for a national blower door testing population. The models are capable of predicting the airtightness of existing homes constructed between the late 1700's through to 2016. All homes represented detached, low rise, single family dwellings. The building types reflected pre-war, post war, and contemporary homes. As such, the housing wall type were heterogeneous, representing masonry, prefabricated systems and contemporary wood framed homes. Two air leakage metrics were used to characterise the whole building airtightness of these populations; normalised air leakage (NL), and air changes per hour ($ACH50$). Nationally representative multiple linear regression models for house populations of 900,000 and 330,000 were modeled with 3 predictor variables and 8 predictor variables respectively. Additional provincial and territorial based models were constructed and their respective predictive strengths evaluated. In addition, univariate exploratory analyses were utilised to establish temporal, geometric, and geographic trends.

4.1.1 Data, Results & Discussion

4.1.1.1 *Univariate Descriptive Statistics for 900,000 homes*

Figure 8 shows a histogram of air leakage at $ACH50$ compared to frequency which confirms a log normal distribution. The shape of the distribution, which contains nearly 900,000 homes, was expected since one tail of the distribution is constrained by zero air leakage while the other tail of the distribution can practically be several orders of magnitude larger than the restricted

tail. A geometric mean often reflects a more meaningful estimate of the sample mean as compared to the arithmetic mean due to the exponential decay of the left biased distribution. Furthermore, in contrast to normal distributions where the mean, median, and mode are identical, the geometric mean is much closer to the median. As a result of this difference of mean calculation, the geometric mean was found to be 5.7 ACH50, while the arithmetic mean was 18% greater at 6.7 ACH.

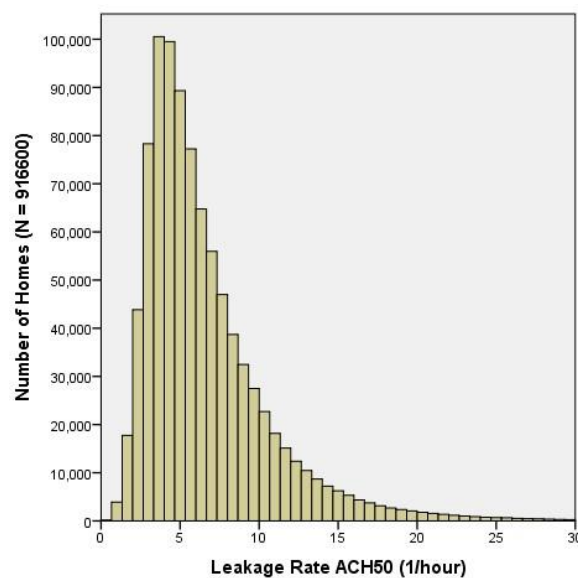


Figure 8 Air Leakage Frequency

Segregating the mean air leakage by province reveals that Nunavut, Manitoba and Saskatchewan have the lowest air leakage rates on an ACH50 basis as seen in Table 4. Note that does not display the geometric standard deviation since its units are dimensionless and thus difficult to interpret. One should also note that the sample size for Nunavut was low and could have possibly biased the mean air tightness results away from the actual population mean airtightness.

Table 4 Mean Air Leakage by Jurisdiction

Province	ACH50			N
	A. Mean	G.Mean	SD	
Alberta	5.6	4.8	3.6	100000
British Columbia	7.9	7.0	4.2	111000
Manitoba	5.2	4.3	3.6	26000
New Brunswick	6.3	5.2	4.4	45000
Nova Scotia	8.5	7.1	5.5	51000
NWT	6.3	5.3	4.1	950
Nunavut	3.9	3.4	2.3	70
Ontario	6.8	5.9	4.2	460000
PEI	6.4	6.4	4.2	4000
Quebec	5.9	5.0	3.9	114000
Saskatchewan	5.1	4.4	3.4	55000

Table 5 Mean Air Leakage by Building Height

Storeys	ACH50		
	A. Mean	G.Mean	SD
1	6.3	5.3	4.1
1.5	9.6	8.4	5.2
2	6.8	5.8	4.2
2.5	9.4	8.5	4.3
3	9.0	8.1	4.2

Table 6 Alternate Mean Air Leakage by Jurisdiction

Province	Normalised Leakage by Province			N
	A. Mean	G.Mean	SD	
Alberta	0.65	0.54	0.47	100000
British Columbia	0.96	0.83	0.55	111000
Manitoba	0.60	0.48	0.48	26000
New Brunswick	0.75	0.59	0.59	45000
Nova Scotia	1.07	0.85	0.78	51000
NWT	0.75	0.63	0.49	950
Nunavut	0.46	0.40	0.26	70
Ontario	0.84	0.71	0.56	460000
PEI	0.80	0.64	0.60	4000
Quebec	0.70	0.57	0.52	114000
Saskatchewan	0.57	0.47	0.44	55000

The arithmetic standard deviation was retained for simplicity and convenience. These lower leakage rates occur despite having some of the smallest interior volumes (Table 11). The provinces of Nova Scotia, British Columbia and PEI were shown to have the higher air leakage rates. Table 5 shows ACH50 when categorised by building height. It was found that single and two storey homes had the lowest leakage by 23%.

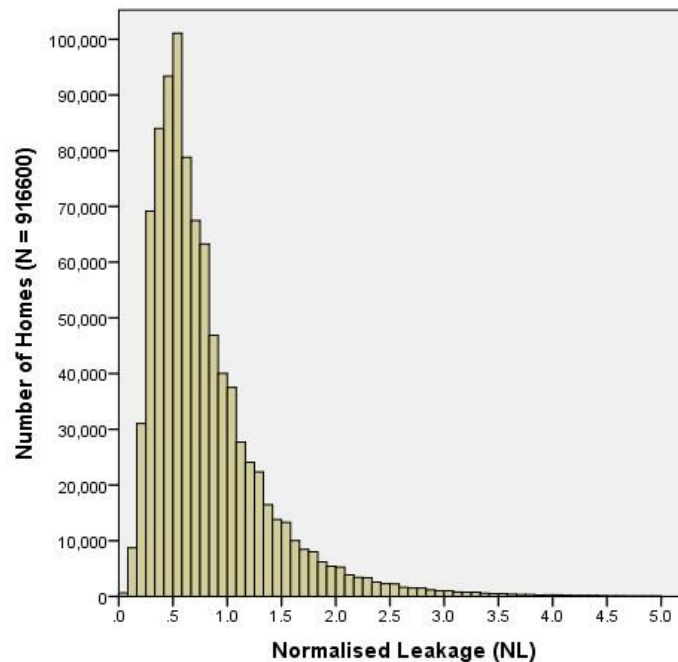


Figure 9 Alternate Mean Air Leakage Rate Frequency

The distribution of the data was generally even as evidenced by the standard deviation averaging 4.4 across all five building heights. These lower leakage rates among the single and two storey buildings may be influenced by the newness of the housing stock which was calculated to be 22 years younger than the mean housing age (Table 8). It may also be related to the reduced housing complexity of full storey buildings versus half storey and three storey buildings which likely optimise the number of leakage joints. As an alternative to air leakage on an ACH basis, Normalised Leakage was plotted for the data set to compare buildings, independent of building

height, and building volume. Not surprisingly the normalised frequency plot (Figure 9) was also log normal with a geometric mean of 0.67 and an arithmetic mean of 0.81.

Table 7 Alternate Mean Air Leakage by Province

Province	Normalised Leakage by Province			N
	A. Mean	G. Mean	SD	
Alberta	0.65	0.54	0.47	100000
British Columbia	0.96	0.83	0.55	111000
Manitoba	0.60	0.48	0.48	26000
New Brunswick	0.75	0.59	0.59	45000
Nova Scotia	1.07	0.85	0.78	51000
NWT	0.75	0.63	0.49	950
Nunavut	0.46	0.40	0.26	70
Ontario	0.84	0.71	0.56	460000
PEI	0.80	0.64	0.60	4000
Quebec	0.70	0.57	0.52	114000
Saskatchewan	0.57	0.47	0.44	55000

Table 7 shows NL for each jurisdiction. Nunavut, Saskatchewan, and Manitoba remained the provinces that produced the tightest homes based on the data set. Nova Scotia, British Columbia, and Ontario were the leakiest homes on normalised basis. It should be noted that Ontario had the largest mean house volumes. Since the NL metric factors in housing size and the relative contribution of the enclosure leakage area, then the impact of housing size on the airtightness metric was reduced. Single storey homes showed even less air permeance (Table 5) as compared to two-storey homes. Single-story buildings were 33% less leaky as compared to the two-storey mean. The relative leakiness between the single and two-storey buildings on an ACH basis was 9% (Table 8). This shows the importance of understanding which metric to use when reporting air leakage as the surface volume to shell area ratio does

change significantly across dwelling typology. The leakiest building configuration became the three- storey house (Table 6) as compared to the 2.5 storey house on the ACH basis (Table3).

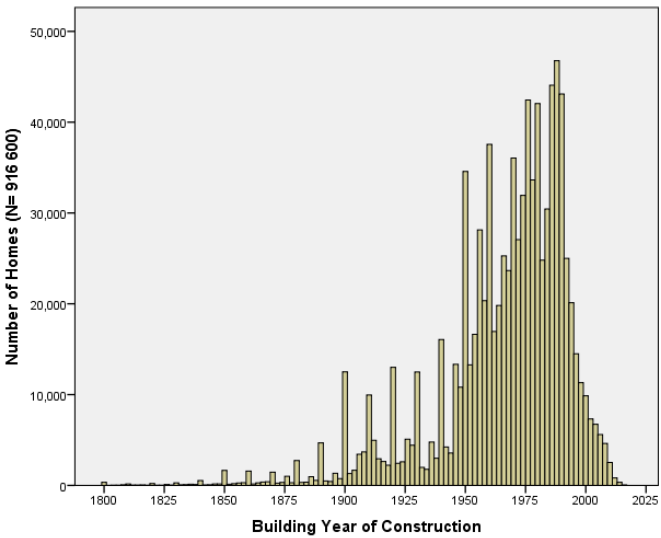


Figure 10 Frequency plot of Building Year of Construction Table

The frequency plot for the Build Year showed a marked heterogeneity (Figure 10). Upon further investigation, it was found that the frequency plot was multi modal. Meaning that plot showed a layering or superposition of many distributions. The multimodal nature of this plot reflected the change and predominance of certain housing styles within different time periods. In this case, the distribution was not log normal and the geometric and the arithmetic mean for building age was found to nearly equal at 1965. On a provincial basis Nova Scotia, Manitoba, and Prince Edward Island had the oldest building stock from the data set (

Table 8). Nunavut and the North West Territories had the newest mean building stock.

Table 8 Mean Building Year by Province

Province	Build Year			N
	A. Mean	G.Mean	SD	
Alberta	1971	1971	19	100000
British Columbia	1971	1971	21	111000
Manitoba	1957	1956	26	26000
New Brunswick	1966	1966	30	45000
Nova Scotia	1955	1955	37	51000
NWT	1981	1981	13	950
Nunavut	1990	1990	13	70
Ontario	1965	1964	29	460000
PEI	1958	1958	39	4000
Quebec	1966	1966	29	114000
Saskatchewan	1964	1964	22	55000

Table 9 shows that building typologies may have changed over time. The 1.5, 2.5 and 3 storey single family detached style homes significantly older than 1 and 2 storey buildings.

Table 9 Mean Building Year by Building Height

Storey	Build Year		
	A.Mean	G.Mean	SD
1	1969	1969	18
1.5	1939	1939	33
2	1965	1964	34
2.5	1923	1923	31
3	1923	1929	34

The mean build year as a function of air leakage rate showed newer buildings comprising the most airtight construction (Table 10). This was confirmed by other studies (Chan et al., 2013)(Hamlin & Gusdorf, 1997).

Table 10 Mean Air Leakage Compared to Mean Building Year

ACHRange	ACH50		Build Year		N
	G.Mean	SD	G.Mean	SD	
0 <ACH <1	0.8	0.1	1997	16	1071
1 <ACH <2	1.6	0.3	1991	16	20267
2 <ACH <4	3.1	0.5	1981	16	220987
4 <ACH <8	6.0	1.1	1968	23	433123
8 <ACH <16	10.4	2.1	1945	31	204947
16 <ACH <32	19.9	3.7	1932	34	31289
32 <ACH <64	37.8	5.5	1935	33	1904
64 <ACH	69.4	4.9	1948	21	6

Table 11 Mean Air Leakage Compared to Mean Building Volume

ACH Range	ACH50		Volume m ³		N
	G.Mean	SD	G.Mean	SD	
0 <ACH <1	0.8	0.1	752	811	1071
1 <ACH <2	1.6	0.3	670	374	20267
2 <ACH <4	3.1	0.5	630	277	220987
4 <ACH <8	6.0	1.1	546	220	433123
8 <ACH <16	10.4	2.1	456	187	204947
16 <ACH <32	19.9	3.7	350	153	31289
32 <ACH <64	37.8	5.5	247	118	1904
64 <ACH	69.4	4.9	177	17	6

Building volume was found to be best described as a log normal distribution. Hence as shown in Table 11, the geometric mean was determined to be a better descriptor of mean volume statistic. The standard deviation of the mean ACH50 for the tighter houses was considerably smaller (SD=0.1) than for homes in the typical range (SD = 1.1). Ontario was found to have the largest homes by volume 18% above the mean, while Nunavut and the North West Territories had the smallest home by volume at approximately 23% below the mean.

Table 12 Mean House Volume by Province

Province	Volume m ³		
	A.Mean	G.Mean	SD
Alberta	568	533	218
British Columbia	589	550	234
Manitoba	498	470	185
New Brunswick	520	488	198
Nova Scotia	502	466	203
NWT	418	376	194
Nunavut	391	374	131
Ontario	621	573	271
PEI	570	531	219
Quebec	521	492	195
Saskatchewan	489	465	162

Interestingly, the similarity in small size and building age for Nunavut and the NWT did not translate to similar air tightness values (Table 12). This may be influenced by construction technique or workmanship on proportionally small samples sizes as compared to other Canadian jurisdictions. More precisely, the probability that a few builders were overrepresented is more likely in small house sample of 70 as compared to a larger housing sample in the hundreds.

4.1.1.2 Multiple Linear Regression Models for 900,000 and 330,000 homes

It was found that Building Year was the most important predictor variable tied to building air leakage in the three-variable, 900,000 house model.

Table 13 Regression Variables for Varying Leakage Metrics

Regression Variable Correlations			
Metric	Year	Storeys	Volume
ACH	-0.500	0.086	-0.315
NL	-0.514	0.234	-0.247

Table 13 shows a summary of the regression correlation matrix to visualise the dependence of the three-variable model on airtightness. The absolute value indicates that the Build Year is the most highly correlated predictor variable followed by building volume in both the ACH and NL model.

Table 14 Comparison of Pearson's Correlation and Coefficient of Determination N=900,000

Regression & Leakage Metric		
Model	R	R ²
ACH50	0.57	0.32
NL	0.59	0.35

Not surprisingly the number of storeys has a higher correlation in the NL model since building height is directly factored in the NL equation. Furthermore, the strength of the respective ACH and NL models where compared in Table 14.

Table 15 Comparison of Pearson's Correlation and Coefficient of Determination N=330,000

Regression & Leakage Metric		
Model	R	R ²
ACH50 I	0.68	0.46
NL I	0.69	0.48

Table 16 Regression Model Strength by R and R2 per Province with Predictor Variables: Height, Volume, Age N=900,000

Multiple Linear Regression Analysis				
Province	R	R ²	N	Sig.
Alberta	0.5	0.27	49000	0.000
British Columbia	0.5	0.29	111000	0.000
Manitoba	0.7	0.46	26000	0.000
New Brunswick	0.6	0.35	45000	0.000
Nova Scotia	0.6	0.39	51000	0.000
NWT	0.6	0.35	950	0.000
Nunavut	0.7	0.43	70	0.000
Ontario	0.6	0.36	460000	0.000
PEI	0.7	0.48	4000	0.000
Quebec	0.5	0.29	114000	0.000
Saskatchewan	0.6	0.42	55000	0.000

The comparison showed a slight improvement in the coefficient of determination for the ACH50 and NL models ($R = 0.57$, $R^2=0.32$, $p<0.0001$) to the ($R = 0.59$, $R^2=0.35$, $p<0.0001$). Hence the ACH50 model explains 32% of the airtightness, while the NL model explains 35% of the airtightness variation. This also suggests that the ACH standard of airtightness can still adequately estimate and predict airtightness to within 2% of the NL method that accounts for building size. Table 15 summarises the 8-predictor variable, 330,000 home model. Here the coefficient of determination improved for both the ACH I ($R = 0.68$, $R^2=0.46$, $p <0.0001$) and NL I metrics ($R = 0.69$, $R^2=0.48$, $p<0.0001$) increasing the explanatory power of both models by approximately 14%. Hence almost half of the housing airtightness can be explained by the expanded 8 variable regression models. A regression analysis was also performed on the data for $N=900,000$ homes and grouped per province (Table 16)

Table 17 Regression Model Strength by R and R² per Province with Predictor Variables: Height, Volume, Age, Climate, Insulation (Wall, Ceiling, Foundation), Windows N=330,000

Multiple Linear Regression Analysis				
Province	R	R ²	N	Sig.
Alberta	0.6	0.31	29000	0.000
British Columbia	0.6	0.40	55500	0.000
Manitoba	0.7	0.54	21000	0.000
New Brunswick	0.7	0.48	32000	0.000
Newfoundland	0.8	0.68	50	0.000
Nova Scotia	0.6	0.40	7200	0.000
NWT	0.8	0.70	230	0.000
Nunavut	0.7	0.45	30	0.000
Ontario	0.7	0.55	165000	0.000
PEI	0.8	0.58	25	0.000
Quebec	0.7	0.49	17000	0.000
Saskatchewan	0.6	0.38	350	0.000

Due to the small p-values of $p < 0.0001$ all regression models explained between 27% to 48% of the variation within the data. Similarly, Table 17 shows the same analysis but for the more detailed data set of 330,000 homes. In this case, the Pearson's Correlation Coefficient range was higher at 0.6 to 0.8 with explanatory power ranging from 31% to 70% of the variation. A further test was performed to consider if the smaller jurisdictions with smaller sample sizes, such as NWT, Nunavut, and PEI had an increased model strength R^2 . The regression test showed that there was little to no correlation ($R^2=0.004$) between the provincial sample size as compared to the model strength. Since Build Year was the most important predictor variable, the authors investigated a temporal regression model based on Canada's building code iterations since 1939.

Table 18 Comparison of R & R^2 with respect to building code issuance dates N=900,000

Regression Analysis: Code Change Periods				
Range Year Built	R	R^2	N	Sig.
<1939	0.4	0.13	121000	0.000
1939 Year <1949	0.4	0.14	48000	0.000
1949 Year <1959	0.4	0.16	113000	0.000
1959 Year <1969	0.4	0.13	123000	0.000
1969 Year <1974	0.3	0.12	78000	0.000
1974 Year <1978	0.4	0.13	73000	0.000
1978 Year <1980	0.4	0.13	37000	0.000
1980 Year <1984	0.4	0.14	64000	0.000
1984 Year <1990	0.4	0.14	130000	0.000
1990 Year <1995	0.4	0.13	65000	0.000
1995 Year <1997	0.4	0.13	15000	0.000
1997 Year <2005	0.4	0.14	35000	0.000
2005 Year <2010	0.4	0.12	12000	0.000
2010 <Year	0.3	0.11	2000	0.000
All Years	0.6	0.35	920000	0.000

Table 18 shows the temporal regression model strength via Pearson's correlation coefficient and the coefficient of determination. The analysis showed that there were no clear discernible trends that would indicate a change in model strength vis a vis building code updates. This result was

not surprising, given that any decrease in airtightness resulting from building code changes would be indirectly related to other factors since the Canadian building code has not included building airtightness as a prescribed metric for single family dwellings. However, it is significant that the majority of homes in this data set belong to the pre-1980 era (65% of tested homes). A similar analysis was performed with the subset data of 330,000 homes. Table 19 shows the temporal regression model strength via Pearson's correlation coefficient, and the coefficient of determination. Again, these time frames represent official changes to Canada's Model National Building code. And as before, there are no clear discernible trends that would indicate a change in model strength vis a vis building code updates.

Table 19 Comparison of R & R² with respect to building code issuance dates N=330,000

Regression Analysis: Code Change Periods				
Range Year Built	R	R ²	N	Sig.
<1939	0.4	0.23	51000	0.000
1939 Year <1949	0.5	0.27	20000	0.000
1949 Year <1959	0.5	0.32	47000	0.000
1959 Year <1969	0.6	0.39	48000	0.000
1969 Year <1974	0.6	0.38	28000	0.000
1974 Year <1978	0.7	0.43	25000	0.000
1978 Year <1980	0.7	0.45	14000	0.000
1980 Year <1984	0.7	0.43	23000	0.000
1984 Year <1990	0.7	0.43	38000	0.000
1990 Year <1995	0.6	0.39	21000	0.000
1995 Year <1997	0.6	0.37	4000	0.000
1997 Year <2005	0.6	0.40	9000	0.000
2005 Year <2010	0.7	0.43	2000	0.000
2010 <Year	0.6	0.35	100	0.000
All Years	0.7	0.48	330000	0.000

Table 20 shows three parameter multiple linear regression model based on air changes per hour. The three-variable model was based upon a sample of over 900,000 individual homes. The predictive variables of volume, building height, and building year were included. Building

volume had its associated coefficient as -0.005. Building height, represented by storeys had the coefficient +1.048. Lastly the build year had a coefficient determined to be -0.065. The lower bound and upper bound confidence intervals were nearly equal due to the very large t-statistic values. All coefficients were found to be extremely significant ($p < 0.0001$).

The resultant model for this regression is shown in Equation 2. Hence both house volume, and build year were negatively correlated with air leakage while building height, and positively correlated to building air leakage.

Table 20 Linear Regression Coefficients 95% CI, N=900,000

Parameter			t	Sig.		
	B	SE			LB 95% C.I.	UB 95% C.I.
(Constant)	135.304	0.267	507.076	0.000	135.827	135.827
Volume	-0.005	0.000	-305.305	0.000	-0.005	-0.005
Year	-0.065	0.000	-478.159	0.000	-0.065	-0.065
Storeys	1.048	0.008	136.366	0.000	1.033	1.063

Table 21 Linear Regression Coefficients 95% CI, N=330,000

Parameter			t	Sig.		
	B	SE			LB 95% C.I.	UB 95% C.I.
(Constant)	126.649	0.670	189.160	0.000	125.337	127.961
Ceiling RSI	-0.288	0.004	-71.794	0.000	-0.296	-0.280
HDD	-0.001	0.000	-154.439	0.000	-0.001	-0.001
Foundation RSI	-0.218	0.028	-7.748	0.000	-0.273	-0.163
Volume	-0.005	0.000	-190.324	0.000	-0.005	-0.005
Wall RSI	-0.400	0.012	-34.167	0.000	-0.423	-0.377
Storeys	0.939	0.010	90.253	0.000	0.918	0.959
Window RSI	-3.264	0.071	-45.740	0.000	-3.404	-3.124
Year	-0.057	0.000	-162.389	0.000	-0.057	-0.056

Similarly, Table 21, shows the regression coefficients for the population subset of 330,000 homes with eight predictor variables. The nominal value of the regression coefficients for building volume, building year and height were in close agreement with the previous 3 predictor

variable model. Additionally, the student-t test found that all coefficients were found to be extremely significant ($p < 0.0001$).

$$ACH = 135.304 - 0.005(\text{Volume}) + 1.048(\text{Storeys}) - 0.065(\text{Year}) \quad (15)$$

$$\begin{aligned} ACH = & 126.649 - 0.005(\text{Volume}) + 0.939(\text{Height}) \\ & - 0.057(\text{Year}) - 0.001(\text{HDD}) - 0.288(\text{Ceiling})RSI \\ & - 0.218(\text{Foundation})RSI - 3.264(\text{Window})RSI - 0.400(\text{Wall})RSI \end{aligned} \quad (16)$$

The additional predictor variables due to climate (*HDD*) and enclosure insulation were also negatively correlated to building air leakage. More precisely, a colder climate building location coupled with an increase in building enclosure insulation showed a decrease in air leakage. Based on Equations 3, and 4 one can predict the air leakage in the existing Canadian detached single-family home building stock with the knowledge of the building volume, building height, year of construction, the buildings local heating degree days, and the insulation values for the ceiling, foundation, windows, and walls. The 3-variable *ACH* model yielded a moderate strength equation which explained a 32% of the variation in air leakage ($R = 0.57$, $R^2 = 0.32$, $p < 0.0001$). The 3-variable *NL* also yielded a moderate strength predictor equation ($R = 0.59$, $R^2 = 0.35$, $p < 0.0001$) explaining 35% of the variation in the data. The 8-variable model showed a marked improvement in model strength and in explanatory power in contrast to the 3-variable models. The model strength for both the 8-variable *ACH* I ($R = 0.68$ $R^2 = 0.46$, $p < 0.0001$) and *NL* I ($R = 0.69$ $R^2 = 0.48$, $p < 0.0001$) regression equations was moderate to strong predicting nearly half for the airtightness variation.

Airtightness results for nearly 900,000 single family Canadian homes were analysed from both a univariate and multiple linear regression approach. The univariate analysis utilised three predictor variables, namely: building age, building height and building volume. These three variables were analysed in conjunction with a single airtightness response variable at a time, be it, in Air Changes per Hour at 50 Pa, or in Normalised Leakage at 50 Pa. Previous studies have shown that building age was an important predictor of airtightness. This relationship between age and airtightness has been supported by Chan et al (Chan et al., 2013), Sfakianaki et al (Sfakianaki et al., 2008), and Bramiana (Bramiana et al., 2016). This study has also confirmed the importance of building age as a prominent predictor variable (Table 10 & Table 13) at the national level. The general relationship has been that older homes have a lower airtightness as compared to more recently built homes. However, this study has also shown that this general trend can differ at the regional level. For instance, Manitoba and Saskatchewan registered among the oldest built (Table 8) Canadian homes, yet these provinces had among the lowest air leakage rates (Table 4). Building height was also analysed from a univariate perspective. In this instance, 1 storey and 2 storey buildings were the most airtight (Table 5). Further investigation showed that 1 and 2 storey homes were most recently built as compared to 1.5, 2.5 and 3 storey homes which were on average 24.5 years older when compared as a group. This difference in air leakage rates may also be an artifact related to the building enclosure complexity in older 1.5 storey, 2.5 storey and 3 storey homes. The largest homes unsurprisingly had the lowest air leakage rates as measured by ACH50 due to this metric being a volume-based unit. However, Table 10 also showed the homes with the lowest air leakage rates demonstrated the greatest variability in volumetric size as evidenced by volumetric standard deviation. This suggests an alternative driver

such as building age or location influences airtightness. The variability in dispersion with regard to ACH50 is also noteworthy.

The standard deviation increased by an order of magnitude, for homes below 1 ACH50, compared to homes between $4 < \text{ACH50} < 8$. At a sampling population level, airtight homes below 2 ACH50 only represent approximately 2.5% of the tested homes. While 72% of the homes tested had an air tightness level ranging from 4 ACH50 to 16 ACH50. In addition, the housing data did reveal a strong regional component, where larger building volumes did not necessarily contribute to increased airtightness at the regional level. In fact, Saskatchewan and Manitoba possessed the smallest mean housing volumes (Table 12) yet they were shown to be among the most airtight homes (Table 4). The authors speculate that the marked regional heterogeneity highlighted in univariate analyses may be an indication of the differences in construction quality, enclosure detail complexity, and possibly a variation in climate-based architectural vernacular present across the Canadian landscape. Regardless of the accuracy of these suggestions, the regression analysis shows that regional differences exist and should be studied further. As a second step in the analysis, multiple linear regression was conducted on a nationally representative sample of 900,000.

Following this analysis, a subset of nearly 330,000 homes were selected for an increasingly detailed study. Three predictor variables were used for the 900,000 tested homes, while eight predictor variables were used for the 330,000 subsets of homes. Regression equations and prediction strength were calculated for a single response variable, be it either NL or ACH. Furthermore, additional analyses were performed on a regional basis, representing 11 of the 13 territories and provinces throughout the country. The provincial and territorial based regression

models (Table 16 & Table 17) developed in this study were shown to either be equal to, or stronger in both explanatory powers, and in predictive model strength as compared to earlier studies [11] [12] [13]. The range in the explanatory power of the provincially and territorially based airtightness models spanned from 54% to 70% ($0.54 < R^2 < 0.70$). The results from this study were the most consistent with both Hamlin et al.'s (Hamlin & Gusdorf, 1997) Canadian study and Chan et al.'s (Chan et al., 2013) United States study. Both Chan et al.'s study and this investigation predicted a mean normalised air leakage of 0.67 across each respective population. The strength of the Chan et al.'s investigation was stronger with $R^2 = 0.68$ as compared to this investigation ($R^2 = 0.46$). However, Chan et al.'s study considered design peculiarities not common in the Canadian context. Furthermore, this study as compared to Hamlin et al.'s (Hamlin & Gusdorf, 1997) smaller Canadian study had found that Prairie provinces had the tighter houses. However, there was less agreement on which houses were the least airtight. Since building age was seen to be the most influential predictor variable, it will be necessary to examine what possible independent factors associated with building age can be isolated explicitly for analysis. This investigation (Khemet & Richman, 2018) and previous studies suggest that building age may be a proxy for specific and measurable building details and building handcraft.

There was a limitation related to data collection that could further clarify the resulting strength of interpretation of the national airtightness models. The variance of the air leakage output variable, ACH50, was not formally determined based on the method of collection from third party collection methods. The variance could only be indirectly inferred from the airtightness test method standard, and not directly ascertained.

The results of this Phase are compared and summarised in Table 22. Phase I results from this study represents, to the best of the authors knowledge, the largest multiple linear regression airtightness analysis on Canadian data for the purposes of airtightness modeling. The resulting national and provincially regression analyses may serve as a lower bound for the future regression analysis in a Canadian context.

Table 22 Comparison of Phase I Model with Existing Literature

Jurisdiction	R ²	Parameters	N	Description
United States (2005)	0.56 ^{a,b}	4	70 000	Heterogeneous Typology Heterogeneous Assembly
Greece (2006)	0.56, 0.93 ^a	1	20	Homogeneous Typology
Spain & France (2009)	0.94 ^{a,b}	2	483	Homogeneous Typology Heterogeneous Assembly
United Kingdom (2010)	0.49	7 – 6	287	Heterogeneous Typology Heterogeneous Assembly
United States (2013)	0.68 ^{a,b}	12	134 000	Homogeneous Typology Heterogeneous Assembly
Netherlands (2016)	0.43 ^b	5	320	Heterogeneous Typology Heterogeneous Assembly
Canada (2018) (Phase I)	0.48 ^b	8 – 3	900,000	Homogeneous Typology Homogeneous Assembly
Notes:				
a. airtightness level known <i>a priori</i>				
b. year of construction used as predictor				

4.2 Summary

Univariate and multiple linear regression analyses were performed on blower door testing data for detached single family homes throughout Canada. Three variable airtightness estimation models were produced for a testing population of 900,000 homes. Building height, building volume and year of construction were found to be significant predictor variables. Normalised Leakage and Air Changes per Hour models were found to account for 35% ($R^2=0.35$, p-value

<0.0001) to 32% ($R^2=0.32$, p-value < 0.0001) of the whole building air leakage estimate respectively. The explanatory power of the 3 and 8 variable models in Phase I were used as a minimum for subsequent models. Eight variable airtightness estimation models were produced for 330,000 homes. Foundation wall insulation, above grade wall insulation, effective window insulation, ceiling insulation, climate, in addition to building height, building volume and year of construction were found to be significant predictor variables. Insulation levels were included to serve as a possible proxy to handicraft associated with regional construction practices. The 8-variable Normalised Leakage and Air Changes per Hour models were found to be stronger than the 3 variable models. Normalised leakage accounted for 48% ($R^2= 0.48$, p-value < 0.0001) of the whole building airtightness estimate. The Air Change per Hour model accounted for 46% ($R^2=0.46$, p-value < 0.0001) of the whole building airtightness estimate. All models were constrained to predict air leakage rates for existing buildings. The three variable models would be used as a lower bound for airtightness estimation for Phase II.

5 Local Airtightness Predictions

5.1 Introduction

This chapter pertains to Phase II of the airtightness estimation approach. Predictive models for a local blower door testing population are presented here. As highlighted in Chapter 4, studies thus far have relied upon predictor variables that include the year of construction as a central prediction parameter. Moreover, previous studies have also included heterogeneous wall construction type, climate zone, and *a priori* knowledge of the buildings' general airtightness levels. This phase of the research builds on current research by eliminating these traditional strong variables (i.e. build year, wall construction type) and develops strong predictor models using traditionally less strong variables. The results presented in this Chapter illustrate a methodology developed as part of this research through which designers could predict airtightness in light-framed, single-family homes at the preconstruction phase.

Two air leakage metrics were used to characterise the whole building airtightness of these populations; normalised air leakage (*NL*), and air changes per hour (*ACH50*). A local sample of 2297 homes constructed approximately between 2013 and 2017 were examined. A further subset of 272 homes with 54 building layouts from a total of four builders was utilised to create predictive models. Univariate exploratory analyses were conducted. A total of six models were developed; four models were builder specific formulations, with two additional models amalgamating the builder specific models to track quality and handicraft. The blower door testing data was synthesised with detailed geometrical data to create several airtightness models. Air leakage predictions in this phase of the research were found to either match or exceed previous multiple linear regression models without relying upon the year of construction,

heterogeneous wall assemblies, heterogeneous housing typologies, or climate zone, thus showing the capability to forecast preconstruction airtightness in conventional constructed homes on a regional or per-builder basis.

5.1.1 Univariate Exploratory Analyses

A univariate analysis of a local blower door testing population was performed on approximately 3000 homes in southern Ontario. The distribution of the airtightness records was found to be log-normal as evidenced by the mean airtightness frequency plot shown in Figure 11. The log-normal distribution was consistent with the findings in both the original research and the cited literature discussed in Phase I. The mean airtightness was found to be 2.17 ACH50 with a standard deviation of 0.50. This average level of airtightness is below the voluntary OBC target of 2.5 ACH50. The higher level of performance may be indicative of the performance standards that these builders were attempting to achieve, namely Energuide and Energy Star rating systems.

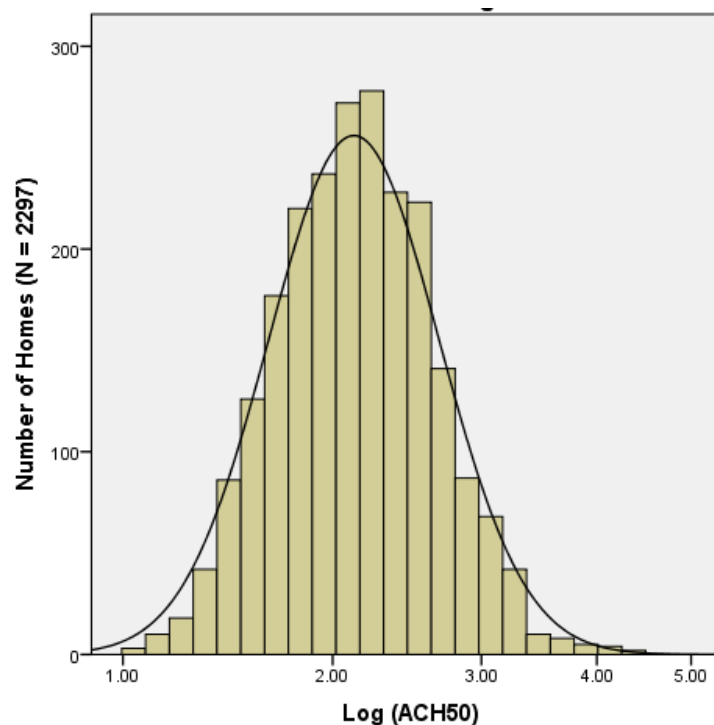


Figure 11 Airtightness Frequency Plot of a Local Blower Door Sample Population

The blower door testing population was further divided into subgroups as shown in Figure 12 . The first subgroup consisted of a non-random population of 272 homes. These homes were selected based on the availability of building geometry. A second subgroup consisted of a mutually independent random sample of the remaining tested homes.

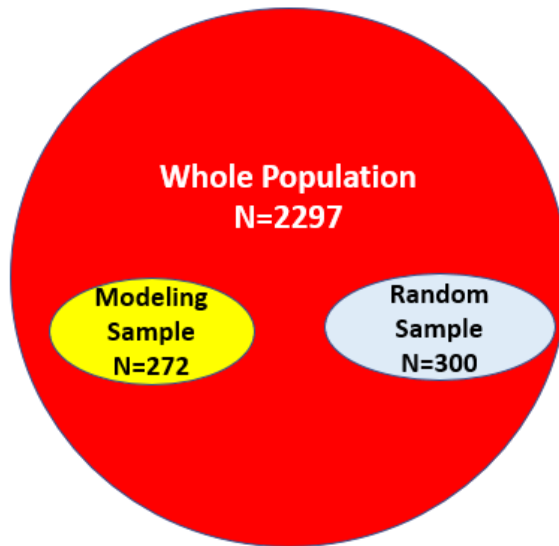


Figure 12 Representation of Population Samples

The descriptive statistics for each group are shown in

Table 23. From inspection, the arithmetic mean, sample standard deviations, and standard errors of the means for both the modelling and random sample seem comparable. The random subsample of 300 airtightness records was selected to determine whether or not the modelling population was representative of the 2297 homes. An independent t-test was conducted to determine any difference or similarity between the two sub groups. The independent t-test includes an F-test. F-tests with p-values > 0.05 would imply equal variances between the

modeling and the random samples. T-tests with a p-values>0.05 would imply that the means were equal between the random sample and the modeling sample.

Table 23 Descriptive Statistics for Population Types

	Population Type		
	Modelling	Random	Whole
Mean ACH	2.44	2.27	2.17
SD	0.52	0.56	0.50
SE	0.03	0.03	0.01
N	272	300	2296

The tests were inconclusive. The t-test statistics was $t = -3.78$, and $p\text{-value} < 0.01$ and indicated that the means between the two subgroups were different. In contrast, the F-test with statistic $F < 0.00$ with $p\text{-value} = 0.99$ indicated equal variance. To provide further resolution the effect size between the Modeling sample and the Random sample was conducted. In contrast to the p-value, the effect sizes have been recognised as an important method to determine the magnitude in the difference between two populations. The effect size has been used to provide interpretation between practical significance and statistical significance (Cohen, 1990). The Cohen's d method estimates the distance between means of two respective populations. As shown in Table 24, Effect sizes near 0.2 are considered small or trivial. Values near or above 0.5 are typically interpreted as significant. Effect Sizes larger than 0.8 are considered large and thus imply important differences between populations (Sullivan & Feinn, 2012). The effect size between the non-random Modelling sample of 272 homes as compared to the random sample of 300 was found to be $d = 0.3$. This implies that the difference between the sample populations were small, or that the populations were somewhat similar. Therefore, the non-random sample of 272 homes were somewhat similar to the whole population of 2297 homes.

Table 24 Effect Size Interpretation (Cohen's d)

Effect Size (d)	Interpretation
0.2	<i>small</i>
0.5	<i>medium</i>
0.8	<i>large</i>

A mean airtightness frequency plot the Modelling sample is shown in Figure 13. The modeling samples means were further categorised by builder. The mean ACH50 for individual builders is shown graphically in Figure 14, and in tabular form in Table 25. The means, medians and geometric means are similar in value indicating the distributions are symmetric as compared to airtightness distributions in Phase I.

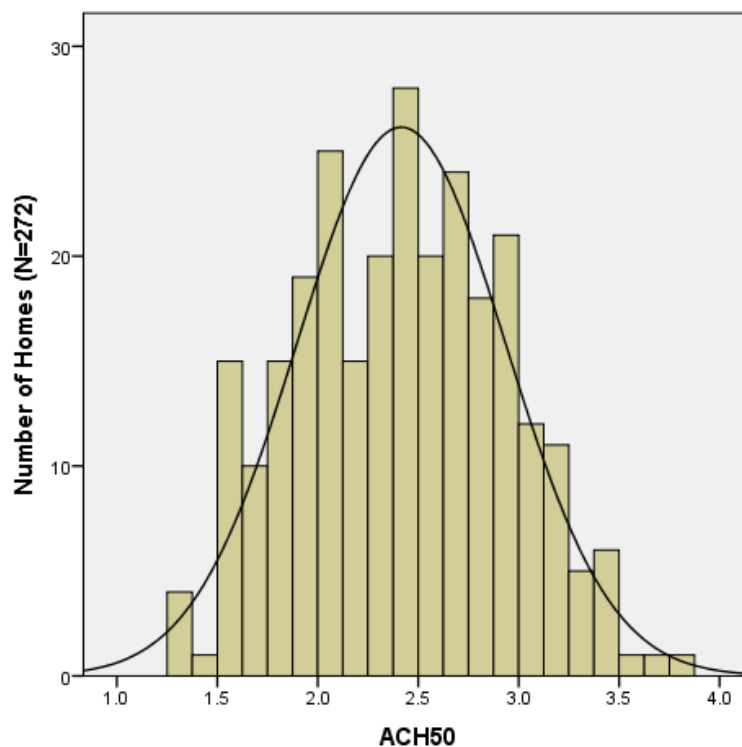


Figure 13 ACH50 Frequency Distribution for 272 Modeled Homes

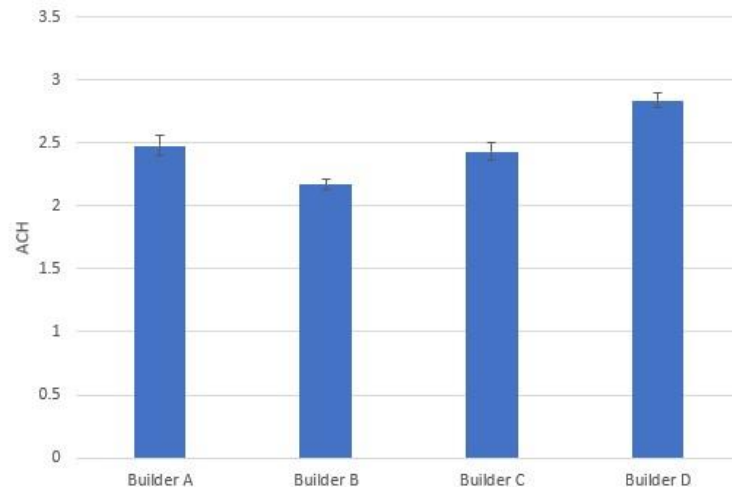


Figure 14 Mean ACH50 by Builder (N=272)

Table 25 ACH50 Descriptive Statistics per Builder (N=272)

	Mean	Median	G.Mean	SE
Builder A	2.49	2.54	2.43	0.08
Builder B	2.18	2.17	2.13	0.04
Builder C	2.44	2.43	2.41	0.07
Builder D	2.84	2.83	2.81	0.05
All Builders	2.42	2.41	2.36	0.03

The mean air leakage rates for Builder A, B, C, D, were, 2.49, 2.18, 2.44, and 2.84, respectively.

The mean airtightness between each builder appear to be similar. An ANOVA was performed to identify any differences in the means of these four builder subpopulations. Table 26 showed the ANOVA based on builder groups. The null hypothesis for this test was that all the mean ACH50 between builders are the same. The alternative hypothesis was that at least one mean is different. The test significance level was set to $\alpha = 0.05$, which satisfied the criteria of being both statistically and practically significant. Therefore, the analysis showed that the at least one of the groups of builders had a significantly different mean.

Table 26 ANOVA, ACH between and Within Builders (N=272)

ACH Builders	SS	DF	MS	F	Sig.
Between Groups	19.052	3	6.351	31.576	0.000
Within Groups	53.900	268	0.201		
Total	72.952	271			

Table 27 Difference of Means Bonferroni Method (N=272)

Bonferroni	Dependent variable: ACH	95% CI				
(i) BuilderID	(j) BuilderID	Mean Diff. (i - j)	SE	Sig.	LB	UB
A	B	0.309	0.076	0.000	0.108	0.510
	C	0.050	0.105	1.000	-0.230	0.330
	D	-0.351	0.086	0.000	-0.578	-0.123
B	A	-0.309	0.076	0.000	-0.510	-0.108
	C	-0.260	0.092	0.032	-0.504	-0.014
	D	0.660	0.068	0.000	-0.841	-0.478
C	A	0.050	0.105	1.000	-0.330	0.230
	B	0.259	0.092	0.032	0.014	0.504
	D	-0.401	0.100	0.001	-0.668	-0.134
D	A	0.351	0.086	0.000	0.123	0.578
	B	0.650	0.068	0.000	0.478	0.841
	C	0.401	0.100	0.001	0.134	0.668

Table 28 Difference of Means Least Significant Difference (LSD) (N=272)

LSD	Dependent Variable	ACH50			95% CI	
(i) BuilderID	(j) BuilderID	Mean Diff. (i - j)	SE	Sig.	LB	UB
A	B	0.309	0.757	0.000	0.160	0.457
	C	0.050	0.105	0.636	-0.160	0.258
	D	-0.351	0.086	0.000	-0.519	-0.182
B	A	-0.309	0.076	0.000	-0.458	-0.160
	C	-0.259	0.092	0.005	-0.440	-0.078
	D	-0.660	0.068	0.000	-0.794	-0.525
C	A	-0.050	0.105	0.636	-0.258	0.158
	B	0.259	0.092	0.005	0.078	0.440
	D	-0.401	0.100	0.000	-0.589	0.203
D	A	0.351	0.086	0.000	0.182	0.519
	B	0.660	0.068	0.000	0.525	0.794
	C	0.401	0.100	0.000	0.203	0.589

However, the test was not able to distinguish which builders had a different mean airtightness. Both the Bonferroni and the Least Significant Difference method were used to identify which builders had different means. Table 27 shows the Bonferroni method of determining if there is a difference in means between any of the group combinations. The test showed that Builder A and Builder C had the same means while every other combination of means were different. Or more precisely, Builder A mean ACH50 is different from Builder B's ACH50, and Builder A's mean ACH50 is different from Builder D's ACH50. The Bonferroni method can be seen as overly restrictive and conservative since its' confidence intervals are shorter. The Least Significant Difference (LSD) method was used and the results can be seen in Table 28. Both the Bonferroni and the LSD method showed that Builders A and Builders C have the same mean ACH50, while other means were different. Further analysis was performed to determine the magnitude of the airtightness differences between these four groups of builders. The effect size for each builder combination was calculated and shown in Table 29. The Cohens' d for Builders' A and Builder C was $d=0.1$, which indicated a negligible difference between the two populations. The similarities between builders A and B were consistent with the conclusions arising from both Bonferroni and LSD methods. The other comparisons showed medium differences such as Builders A&B, B&C ($d=0.7$, $d=0.6$) or large differences in remaining combinations (A & D, $d= 0.8$; B & D, $d =1.5$; C & D, $d=1.1$).

Table 29 Effect Sizes Between Builders (Cohen's d Method)

Effect Size (d)					
A vs B	A vs C	A vs D	B vs C	B vs D	C vs D
0.7	0.1	0.8	0.6	1.5	1.1

A univariate analysis was performed on each predictor variable. Table 30 shows how the 20 selected variables relate linearly with ACH. Above Grade Height, Total Height, were positively correlated to ACH50 at 0.319 and 0.532, respectively. The Exposed Floor Area had an equally negative correlation of -0.304. The newly devised area-based ratios of Ceiling Area to Wall Ratio, and Exposed Floor Area were found to be positively correlated with 0.310 and 0.392, respectively. The only discrete predictor variable, Building Identification, was also positively correlated with an $R = 0.380$.

Table 30 Univariate Analysis of ACH Compared to Predictor Variables

Predictor Variable	R	Sig.
AGradeH	0.319	0.000
TotalH	0.352	0.000
RJoistL	0.122	0.044
RJoistA	-0.039	0.521
Volume	0.168	0.005
ShellA	0.188	0.002
ExFloorA	-0.304	0.000
FloorA	0.141	0.020
CeilingA	0.040	0.507
DoorP	0.226	0.000
WindowP	0.236	0.000
DoorA	0.064	0.293
WindowA	0.113	0.062
FWR	-0.078	0.199
PerimR	-0.022	0.724
RJoistR	0.136	0.025
CWR	0.31	0.000
FenPerimHR	0.181	0.003
ExCondFAR	0.392	0.000
BuilderID	0.380	0.000

5.1.2 Builder Specific, Geometry Based Multiple Linear Regression Analyses

The results for the predictive multiple linear regression models are presented here. The next four builder specific models are exclusively geometric in nature. The steps to develop the models are in accordance with Chapter 3 discussed above.

Table 31 Builder A Regression Model

Model	R	R ²	Adj.R ²	SE
Builder A	0.734	0.539	0.508	0.373

Table 31 shows the results of linear regression using Builder A's pressurisation data set which contained 48 houses. Pearson's correlation coefficient was strong with $R = 0.734$ with an R^2 of 0.539. The adjusted R^2 showed that this model explains approximately 51% of the variation. Table 32 shows the analysis of variance for Builder A. The F test revealed a value of $F=17.2$ which is extremely significant with $p < 0.001$.

Table 32 ANOVA Builder A

Builder A	SS	DF	MS	F	Sig.
Regression	7.176	3	2.392	17.2	0.000
Residual	6.134	44	0.139		
Total	13.309	47			

Table 33 Builder A Regression Model Parameters

Predictors	B	SE	t	Sig.	LB 95.0% CI	UB 95.0% CI	VIF
(Constant)	18.465	4.218	4.38	0.0001	9.964	26.967	
Volume	0.001	0.000	2.86	0.0064	0.000	0.002	3.5
RJoistR	-0.178	0.048	-3.74	0.0005	-0.274	-0.082	2.9
FenPerimHR	-0.068	0.022	-3.09	0.0034	-0.113	-0.024	4.3

The parameters for the regression predictor variables for Builder A are shown in Table 33. Only three out of the original 20 parameters were shown to be significant for Builder A's airtightness model. These significant parameters were building volume, the joist ratio and the fenestration to perimeter height ratio. The significance of each of the corresponding parameters were found using the student-t test with p-values < 0.01. The measure of multicollinearity was quantified by the variance inflation factor. The predictor variable variance inflation factors were well below the threshold value of 10 identified in the methodology. VIF were less than 5 for all three parameters indicating a relative independence between each predictor.

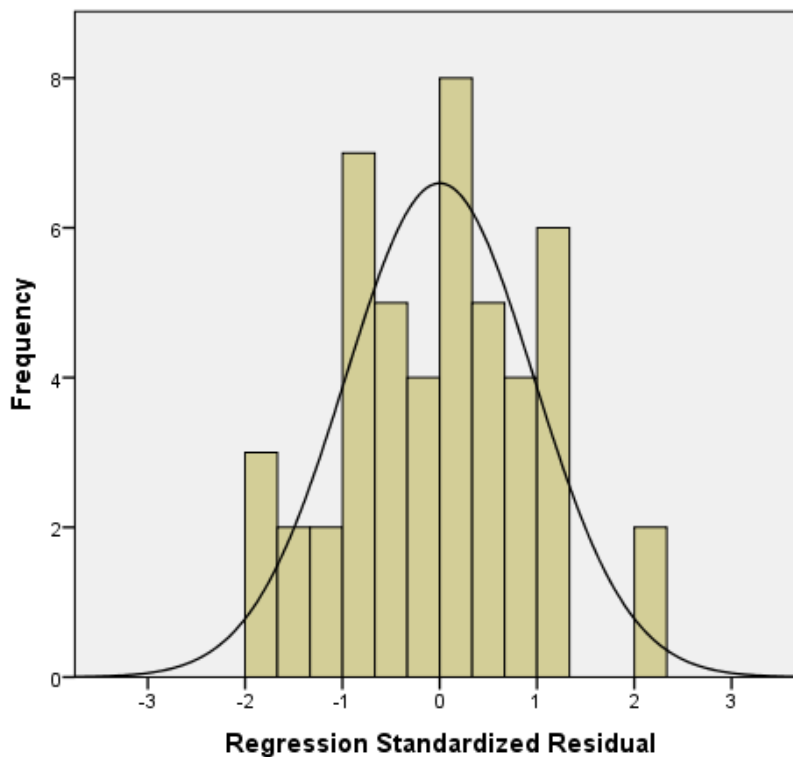


Figure 15 Builder A Standardised Residual Frequency Plot

The mean and standard deviation for the regression standardised residuals for Builder A were calculated. The frequency distribution of the regression standardised residuals is shown in Figure 15. The mean was

found to be $\mu < 0.000$ and the regression standardised standard deviations was nearly unity with $SD = 0.945$ indicating a normal distribution of the modeling error. The probability-probability plot of the expected standardised cumulative probability against the observed and standardised cumulative probability seem to indicate the same measure of normality as shown in Figure 16.

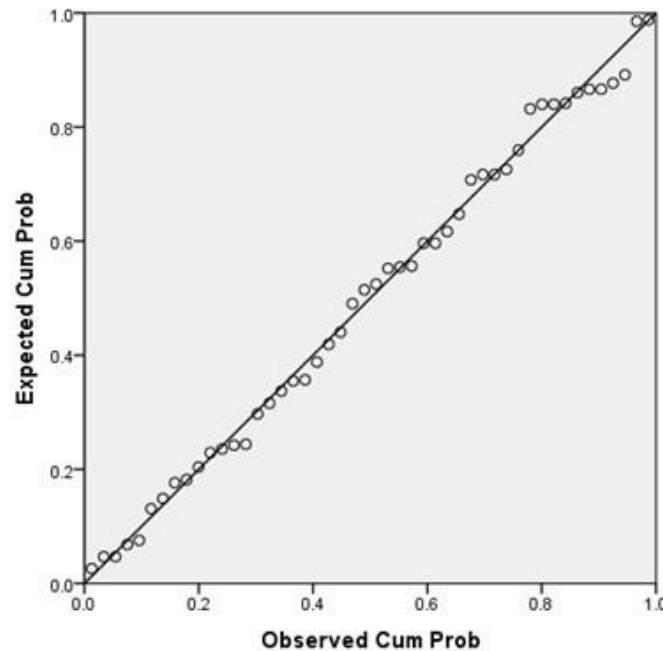


Figure 16 Builder A Standardised Residuals Probability-Probability Plot

Table 34 Builder B Regression Model

Model	R	R ²	Adj R ²	SE
Builder B	0.602	0.363	0.348	0.373

131 homes were used to represent Builder B's blower door testing population. Pearson's correlation coefficient of $R = 0.602$ was moderate for Builder B's predictive model. The adjusted R^2 suggested that the model explained 35% of the variation. Table 35 showed the analysis of variance for Builder B. The F test revealed a value of $F = 24.0$, hence a predictive model which was extremely significant with $p\text{-value} < 0.001$.

Table 35 for Builder B ANOVA

Builder B	B	DF	MS	F	Sig.
Regression	10.07	3	3.36	24.11	0.000000
Residual	17.69	127	0.14		
Total	27.76	130			

Table 36 Builder B Regression Model Parameters

Predictors	B	SE	t	Sig.	LB 95.0% CI	UB 95.0% CI	VIF
(Constant)	3.460	1.37	2.526	0.0128	0.749	6.171	
FenPerimHR	0.027	0.007	3.898	0.0002	0.013	0.041	1.6
CWR	1.526	0.183	8.357	0.0000	1.164	1.887	1.9
AGH	-0.942	0.280	-3.369	0.0010	-1.496	-0.389	1.2

Builders B's predictor variables were different as compared to Builder A. Both the joist, and fenestration were implicated, however the ceiling detail was found to be important as well. All the parameters were found to be extremely significant with p values < 0.0001. The multiple collinearity was found to be low with the VIF < 2.

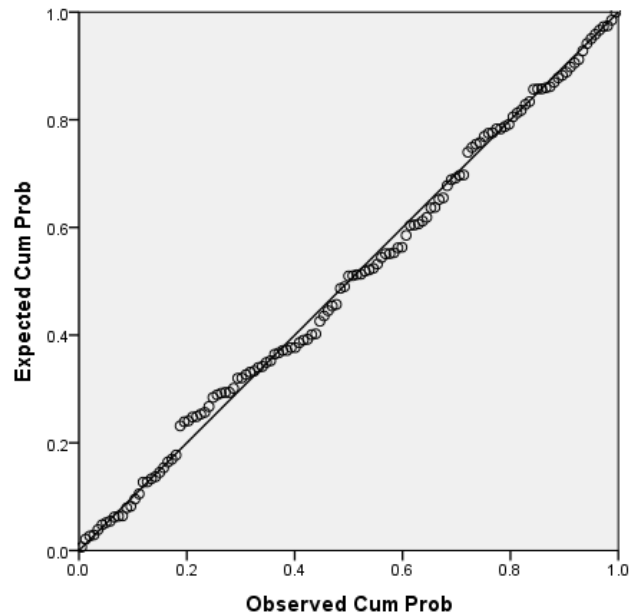


Figure 17 Builder B Standardised Residual Probability-Probability Plot

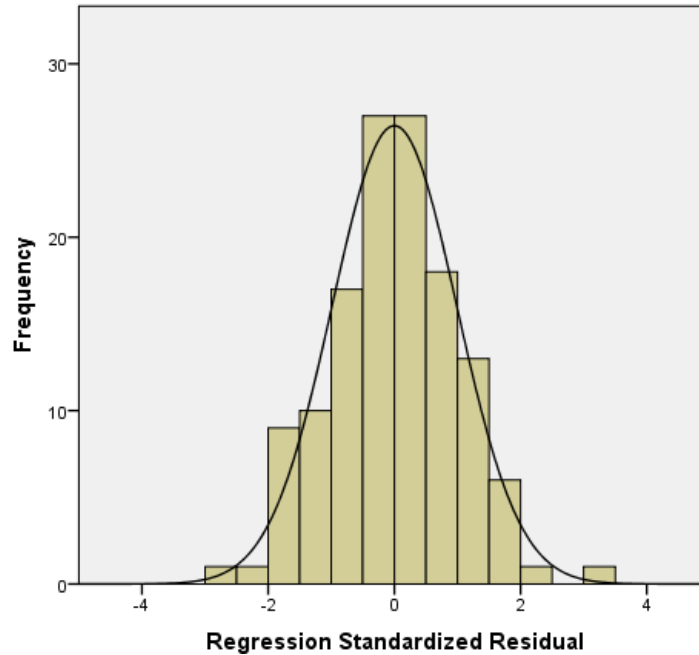


Figure 18 Builder B Standardised Residual Frequency Plot

The normality Builder B's residuals was confirmed with the Probability-Probability plot in Figure 17 and the frequency plot of the regression standardised residuals in Figure 18. The standardised residuals were also found to distribute normally with $\mu = 0.000$ and $SD = 0.988$. Furthermore, although the explanatory power for Builder B was weaker than Builder A's model, the overall model significance was still high.

Table 37 Builder C Regression Model

Model	R	R ²	Adj R ²	SE
Builder C	0.793	0.628	0.584	0.256

Table 37 shows the multiple linear regression for Builder C which contained a data set of 29 homes. Pearson's Correlation coefficient was found to be strong with $R = 0.752$ and an adjusted R^2 suggesting that the regression model explains more than half of the air leakage ($R^2=53\%$, $p\text{-value}<0.001$).

Table 38 Builder C ANOVA

Builder C	SS	DF	MS	F	Sig.
Regression	2.778	3	0.926	14.08	0.00001
Residual	1.644	25	0.066		
Total	4.422	28			

The model's ANOVA shown in Table 38 was found to be extremely significant with $F = 16.9$ yielding a $p < 0.0001$. The regression parameters for Building C model were all found to be extremely significant with $p < 0.0001$. The parameters were also found to have a low multicollinearity with $VIF < 5$ for the joist length, building height, and the volume. The combined ANOVA and variable inflation factor analyses indicate that the developed model was strong, and unlikely a result of chance, with a set of predictor variables with reasonable independence.

Table 39 Builder C Regression Model Parameters

Predictors	Beta	SE	t	Sig.	95% CI LB	95% CI UB	VIF
(Constant)	5.389	2.049	2.631	.01438	1.170	9.609	
Volume	-0.0011	0.0003	-3.030	.00562	-.002	.000	4.5
PerimR	0.0219	0.0151	1.451	.15916	-.009	.053	1.3
ShellA	-0.0056	0.0012	-4.546	.00012	-.008	-.003	5.1

The analysis of the standardised model error revealed a normal distribution with $\mu < 0.000$ and a regression standardised residual standard deviation of $SD = 0.945$. Figure 19 and Figure 20 show that the frequency plot and the probability-probability plot distribute normally. Hence the assumed normal distribution of the data set for Builder C was confirmed.

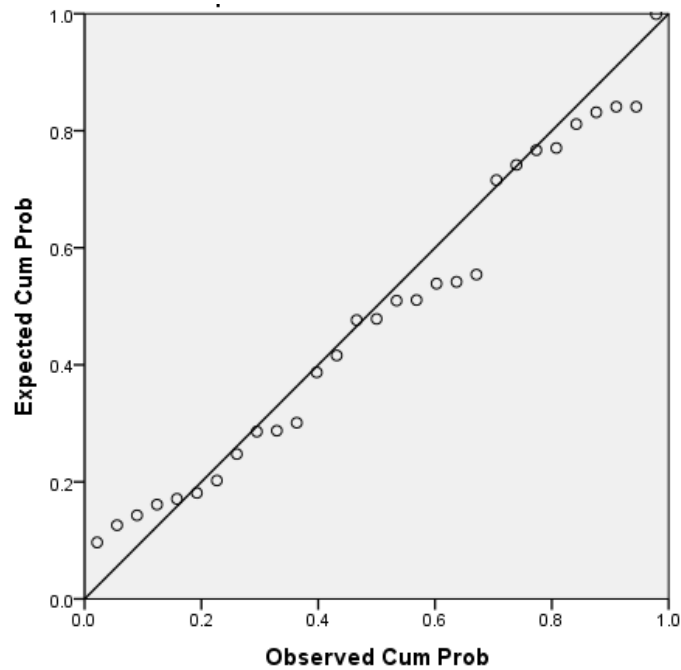


Figure 19 Builder C Standardised Residual Probability-Probability Plot

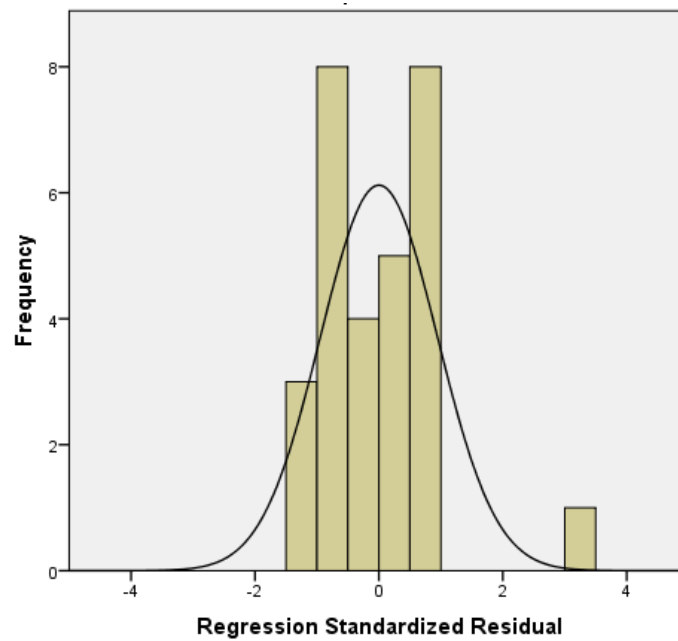


Figure 20 Builder C Standardised Residual Frequency Plot

Although builder specific models for Builders A, B, and C were proven to be significant, the modeling for a predictive airtightness model for Builder D was found to be unsuccessful. The model strength as assessed

by the Pearson correlation coefficient was very weak with $R = 0.265$, with an $\text{Adj.}R^2 = 0.024$. This indicated that model only explained 2% of the variation in airtightness (See Table 40).

Table 40 Builder D Multiple Linear Regression Model

Model	R	R^2	Adj R^2	SE
Builder D	0.265	0.070	0.024	0.361

Table 41 Builder D ANOVA

Builder D	SS	DF	MS	F	Sig.
Regression	0.589	3	0.196	1.508	0.222
Residual	7.814	60	0.130		
Total	8.404	63			

Furthermore, the ANOVA (Table 41) indicated the one must fail to reject the null hypothesis since the p value = 0.22, which was above the significance level initially prescribed as $\alpha = 0.05$. Unsurprisingly none of the regression parameters were significant. The p-values were 0.61, 0.31 and 0.91 for the predictors shown in

Table 42. Based on the methodology outlined in Chapter III, Builder D's blower door testing sample size would need to be increased so that the analysis could be performed anew. It is also possible that there are other yet to be discovered differences in Builder D's homes have prevented the development of a strong airtightness model. These results further highlight that different population sizes maybe required for different builders in order to create predictive models. While 64 tested homes proved to be insufficient for Builder D, 29 tested homes were sufficient for Builder C, and 48 homes were sufficient for Builder A.

Table 42 Builder D Regression Model Parameters

Predictors	Beta	SE	t	Sig.	LB 95.0% CI	UB 95.0% CI	VIF
(Constant)	0.579	4.164	0.14	0.890	-7.750	8.908	
Volume	0.002	0.005	0.51	0.608	-0.007	0.012	1.7
FenPerimHR	0.040	0.038	1.04	0.301	-0.036	0.115	4.6
PerimR	0.006	0.053	0.10	0.914	-0.100	0.112	5.2

5.1.3 Handicraft & Geometry based Multiple Linear Regression Analyses

Airtightness modelling was also performed using the addition of a single, non-geometric predictor. *BuilderID* was used to account for the variation in handicraft and/or construction quality between subsets of the blower door tested housing populations. The same approach from Figure 3 used to construct airtightness prediction models controlling for handicraft. Both normalised leakage (NL) and air changes per hour (ACH50) were used as output metrics. The NL model utilised 223 blower door test records since the ELA was not available for Builder A. The ACH50 model utilised both data sets of 223 and 272 blower door test records. The 223 record was chosen such that the predictive power between the ACH50 and NL models could be directly compared. The modeling of the NL model showed that the Pearson's Correlation Coefficient (Table 43) was strong, with $R = 0.865$ explaining over 74% for the variation in airtightness. The F-test shown in the ANOVA Table 44 for the regression model demonstrates an extremely significant model based on the $p\text{-value} < 0.001$.

Table 43 NL II Multiple Linear Regression

Model	R	R ²	AdjR ²	SE
NL II	0.865	0.748	0.742	0.025

Table 44 NL II ANOVA

NL II Parameter	SS	DF	MS	F	Sig.
Regression	0.403	5	0.081	128.925	0.000
Residual	0.136	217	0.001		
Total	0.539	222			

Furthermore, a high degree of significance ($p\text{-value} < 0.01$) was found for all five predictor variables, *ExCondFA*, *FenPerimH*, *CeilingA*, *AGradeH* and *Builder ID*. The degree of multicollinearity between retrospective parameters and the model was low, save *BuilderID* which had a VIF near the threshold factor value of 10.

Table 45 NL II Regression Model Parameters

NL II Parameter	Beta	SE	t	Sig.	LB 95%CI	UB 95%CI	VIF
(Constant)	0.335	0.052	6.41	0.0000	0.232	0.438	
ExCondFA	0.002	0.001	3.03	0.0027	0.001	0.004	2.3
FenPerimHR	0.002	0.000	4.90	0.0000	0.001	0.003	3.2
CeilingA	-0.001	0.000	-5.56	0.0000	-0.001	0.000	3.5
AGradeH	-0.030	0.009	-3.49	0.0006	-0.047	-0.013	6.0
BuilderID	0.037	0.004	9.91	0.0000	0.030	0.045	9.4

A large F-value of 129 showed that the NL II model was highly significant with p-value < 0.001. Table 45 shows that five significant parameters could be used to predict airtightness. The five parameters corresponded to: fenestration perimeter to building height, ceiling area, above grade height, and building identification. The parameter for exposed floor area to conditioned floor area was found to significant with p-value < 0.01. AGHeight had a significance of p-value < 0.001. The remaining three variables; *FenPerimHR*, *CeilingA*, *BuilderID* had a significance of p-value < 0.0001. It is important to note that the multicollinearity was kept to reasonable levels for two predictor variables that shared a divisor. The VIF of *FenPerimHR* and *AGradeH* were 3.2 and 6.0 respectively. The controlled multicollinearity was likely a result of the transformation of the *FenPerimHR* from an absolute variable to a ratio of independent variables. Therefore, fenestration crack length divided by building height becomes independent to building height. *BuilderID* was found to have the highest measure of multicollinearity yet within the acceptable range with a VIF =9.4. This means that BuilderID is on the threshold of collinearity with the remaining portions of the airtightness model. The implications are that handicraft may be heavily dependent on geometric description.

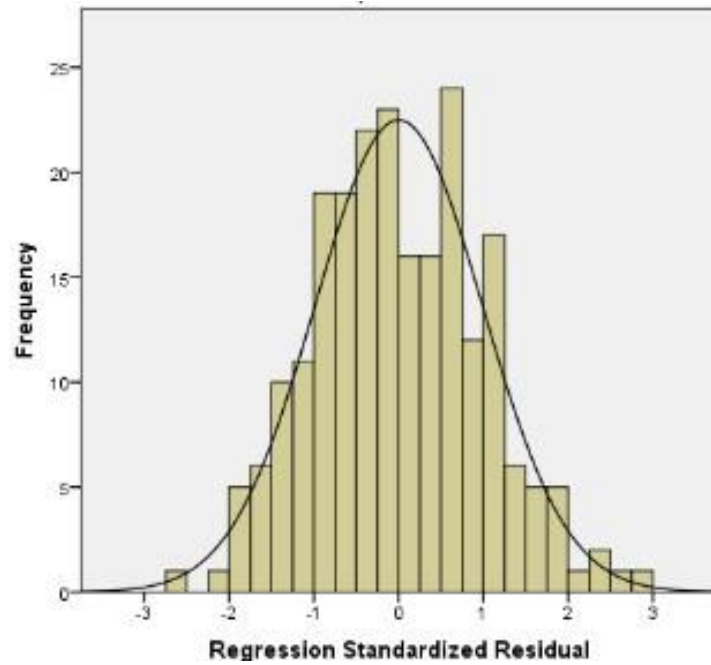


Figure 21 NL II Standardised Residual Frequency Plot

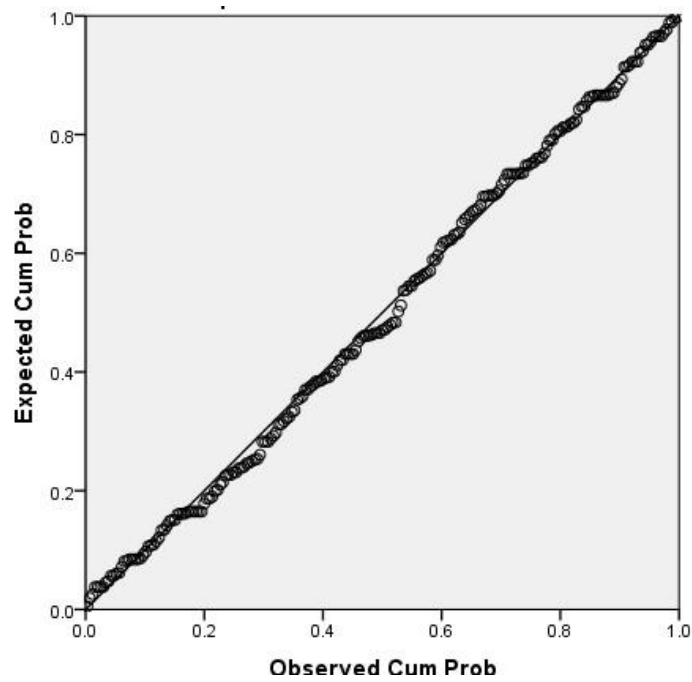


Figure 22 NL II Standardised Residual Probability-Probability

The error analysis of model NL II is shown in Figure 21 and Figure 22. The standardised residuals shown in both the frequency plot and the probability-probability plot show well behaved residuals. The resulting mean was $\mu < 0.000$ and the standardised standard deviation was $SD = 0.989$, which satisfied the condition of assumed normality.

Two models ACH50 IIa, and ACH50 IIb based on air change rates were also investigated utilising the same data set for normalised leakage as above. All predictor variables were geometric in nature save *BuilderID*. The analysis was performed with 272 detached homes as well as a subset of 223 homes so that the models could be easily compared to the *NL II* model developed above.

Table 46 ACH IIa Multiple Linear Regression

Model	R	R ²	Adj. R ²	SE
ACH50 IIa	0.589	0.347	0.337	0.42

The airtightness model ACH50 IIa is summarised in Table 46. The Pearson correlation coefficient was found to moderate in strength with $R = 0.589$, $R^2 = 0.347$ and an adjusted R^2 suggesting that nearly 34% of the airtightness could be explained by the model. The model was found to be highly significant with $F = 35$ corresponding to a $p < 0.001$ as shown in Table 47.

Table 47 ACH IIa ANOVA

ACH50 IIa	SS	DF	MS	F	Sig.
Regression	25.29	4	6.32	35.425	0.0000
Residual	47.66	267	0.18		
Total	72.95	271			

Four geometric predictor variables and one External type of predictor variable were found to be relevant to the model. All predictors, *BuilderID*, *FenPerimH*, *ExCondFAR*, *CeilingA* were found to

be extremely significant with p-values < 0.0001. Low levels of multicollinearity were detected with VIF < 4.0 for all predictor variables.

Table 48 ACH Ila Regression Model Parameter

Predictor	Beta	SE	t	Sig.	LB 95%CI	UB 95%CI	VIF
(Constant)	2.672	0.21	12.90	0.0000	2.26	3.08	
BuilderID	0.150	0.03	5.61	0.0000	0.01	0.20	2.35
FenPerimH	0.039	0.01	5.86	0.0000	0.03	0.05	2.82
ExCondFAR	0.053	0.01	4.79	0.0000	0.03	0.07	1.93
CeilingA	-0.015	0.001	-8.32	0.0000	-0.02	-0.01	3.70

The analysis of the residuals indicate that the error distributes normally with $\mu < 0.0000$ and SD =0.989. The probability-probability plots and the frequency plot of the regression standardised residuals demonstrated the errors are normal distributed. The residual analysis is shown graphically in Figure 23 and Figure 24.

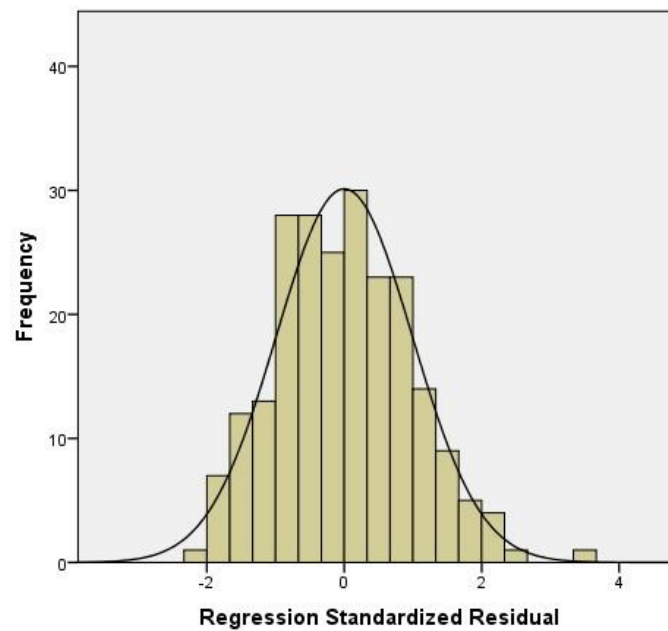


Figure 23 ACH50 Ila Standardised Residual Frequency Plot

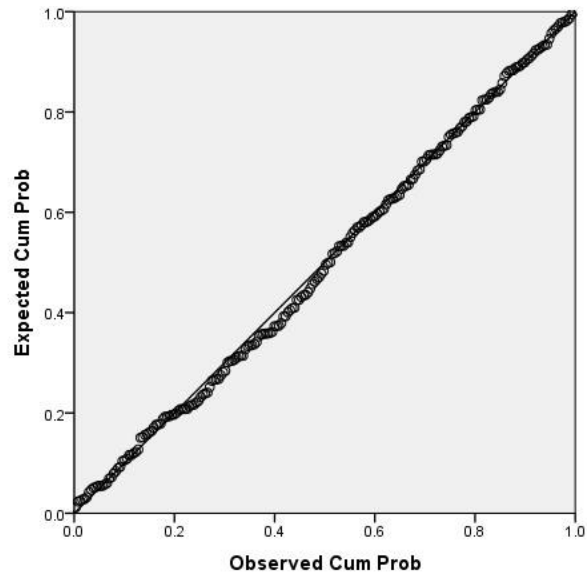


Figure 24 ACH Ila Standardised Residual Probability-Probability Plot

The ACH IIb model utilising a subset of 223 homes was also constructed. The model explained up to 45% for the airtightness of the data set. The model had a moderate strength of $R = 0.676$ as shown in Table 49. The analysis of variance showed that the overall model was extremely significant with $p\text{-value} < 0.0001$.

Table 49 ACH IIb Multiple Linear Regression

Model	R	R ²	Adj. R ²	SE
ACH50 IIb	0.676	0.458	0.448	0.38

Table 50 ACH IIb ANOVA

ACH50 IIb	SS	DF	MS	F	Sig.
Regression	27.15	4	6.788	46.187	0.00000
Residual	32.19	219	0.147		
Total	59.34	223			

ACH IIb utilised the same four parameters as ACH50 Ila; *BuilderID*, *FenPerimH*, *ExCondFAR*, *CeilingA*. All the parameter values were in the same order of magnitude between models ACH50

Ila, and ACH50 IIb. All the parameters were also found to be extremely significant with p-values < 0.00001. Multicollinearity was interpreted as low with all variable inflation factors to be VIF < 4 as seen in Table 51

Table 51 ACH IIb Regression Model Parameters

Parameters	Beta	SE	t	Sig.	LB 95%CI	UB 95%CI	VIF
(Constant)	2.929	0.224	13.08	0.00000	2.487	3.370	
BuilderID	0.249	0.034	7.36	0.00000	0.183	0.316	3.2
FenPerimH	0.028	0.007	4.25	0.00000	0.015	0.042	3.1
ExCondFA	0.028	0.011	2.55	0.00000	0.006	0.050	2.2
CeilingA	-0.013	0.002	-7.66	0.00000	-0.016	-0.010	3.5

The assumption of normal distribution was well supported based on $\mu = 0.000$ and $SD = 0.991$.

The normality assumption was also well illustrated by the standardised residual frequency plot (Figure 25 & Figure 26).

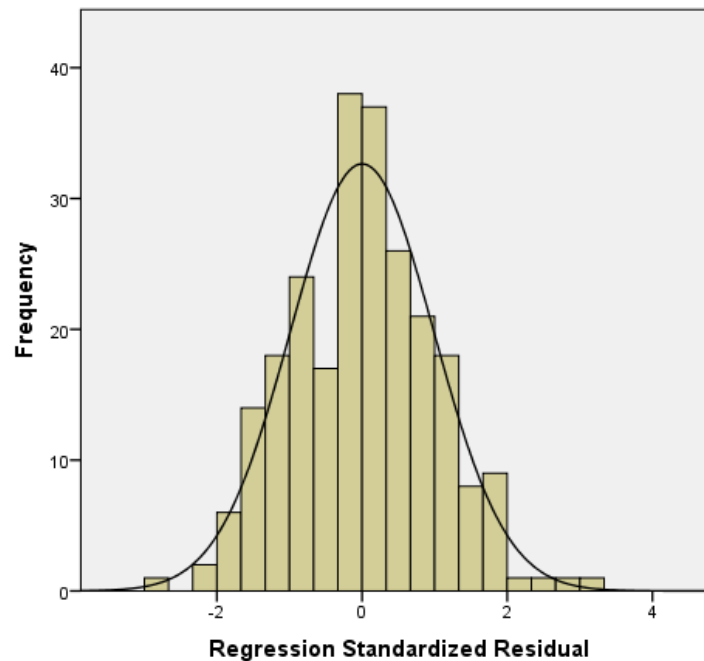


Figure 25 ACH50 IIb Standardised Residual Frequency Plot

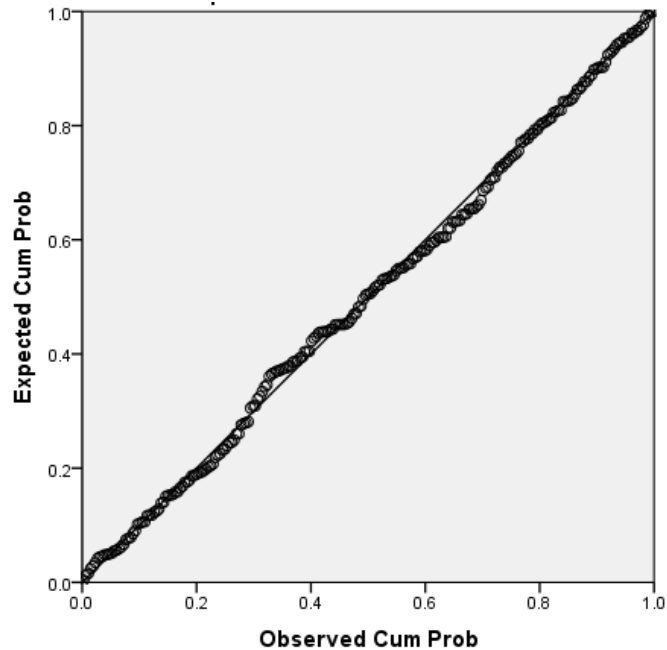


Figure 26 ACH IIb Standardised Residual Probability-Probability Plot

The Phase II geometry-based airtightness models that were investigated are summarised in Table 52. Four builder specific models for Builders A,B,C,D were constructed. These four models relied solely on building geometry, with no considerations for building age or handicraft. The builder specific models for Builder A, & C were shown to be strong both with $R > 0.7$ and explaining over 51% and 58% of the air leakage in their respective population samples. Builders A, B, C used volume as a significant predictor indicating absolute building size was important in airtightness for these builders. Air leakage at the rim joist seemed to be an important parameter for Builders A and C. Builders A & B, and C did share Volume as a predictor variable, while Builder A and Builder B both used *FenPerimHR*. These results suggest that the development of this new predictor variable was justified. The effects of crack lengths around windows and doors as a ratio to total building height was shown to be more important than the absolute length of cracks for this Builder.

The CWR was shown to be important for Builder B. The appearance of CWR for Builder B as an important predictor variable may have indicated that leakage at the ceiling to roof interface is significant for this builder. The strength of Builder D model was shown to be extremely weak in strength and had little to no practical value. The Builder D model's adjusted R^2 revealed that the model could only predict 2% of the variation in airtightness. The analysis of variance analysis showed that the model failed to reject the null hypothesis since the p-value was well above the significance limit of $\alpha = 0.05$.

Table 52 Phase II Airtightness Model Summary Table

Model	Parameters	R	adj R^2	ANOVA	Collinearity	Residuals
NL II	5	0.865	74%	$p < 0.0001$	VIF < 10	$\mu = 0$, SD = 0.99
ACH50 IIa	4	0.589	34%	$p < 0.0001$	VIF < 4	$\mu = 0$, SD = 0.99
ACH50 IIb	4	0.676	46%	$p < 0.0001$	VIF < 4	$\mu = 0$, SD = 0.99
Builder A	3	0.734	51%	$p < 0.0001$	VIF < 5	$\mu = 0$, SD = 0.94
Builder B	3	0.602	35%	$p < 0.0001$	VIF < 4	$\mu = 0$, SD = 0.99
Builder C	3	0.752	58%	$p < 0.0001$	VIF < 6	$\mu = 0$, SD = 0.99
Builder D	3	0.262	2%	$p = 0.222$	VIF < 6	N/A

The models controlling handicraft had varying degrees of predictive strength. The strength of the ACH50 IIa model was moderate with $R = 0.59$, and explained close to 34% of the airtightness in the homes. The ACH50 IIb model was considerably stronger with $R = 0.68$ and explained 45% of the airtightness. The strongest model was that which used normalised leakage as an output variable. Nearly 74% of the variation in airtightness was explained by the NL II model. The model was considered strong with $R = 0.865$ and an ANOVA with a p-value < 0.0001 . Multicollinearity was kept to a minimum for four of the five variables save *BuilderID* whose VIF = 9.4 which was just within the established acceptability limits.

A contrast between the modeling improvement between Phase I and Phase II was examined. First, an eight-variable model from Phase I was constructed for Ontario homes to best match the population pool under consideration. Homes built after the year 2000 totaling N = 1975 homes were used to construct a predictive 8 variable normalised leakage model. This model with a constrained geographic region and year of constructed and is shown in Table 53. The model was said to be moderate in strength with $R = 0.564$ and explaining up to 32% of the variation in airtightness. By contrast, the Phase II (Table 52) *NL II* model predicted 74% of the variation in airtightness. Not only has the Phase II model explained more than twice the airtightness than *NL I**, it maintained strong predictive power without using year of construction as an independent variable. To date, detached, low-rise, residential airtightness models have not been able to produce equally as strong predictions using postconstruction approaches.

Table 53 Comparative Phase I Regression Model

Model	R	R²	Adj.R²	SE
NL I* Model	0.564	0.318	0.315	0.26

5.1.4 Phase II Models - Comparison to Previous Literature and Current Contributions

A comparison of selected airtightness regression-based models with models developed in Phase II of this study are shown in Table 54. Many models of the models presented in Table 54 utilised *a priori* information concerning the level of airtightness of the homes in advance of the analysis. For example, the participation in weatherisation programs, or the income level of the dwelling occupants were all means of which to triage homes by an airtightness-based predictor variable. Phase II models developed here held no such variables to enhance model strength. Despite this disadvantage, Phase II models were stronger or equal in strength as compared to older regression models. Moreover, Phase II models achieved their strength with relatively small sample sizes.

Table 54 Airtightness Model Comparison to Preceding Studies

Jurisdiction	R ²	Parameters	N	Description
United States (2005)	0.56 ^{a,b}	4	70 000	Heterogeneous Typology Heterogeneous Assembly
Greece (2006)	0.56, 0.93 ^a	1	20	Homogeneous Typology
Spain & France (2009)	0.94 ^{a,b}	2	483	Homogeneous Typology Heterogeneous Assembly
United Kingdom (2010)	0.49	7 – 6	287	Heterogeneous Typology Heterogeneous Assembly
United States (2013)	0.68 ^{a,b}	12	134 000	Homogeneous Typology Heterogeneous Assembly
Netherlands (2016)	0.43 ^b	5	320	Heterogeneous Typology Heterogeneous Assembly
Canada (2018) (Phase I)	0.48, 0.46 ^b	8 – 3	900,000	Homogeneous Typology Homogeneous Assembly
Ontario (2019) (Phase II)	0.74, 0.58	5 -3	3000	Homogeneous Typology Homogeneous Assembly
^{a.} airtightness level known <i>a priori</i> ^{b.} year of construction used as predictor				

For example, the *ACH50 IIb* model was equally strong as the predictive model in Phase I that utilised more than 330,000 testing records. Furthermore, the *ACH IIb* used a sample population with homogeneous wall assemblies, and a homogeneous climate region. Additionally, year of construction, a variable shown to have had the most significant impact on airtightness predictions is absent from all Phase II models.

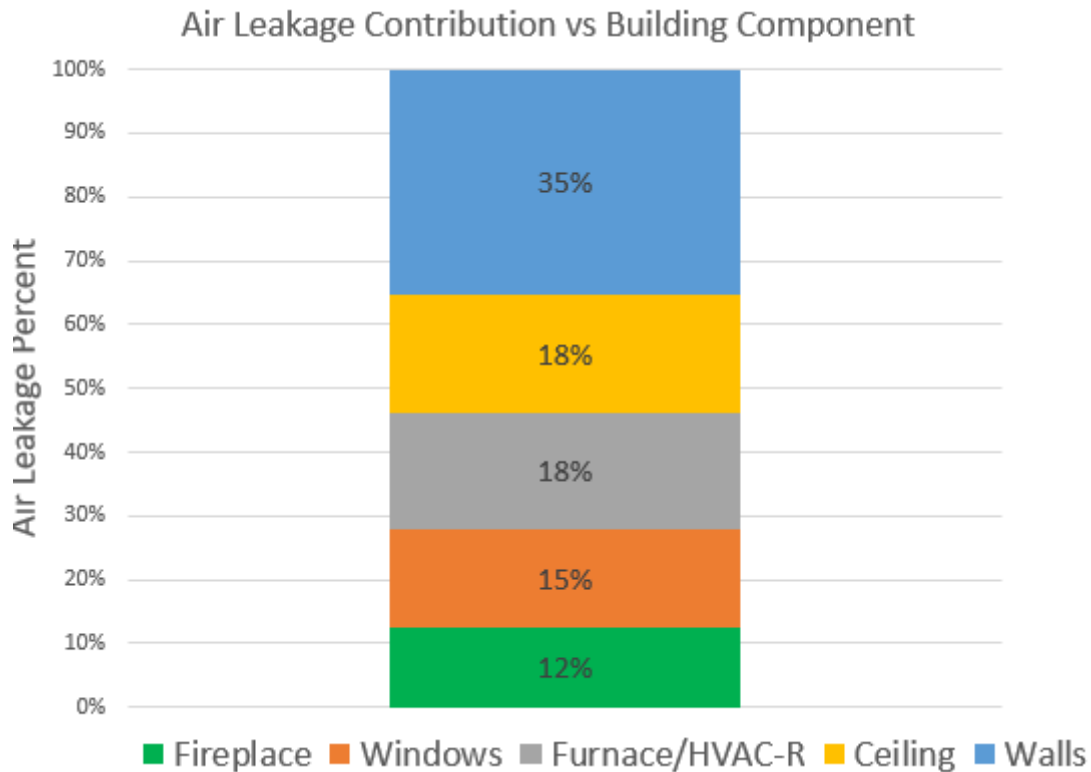


Figure 27 Proportion of Air Leakage in Low Rise Residential Homes (ASHRAE – Fundamentals)

The contribution to building airtightness by proportion has been shown in Figure 27. As discussed in Chapter 2, the Air Barrier System comprising of walls, ceilings and windows account for 68% of the total air leakage, on average. Hence the model strengths for Builder A, and Builder C ($\text{Adj } R^2 = 51\%$ and 58%) accounted for 75% to 85% of the attributable air leakage in such dwellings.

There were a number of differences between the predictive models developed during Phase I and Phase II of this investigation. Phase II models possessed: wall homogeneity, housing homogeneity, temporal independence, climate independence and a handicraft estimation.

Previous studies have used heterogeneous wall types in their regression formulations. These housing types included wall systems made from prefabricated panels, solid masonry walls (such as brick and concrete masonry units) and light framed wood walls. The heterogeneity of

these wall types introduced an inherent variability in airtightness at the population level. The heterogeneity also adds predictive power models linked to those population of houses, increasing the R^2 .

Temporal predictor variables such as build year have been demonstrated to be an important variable both in previous research(Chan et al., 2013, 2005) and Phase I. In addition, the year of construction have been shown to be the most influential predictor variable in regression models. The age of a building may have been an indication of handicraft and material quality for older buildings. The year of construction may have also represented material degradation over time. The models in Phase II have no temporal dependence by contrast. Hence time independent air leakage models from Phase II could allow builders and designers to predict preconstruction airtightness of new homes based primarily on house geometry and detail characteristics. The development of predictive models without temporal dependence is an important contribution to the field and separates the Phase II models from those in related literature.

Climate zones in the form of heating degree days were shown to be strongly related to local building code and construction practices. Hence comprehensive airtightness models to date have often used climate as a predictor variable. On average, an increase in HDD and wall insulation thickness have been shown to reduced the air leakage in residential homes(Chan et al., 2013). This inference is supported by the regional, often climate dependant construction practices and codes found in North America. The prediction models from Phase I used climate as a predictor variable while the models developed in Phase II were climate independent. Yet,

models developed in Phase II were still able to make equal or stronger airtightness predictions than that of those in Phase I.

The modeling in Phase II allowed for the identification of handicraft. Categorising buildings according to *BuilderID* has shown that model strength could be increased. In the case of NL II the model was able to predict 74% of the whole building airtightness.

There are several practical implications to be considered as a consequence of the Phase II analyses. Many previous models focussed primarily on predicting airtightness on existing buildings that were representative of the existing housing stock. Many of these earlier models therefore used predictor variables for wall types, housing types, climate and year of construction. Conversely, Phase II of this research focussed on providing designers and builders the ability to forecast airtightness levels based on their respective housing portfolios. Hence the models for Phase II utilised builder specific geometry and wall types to estimate airtightness for buildings that match their portfolio. The specificity of these models resulted in forecasting equations that were unique to every builder. For example, while leakage at the rim joists were important for all builders, other factors were of greater or lesser importance to others. Additionally, air leakage at the ceiling was important for one builder while leakage around windows was more important for others.

The specificity of the airtightness models were not the only advantages of the approach illustrated in Phase II. The ability provided by controlling for handicraft was shown to have an important effect on the improvement of model strength. For instance, by using the discrete variable named *BuilderID*, the *ACH II* and *NL II* airtightness models were found to be either equal to ($\text{Adj } R^2 = 53\%$) or to surpass ($\text{Adj } R^2 = 74\%$) the predictive strength of previous models.

Moreover, the *ACH II* and *NL II* airtightness models were shown to predict anywhere from 78% to 100% of the attributable air leakage through walls, windows, and ceilings in low rise detached residential homes in North America.

5.2 Summary

An approach to estimating preconstruction airtightness in low-rise, detached, light-framed residential homes was demonstrated using 2297 homes in Southern Ontario. The subpopulations consisted of four builders, adhering to the Ontario Building Code blower. Building depressurisation data as well as construction and architectural details were collected from these builders for analysis. The degree of training, and construction management between each builder was not controlled in the analysis. Three builder specific models were able to account for 58%, 51%, and 34% of whole building airtightness. Three airtightness models controlling for handicraft were developed and could account for 74%, 46%, and 34% of whole building airtightness. The builder specific models were able to account for 78%, 75%, and 50% of the attributable air leakage through walls, windows and ceilings. The models were found to dependent on building select size attribute as well as custom developed geometric ratios. The modeling approach developed in Phase II allowed designers to forecast preconstruction airtightness for future residential buildings with conventional construction using a building specific methodology.

6 Transition Detail Airtightness Predictions

A novel methodology to estimate air leakage simultaneously utilising both conventional and next-generation enclosure details for the purposes of predicting whole building airtightness was developed. A laboratory based, 2^3 factorial design assessed the importance of pressure, detail length, and air barrier system approach applied to a rim joist enclosure detail. The assessment was then used to create a set of parameter weighting functions. The empirically based weighting functions were then used to update builder specific, whole building airtightness models created in Chapter 5 showing how this novel testing approach can strengthen whole house air leakage prediction when builders alter specific enclosure details.

6.1 Laboratory Testing Design & Calibration

The rim joist air enclosure detail was chosen for this phase of the research since it was shown to be an important whole building airtightness variable in many of the mathematical models created in Chapter 5. Current, ongoing laboratory-based research is evaluating air leakage at window frames since window to wall joints were also shown to be important contributors to whole building air leakage.

6.1.1 Sample and Test Chamber Construction

Eight floor-to-exterior wall samples details were built with varying configurations. The samples total detail length was 2380 mm. The sheathing board joints were chosen to replicate the worst-case conditions at the rim joist detail (refer to Figure 28). Hence, board joints at the base of the 2nd floor sheathing, and the top of the 1st floor were included. Additionally, a third sheathing joint

was included along the rim joist. The joints, shown as dashed lines in Figure 28 were also offset for all the testing samples. Framing joints were made in the bottom plate (J1), subfloor (J2), rim joist (J3) and double top plate (J4, J5) as shown in Figure 29

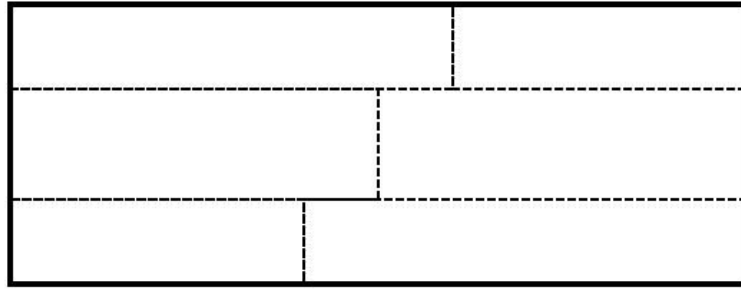


Figure 28 Elevation View Showing Sheathing Board Joints

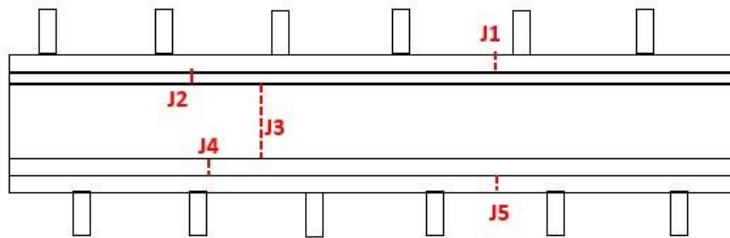


Figure 29 Rim Joist Detail Showing Framing Joint locations

Care was taken to reduce any inherent bias in the sample manufacturing process. This sample manufacturing protocol was utilised to reduce effects due to operator learning, or gradual machinery cutting tool displacements that could potentially affect the resultant sample assembly performance as a result of the manufacturing process. Steps in the sample preparation process were therefore performed in batches, rather than completing constructing one sample detail at a time. In effect, the sample preparation employed a high-volume production methodology. For instance, dimensional lumber was cut to the same size for both the bottom and top plates. Sheathing strips and joints were cut such that a single assembler was performed the same operations. The machinery was adjusted to cut all of the offset joints sequentially. The top plates

were then fastened together with framing screws. Similarly, the Rim Joists were all cut in one operation, while the floor joists were cut in another operation. Pilot holes were applied to all the floor joists first, then were used to be assembled to the rim joists methodically. Bottom plates, stud preparations and subfloor preparations were all cut, prepared and screwed in this same manner. The 40mm x 140mm studs were all predrilled for eventual toenailing with pilot holes. Wood screws were then inserted for each stud. A similar process was observed for cutting the sheathing. All stock OSB sheets were cut in half first with the same dimensional table saw setting. The strips were then cut to for the 1st floor, 2nd floor and rim joist filler board. Sheet and self-adhering air barriers membranes were then applied to the completed samples (refer to Figure 31). Cavity insulation was not used in the assembly since would not form as part of the air barrier system. The rim joist details treated with the sheet membranes represented the conventional code compliant assembly, while the self adhered membranes represented the advance, atypical material application on the advanced joint detail. Each assembly operation was completed in a single day to reduce temporal-based variances in sample construction.

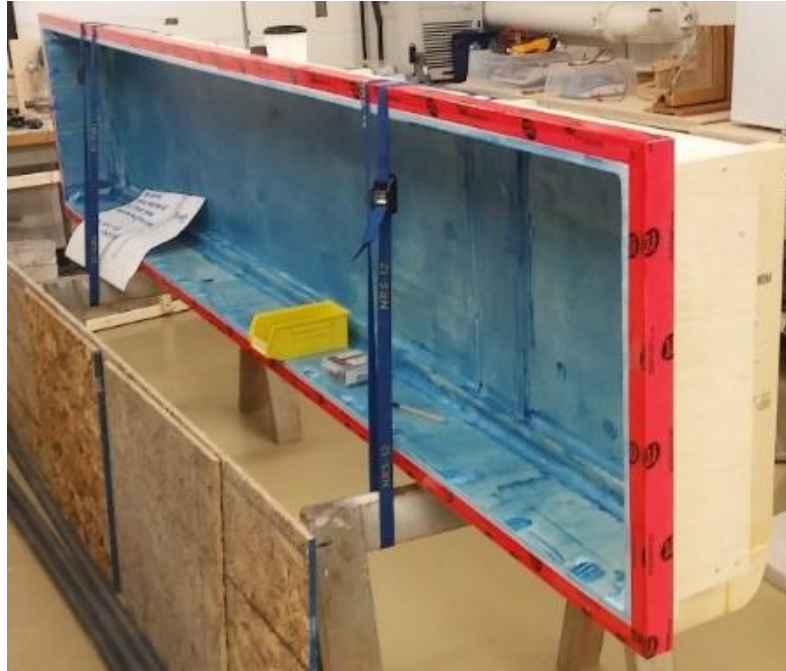


Figure 30 Empty Test Chamber



Figure 31 Membrane Application in Conventional and Advanced Samples

The method of assembly helped to avoid using blocking for day of assembly. Removing the need for a blocking reduced the addition of confounders to factorial analysis. A reduction of confounders was also possible in the testing phase since the design of experiments stipulated that all air leakage tests were to be performed on the same day to minimise changes in environmental conditions such as temperature, atmospheric pressure, and relative humidity.

Similarly, all calibration tests were performed on separate days/weeks. Any fine tuning of the test procedure or equipment adjustments were performed at an earlier date with a prototype sample. The prototype sample was then segregated from the 8 test samples. An airtight test chamber made of plywood and dimensional lumber was constructed. Every joint was pre-caulked, then re-caulked after assembly. Two thick coats of an elastomeric water, air and vapour impermeable liquid applied membrane (shown in Figure 30) was applied to the inner surface of the test chamber.



Figure 32 Chamber with Sample Under Test



Figure 33 Prototype sample

6.1.2 Instrumentation

The instrumentation consisted of; a microleakage meter with part number of MLM-1071, a digital manometer (Figure 34) with model DG1000 and part number 1885 , a flow modulating blower (Figure 37) chamber pressure was determined using a series of calibrated orifice plates (Figure 36) Flow based pressure measurement recordings were made at 50Pa, 75Pa, 100Pa and 150Pa for a total of four measurements per sample. All measurements were time averaged over 10 seconds with the digital manometer. All pressure inputs from 50Pa to 150Pa were kept within +/- 1 Pa of the desired target pressure. Calibration curves (Figure 38) were used to translate pressure readings from Pascals to m³/hour and to L/s.



Figure 34 Digital Manometer



Figure 35 Microleakage Meter



Figure 36 Microleakage Orifice Disks



Figure 37 Variable Speed Depressurisation Fan

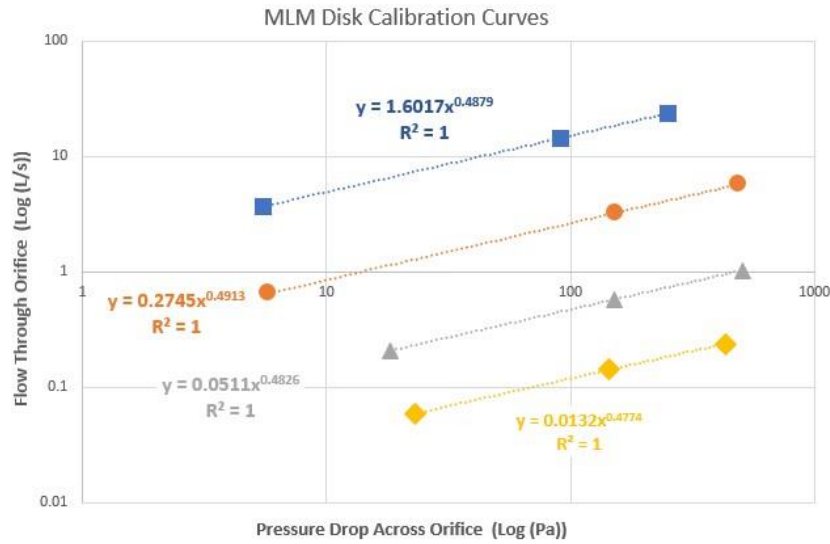


Figure 38 Micro Leakage Meter Calibration Curves

6.1.3 Calibration

The experimental apparatus was calibrated using two methods: (1) background leakage testing and, (2) crack flow verification. Testing background air leakage comprised measuring a control sample. The control sample satisfied the requirements of an air barrier system to ensure the highest performance. A single piece of plywood sheathing covered in a self-adhered membrane was used due to its strength and rigidity, air impermeability, durability, and ability to be continuous. The control sample was measured at four pressures (50, 75, 100, and 150 Pa) and repeated in quadruplicate. The quadruplicate measures (QM) are shown in Table 55. The volumetric leakage rate was also converted to a chamber air change rate (ACHc) for comparative convenience.

Table 55: Quadruplicate Measures Ideal ABS at 4 Pressures

Pa	Leakage (L/s)				Pa	Leakage (ACHc)			
	QM1	QM2	QM3	QM4		QM1	QM2	QM3	QM4
50	0.013	0.013	0.013	0.013	50	0.178	0.178	0.178	0.169
75	0.020	0.017	0.017	0.016	75	0.270	0.229	0.229	0.215
100	0.026	0.024	0.023	0.024	100	0.348	0.318	0.309	0.327
150	0.037	0.036	0.036	0.035	150	0.501	0.482	0.482	0.476

The logarithm of each flow reading was calculated and plotted on a log-log graph shown in Figure 34. The first set of quadruplicate readings, *QM1*, had a flow exponent of $n=0.9414$ based on the slope of the curve. The flow exponents for *QM2*, *QM3* and *QM4* were $n=0.9245$, $n=0.9180$ and $n=0.9766$, respectively. These flow exponents indicated that the leakage rate from the depressurisation system is effectively laminar since the values are close to $n = 1.0$ (Hutcheon & Handegord, 1983; Pritchard et al., 2016).

The coefficients of determination showed high degree of fit with $R^2 = 0.9985$, 0.9844 , 0.9823 and 0.9772 for *QM1* through *QM4* respectively. The control sample allowed for the calculation of the equivalent leakage area of the testing system. The ELA of the test setup was found to have ranged from 1.7 mm^2 to 2.8 mm^2 , and averaged 2.2 mm^2 . This implies that the test apparatus was well sealed and reliable.

Flow C & n Values using Tare Readings Quadruplicate Measurements at Four Pressures 50,75,100,150Pa

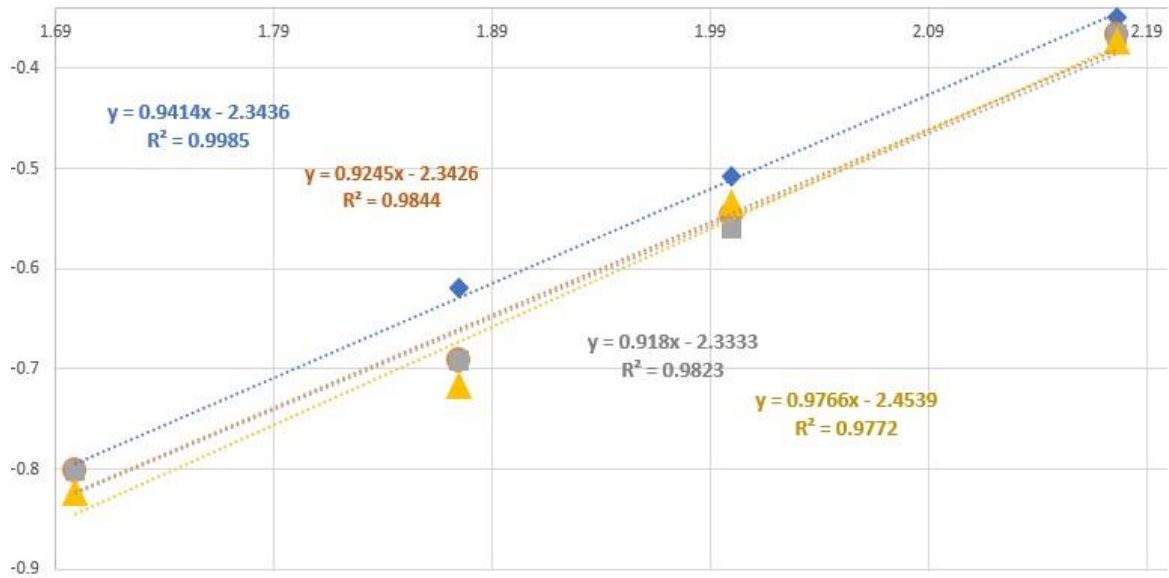


Figure 39 Flow Characterisation of Apparatus via Tare Background Leakage Log (L/s)

Air Flow Characteristics Through Progressivess Plywood Cracks

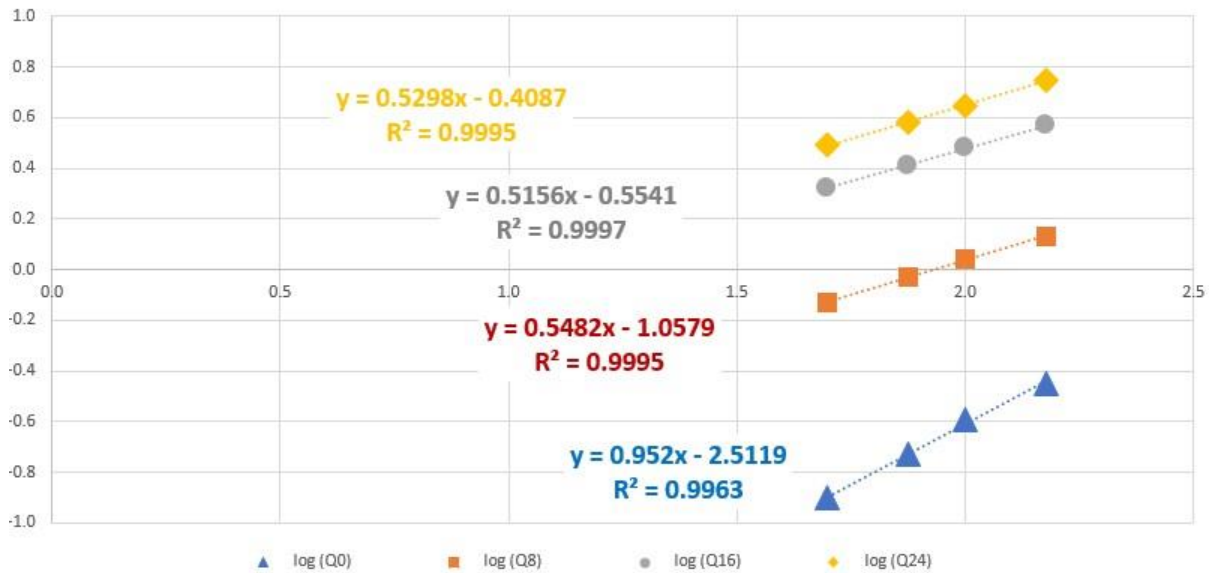


Figure 40 Flow Characterisation of With Crack Length (Qx) Log (L/s)

The second method used to calibrate the test apparatus was a ‘crack study.’ A plain piece of plywood was cut with a 1.5 mm wide saw blade. Progressive lengths were cut starting with 8 cm, 16 cm and ending with 24 cm. The area openings resulted in nominal 120 mm², 240 mm², and 360 mm² cracks areas. Each area opening was then depressurised at intervals of 50 Pa, 75 Pa, 100 Pa and 150 Pa. The pressure readings were converted to volumetric flow and then linearized using a logarithm. Best fit equations for the various crack lengths are shown Figure 40. The flow exponents taken from the lines of best fit were $n = 0.5444, 0.5298, 0.5156$ for the three cracks as compared to the same sample without a crack ($n = 0.9520$). These results were in strong agreement with fluid mechanics theory prediction of turbulent crack flow ($n=0.5$) and laminar flow ($n = 1.0$) for the uncut plywood (Pritchard et al., 2016) (Hutcheon & Handegord, 1983).

Table 56 ELA compared to Crack Area & Pressure

	Corresponding Crack Area (mm ²)			
	0	120	240	360
(Pa)	ELA (mm ²)			
50	13.8	81.9	231.2	342.5
75	16.9	84.3	231.6	345.1
100	19.9	85.5	234.8	346.0
150	22.5	86.3	234.6	354.5

In addition, the best fit lines demonstrated further confidence in the testing apparatus since the line of best fit showed coefficients of determination of $R^2=0.9995$, $R^2=0.9995$, and $R^2=0.9997$ while the plain plywood sample had $R^2 = 0.9963$ or 99.6%. The average ELA derived from crack experiment was plotted against measured cracks areas. The line of best fit between the measure and calculated crack area is shown in Figure 41. There was close to a 1:1 agreement between the

theoretical and the empirically derived crack size values with the slope of 0.9456 and $R^2 = 98.1\%$. Only a negligible offset of 0.5mm^2 was found. A small offset indicates that chamber and apparatus is virtually impervious to air flow. An idealised, air impermeable testing system would yield an input to output relationship of $Y=sX + i$, where the slope $s = 1$ and the intercept of $i=0$. The equivalent leakage area of the complete testing apparatus was found to be approximately 18.3mm^2 which represent a hole with a 2.4 mm diameter. The error between the mean ELA and the actual crack area was minimized at larger crack openings. This was likely due to the reduced flow disturbances caused by the opening's rough edges to the overall fluid flow at larger openings.

Table 57 Equivalent Leakage Area compared to Sample Crack Area

Crack Area (mm^2)	Mean ELA (mm^2)
0	18.3
120	84.5
240	233.1
360	347.0

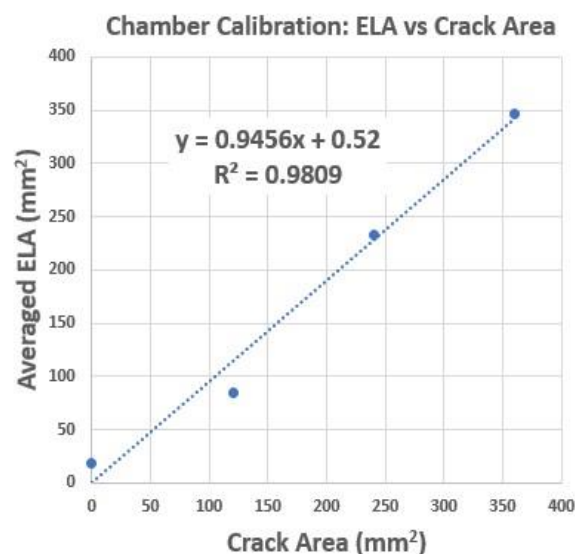


Figure 41 Comparison of Equivalent Leakage Area to Crack Area

In summary, a two-step calibration quantified background leakage and verified crack flow through known orifices. The background leakage procedure allowed for an equivalent leakage area of 18.3mm^2 for the whole system. The ELA represented the approximate sum of all cracks and holes in the test apparatus when it was tested with an impermeable sample. The flow through the ELA was characterised as laminar based on the observed flow exponent. The flow exponent was only 4.8% in error as compared to its expected value of $n = 1.0$. A fitted curve between the actual crack area as compared to the estimated leakage area was plotted. There was a very high correlation between the actual and estimate crack opening. The error between the slope of the line and its expected value was only 5.4%.

The calibration study results were in very strong agreement with fluid mechanics theory. The two-step calibration procedure could therefore be used during future enclosure details testing.

6.2 Data, Results & Discussion

Eight floor-to-wall details were tested in a randomised order over material (M) and length (L). The testing conditions could be visualised using the cube plot (Figure 6) discussed in Chapter 3. Each factor M,L,P had two levels corresponding to +1 and -1. A "+1" was assigned to a The pressure factor (P) could not be randomised due to the progressive nature of depressurisation associated with the experimental apparatus. The air leakage outputs for all testing combinations are shown in Table 58.

Table 58 Air leakage Output in Standard Order

SO	M	L	P	Rep	DM	M·L	M·P	L·P	M·L·P	L/s	ACHc
1	1	1	1	1	1	1	1	1	1	0.0909	1.222
2	1	1	1	1	-1	1	1	1	1	0.0896	1.205
3	1	1	1	-1	1	1	1	1	1	0.0998	1.342
4	1	1	1	-1	-1	1	1	1	1	0.0973	1.308
5	-1	1	1	1	1	-1	-1	1	-1	0.0592	0.796
6	-1	1	1	1	-1	-1	-1	1	-1	0.0576	0.775
7	-1	1	1	-1	1	-1	-1	1	-1	0.0540	0.726
8	-1	1	1	-1	-1	-1	-1	1	-1	0.0509	0.684
9	1	-1	1	1	1	-1	1	-1	-1	0.0780	1.049
10	1	-1	1	1	-1	-1	1	-1	-1	0.0748	1.006
11	1	-1	1	-1	1	-1	1	-1	-1	0.1452	1.953
12	1	-1	1	-1	-1	-1	1	-1	-1	0.0896	1.205
13	-1	-1	1	1	1	1	-1	-1	1	0.0416	0.559
14	-1	-1	1	1	-1	1	-1	-1	1	0.0402	0.541
15	-1	-1	1	-1	1	1	-1	-1	1	0.0442	0.594
16	-1	-1	1	-1	-1	1	-1	-1	1	0.0427	0.574
17	1	1	-1	1	1	1	-1	-1	-1	0.0558	0.750
18	1	1	-1	1	-1	1	-1	-1	-1	0.0535	0.719
19	1	1	-1	-1	1	1	-1	-1	-1	0.1163	1.564
20	1	1	-1	-1	-1	1	-1	-1	-1	0.0660	0.888
21	-1	1	-1	1	1	-1	1	-1	1	0.0415	0.558
22	-1	1	-1	1	-1	-1	1	-1	1	0.0381	0.512
23	-1	1	-1	-1	1	-1	1	-1	1	0.0392	0.527
24	-1	1	-1	-1	-1	-1	1	-1	1	0.0345	0.464
25	1	-1	-1	1	1	-1	-1	1	1	0.0621	0.835
26	1	-1	-1	1	-1	-1	-1	1	1	0.0660	0.888
27	1	-1	-1	-1	1	-1	-1	1	1	0.0780	1.049
28	1	-1	-1	-1	-1	-1	-1	1	1	0.0731	0.983
29	-1	-1	-1	1	1	1	1	1	-1	0.0285	0.383
30	-1	-1	-1	1	-1	1	1	1	-1	0.0276	0.371
31	-1	-1	-1	-1	1	1	1	1	-1	0.0308	0.414
32	-1	-1	-1	-1	-1	1	1	1	-1	0.0290	0.390

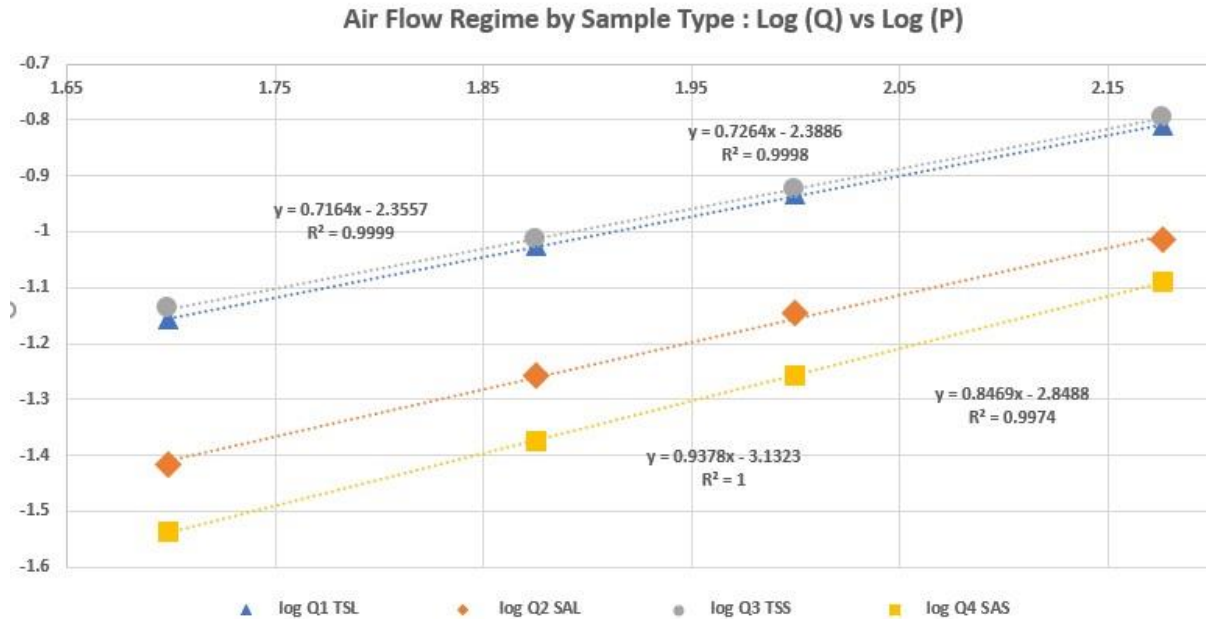


Figure 42 Log-Log Plot of Depressurisation Air Flow Regime by Sample Configuration

Four characteristic linearized curves for four test configurations (TSL, SAL, TSS, SAS as defined below) are shown in Figure 42. These curves are averaged over the sample types and replicates such that each point represents the average of four measurements. The long, taped sheets samples (TSL) are shown as curve Q1. The shorter samples with taped sheets (TSS) are Q3. The long surface applied membranes (SAL) are shown with curve Q2, and the shorter samples with surface applied membranes (SAS) is Q4. The characteristic curves show that the conventional details have flow exponents near the $n = 0.65$ typically assumed for light-framed dwelling construction. The samples using the advanced air barrier approach (i.e. self adhered house wrap ABS) details have flow exponents indicating near laminar flow ($n=0.94$ and $n=0.85$).

6.2.1 Regression Models for Rim Joist Detail

Multiple linear regression airtightness models were created based on the experimental results above. The main effects of M, L, P (Table 57) together with all their respective interactions were considered. The significance of each parameter was determined using the t-test. The significance limit of $\alpha = 0.05$ was used. However, parameters with p-values above 0.10 were discarded between model iterations. For example, in Model 1, interactions $M \cdot L$, $M \cdot P$, and $M \cdot L \cdot P$ were removed based on their respective p-values were above 0.10 threshold value. The significance values for $M \cdot L$, $M \cdot P$, and $M \cdot L \cdot P$ were; 0.138, 0.232 and 0.204 respectively. The multiple linear regression was performed a second time to create Model 2. The one of the main effects, L, which represented the sample length was discarded due to a high parameter p-value. The interaction term L·P representing the effect of both length and pressure simultaneously was also discarded from Model 3 due to a higher than acceptable p-value. Finally, Model 4 was shown to be dependent solely on membrane type and pressure level (M and P). The independence of sample length was an important result. The model's length independence indicates that the sample lengths chosen were appropriate and that air leakage along the sample detail is uniform. A length dependent regression model would imply that airflow through the detail is characterised by locations of higher concentrations of airflow. Furthermore, the magnitude of the of the parameter M shows that material is almost twice as important as pressure.

A summary of the model strengths of the four multiple linear regression was shown in *Table 62 Regression Strength for Empirical Models of Floor to Wall Details*. The model strength was initially evaluated using the adjusted R^2 . Models 1,2,3 and 4 can thus explain; 93%, 91%, 90% and 88% of the air leakage through the wall details (Table 59) The apparent decrease model strength

between model iteration does take ANOVA and Residual analysis under consideration. Only a small change in standard error was detected between all four models. A second method to assess model strength was conducted via an ANOVA. The respective F-tests (Table 61) show that these models were not likely a result of chance since their respective ANOVAs had extremely significant with p-values < 0.0001. The ANOVA p-values decrease by 3 orders of magnitude between Model 1 (the first iteration) and Model 4 (the final iteration). Lastly the residual indicated that Model 4 was an improvement to Model 1 as the assumption of normality was truer for the former model.

Table 59 Regression Summary for Floor to Wall Detail Air Leakage Models

Model	R	R ²	AdjR ²	SE
1	0.981	0.963	0.931	0.079
2	0.967	0.934	0.910	0.090
3	0.958	0.918	0.897	0.096
4	0.946	0.896	0.880	0.104

Table 60 Multiple Linear Regression for Empirical Models

Model	Predictors	Parameter	SE	T	Sig.	LB 95%CI	UB 95%CI
1	(Constant)	0.782	0.020	39.603	0.000	0.737	0.828
	M	0.243	0.020	12.315	0.000	0.198	0.289
	L	0.037	0.020	1.889	0.096	-0.008	0.083
	P	0.130	0.020	6.593	0.000	0.085	0.176
	MxL	-0.033	0.020	-1.649	0.138	-0.078	0.013
	MxP	0.026	0.020	1.294	0.232	-0.020	0.071
	LxP	0.043	0.020	2.200	0.059	-0.002	0.089
	MxLxP	0.027	0.020	1.383	0.204	-0.018	0.073
Model	Predictors	Parameter	SE	T	Sig.	LB 95%CI	UB 95%CI
2	(Constant)	0.782	0.023	34.725	0.000	0.732	0.832
	M	0.243	0.023	10.798	0.000	0.194	0.293
	L	0.037	0.023	1.657	0.126	-0.012	0.087
	P	0.130	0.023	5.781	0.000	0.081	0.180
	LxP	0.043	0.023	1.929	0.080	-0.006	0.093
Model	Predictors	Parameter	SE	T	Sig.	LB 95%CI	UB 95%CI
3	(Constant)	0.782	0.024	32.446	0.000	0.730	0.835
	M	0.243	0.024	10.089	0.000	0.191	0.296
	P	0.130	0.024	5.401	0.000	0.078	0.183
	LxP	0.043	0.024	1.802	0.097	-0.009	0.096
Model	Predictors	Parameter	SE	T	Sig.	LB 95%CI	UB 95%CI
4	(Constant)	0.782	0.026	29.959	0.000	0.726	0.838
	M	0.243	0.026	9.316	0.000	0.187	0.300
	P	0.130	0.026	4.987	0.000	0.074	0.187

Table 61 Regression Strength for Empirical Models of Floor to Wall Detail via ANOVA

Model		SS	DF	MS	F	Sig.
1	Regression	1.309	7	0.187	29.976	0.00004
	Residual	0.050	8	0.006		
	Total	1.359	15			
2	Regression	1.270	4	0.317	39.119	0.000002
	Residual	0.089	11	0.008		
	Total	1.359	15			
3	Regression	1.248	3	0.416	44.739	0.000001
	Residual	0.112	12	0.009		
	Total	1.359	15			
4	Regression	1.217	2	0.609	55.831	0.0000004
	Residual	0.142	13	0.011		
	Total	1.359	15			

The analysis of residuals was also conducted to assess model strength and verify the assumptions of a normal distribution (Montgomery, Peck, & Vining, 2012). The means and standard deviations of the regression standardised residuals are summarised in Table 62. All means (μ) were all effectively zero. However, the standardised residual standard deviation progressively increased from 0.730 to 0.931. Thus Model 4 had the closest to ideal residual distribution ($\mu = 0.0$, and $SD = 0.9$). Hence Model 4 best satisfies the normality assumption required for the regression analysis.

Table 62 Regression Strength for Empirical Models of Floor to Wall Details

Model	R	R ²	Adj R ²	p-value	Regression Predictors	μ	SD
1	0.981	0.963	0.931	0.00004	M, L, P, MxL, MxP, LxP, MxLxP	0.000	0.730
2	0.967	0.934	0.910	0.000002	M, L, P, L x P	0.000	0.865
3	0.958	0.918	0.897	0.000001	M, P, L x P	0.000	0.894
4	0.946	0.896	0.880	0.0000004	M, P	0.000	0.931

The strongest model describing air leakage through a floor to wall detail for light framed homes takes the form of Equation (17). This equation was derived from Model 4 in Table 62. The constants are derived from the beta parameters and the variables are the only remaining significant predictors selected post-analysis.

$$ACH_c = 0.782 + 0.243M + 0.130P \quad (17)$$

6.2.2 Results and Integration into Whole House Prediction Models

Table 63 Output for Model #4 for Rim Joist Details

Configuration Description	Configuration Input	ACH _c = 0.782 + 0.243M + 0.130P
SAM, 50Pa	M = -1, P = -1	ACH _{50c} = 0.409
SAM, 75Pa	M = -1, P = +1	ACH _{75c} = 0.669
TSSM, 50Pa	M = +1, P = -1	ACH _{50c} = 0.895
TSSM, 75Pa	M = +1, P = +1	ACH _{75c} = 1.155

The estimated volumetric chamber air change rate was calculated and shown in Table 63. The configuration inputs are from the extreme conditions from the cube plot in Figure 6. These air leakage estimates were used to construct two proposed weighting functions Table 64. One weighting function was based on a percentage difference between the proposed floor to wall detail and advanced floor to wall detail (Equation (10)). The other weighting function was based on the ratio between the advanced floor to wall detail to the conventional detail (Equation (12)).

Table 64 Weighting Factor for Model #4's Floor to Wall Detail

Pressure Level	Weighting Factors W_i	
	Percentage	Proportional
50 Pa	0.543	0.457

The use of the weighing function can be illustrated using the builder specific results from Chapter 5. Whole building air leakage for Builder A was determined to be related to three factors, building volume, Joist Ratio, and Fenestration Perimeter to building Height Ratio as illustrated in Equation (18).

$$ACH50_{(Builder A)} = B_0 + B_1 \cdot Volume + B_2 JoistR + B_3 FenPerimHR \quad (18)$$

By substituting the parameter values to the builder specific model as shown in Equation (19).

$$ACH50_{(Builder A)} = 18.465 + 0.001 \cdot Volume - 0.178 \cdot JoistR - 0.068 \cdot FenPerimHR \quad (19)$$

The application of the weighting functions to the Joist ratio produces a set of equations giving an upper bound and lower bound estimate (Equation (20)& Equation (21)) of whole building airtightness based on the improvement of a floor to wall detail.

$$ACH50_{(Builder A)} = 18.465 + 0.001 \cdot Volume - 0.097 \cdot JoistR - 0.068 \cdot FenPerimHR \quad (20)$$

$$ACH50_{(Builder A)} = 18.465 + 0.001 \cdot Volume - 0.081 \cdot JoistR - 0.068 \cdot FenPerimHR \quad (21)$$

Builder-specific preconstruction airtightness estimates for Builder A were presented in Equation's (20) & (21). Builder A could now estimate the effect of changing the floor-to-wall's ABS, from stapled and taped house wrap, to a self adhered membrane. Designers for Builder A would also have the flexibility to make dimensional changes to the building plan, volume, height, and window, without affecting the model.

The models presented for Builder A are exemplary. The same approach could have been used for other building enclosure details. The criteria for choosing new details depended on the geometry-based, builder-specific model developed in Phase II. For example, windows were found to be important contributors to air leakage for Builder A, and Builder B based on significance of the predictor variable *FenPerimHR* from Phase II. An empirical based factorial design approach utilising laboratory assembled window-to-wall details could be used to construct new weighting factors. The new weighting factors (Phase III), in combination with the predictive equation (Phase II), would provide designers the opportunity to estimate whole building airtightness between a set of window improvement, and its' own conventionally constructed windows.

Two weighting functions have been proposed; the proportional approach (Equation (20)) and the percent difference approach (Equation (21)). These weighting approaches were by no means exhaustive. It was possible that a more complex weighting formulation could have yielded improved scaling or proportional values for W_i . For example, higher or lower powers ($W_i^{1.5}$, $W_i^{0.5}$) weighting could be used. However, the effective change to whole building airtightness based on

weighting factors adjustments would need to be calibrated against a new blower door testing population that contained homes with and without an improved enclosure detail. This would be accomplished by performing in-situ airtightness tests on floor joist that utilise two configurations. The in-situ testing population would be compared with the laboratory-based testing population. The Beta coefficients and the overall detail airtightness from the two modeling approaches would be compared.

Another strength of the overall airtightness approach is that airtightness of the detail could under test could be converted from chamber ACH50, to another airtightness metric. For instance, the leakage rate could be expressed as L/s at 50 Pascals (Q50) or normalised to convenient units such as air leakage per unit detail length L/s/m (Q50/m) or air leakage per detail area L/s/m² (Q50/m²). The metric selected would be based on the preference of the builder based on practicality or convenience.

6.3 Summary

A methodology to calibrate and test air leakage through typical details in Canadian residential construction was proposed. Full scale, code compliant, construction details representing both conventional and advanced air barrier material applications were compared and analysed. The results were applied as a weighting function to builder specific whole building airtightness models. The testing apparatus was successfully calibrated and was in close agreement with theory. A building enclosure detail shown have a large impact on whole building airtightness in Phase II was constructed for testing. A 2³ full factorial design with 2 replicates performed for a floor to exterior wall detail. The three factors were Pressure (P), Air Barrier Material (M) and sample length (L). The strong empirical model ($R^2 = 0.896$, $p < 0.001$) was found to be governed

by the main effects of M and P and independent of L and all interactions. The combination of whole building airtightness models from Phase II and the weighting function from Phase III can allow builders to estimate preconstruction airtightness for buildings with next generation building enclosure details that form part of the air barrier system.

7 Conclusions

The prime objective of this research was to develop and test an approach to estimating preconstruction airtightness in new, detached, low-rise, light framed, residential homes that could quantify airtightness evolution of next generation exterior wall details. The approach utilised a three-phase methodology that combined national, local, and laboratory-based modeling. The main objective in Phase I was to establish a lower bound of airtightness model prediction strengths based on a national blower door testing database of over 900,000 detached homes. The primary objective of Phase II was to demonstrate whether building-specific airtightness models could be used to predict preconstruction airtightness for conventionally constructed detached homes. Phase III's primary objective was to illustrate how empirical methods could be used to refine builder-specific whole building airtightness models with next-generation details. The interconnectedness of the three-phase approach is illustrated graphically in Figure 43.

7.1 Significance of Work

The Canadian federal government has targeted the reduction of Green House Gas emissions and overall energy consumption for multiple of reasons including tackling climate change and fostering energy security. Residential buildings are an important contributor to energy consumption and Green House Gas emissions. In addition, low rise detached homes disproportionately consume the most energy and emit the most carbon equivalence in both absolute and relative terms. Uncontrolled air leakage is a major contributor to long-term building energy use and GHG emissions. Although poor airtightness drives energy use, the control of

airtightness offers potential solutions. The quantification, control, and predictions of building air leakage is a fundamental design, construction and maintenance of conventional and low energy buildings. The ability to reliably predict preconstruction airtightness for both conventional and next-generation construction details can offer a path to Canada's low carbon future. The content of the research provided a methodology which combines builder-specific, temporally independent, whole building preconstruction airtightness models with laboratory generated estimates of air leakage at wall details. Furthermore, novel ratio-based predictor variables such as *FenPerimHR*, *RJoistR*, and *PerimR* were shown to be stronger indications of air leakage as compared to absolute geometric joint lengths. Finally, the approach to preconstruction airtightness estimation presented herein, yielded models that had stronger explanatory power (74% – 58%) than past postconstruction models.

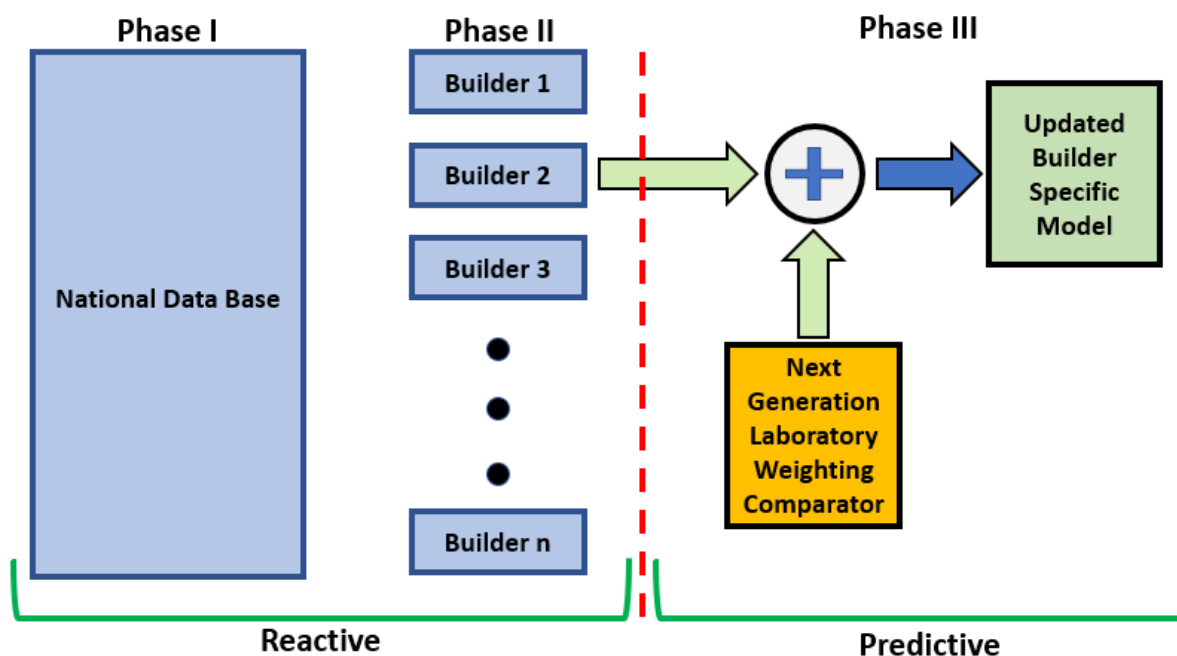


Figure 43 Summary of Approach to Preconstruction Airtightness Prediction

7.2 Resolved Research Questions

7.2.1 Chapter 5 Summary: National Level Airtightness Predictions

A national blower door testing population was analysed and predictive airtightness models were constructed based on significant variables, post-construction. The research question guiding this Phase was:

Can a linear regression model estimate building airtightness in conventionally constructed, low rise, residential buildings in a Canadian cold climate?

A detailed exploration found that multivariate linear regression models could be used to predict airtightness levels in existing, detached buildings. The models that used three predictor variables; Building Volume, Year of Construction, and Building Height, were able to predict 32% to 35% ($p < 0.001$) of whole building air leakage rates. The models that used 8 predictor variables, namely: Wall Insulation, Foundation Wall insulation, Ceiling Insulation, Window Insulation, Climate, Building Volume, Year of Construction, and Building Height predicted 46% - 48% ($p < 0.001$) of whole building air leakage rates. The year of construction was found to be the most significant predictor variable for all models and thus the preconstruction air tightness could not be reliably predicted for new buildings. Therefore, linear regression models were successfully created to estimate air leakage in existing buildings with heterogeneous wall types. These regression models were in some cases equal to or stronger in explanatory power than the existing literature.

7.2.2 Chapter 5 Summary: Predicting Airtightness in Local Populations

A blower door testing population from four builders in southern Ontario was analysed. Predictive airtightness models were constructed based on significant variables. The research question guiding the investigation for Phase I was:

- *Can a builder-specific blower door testing population be used to estimate airtightness in conventional construction based on geometric details associated with air barrier leakage, in low rise, residential, light framed homes, in a Canadian cold climate?*

Two classes of regression-based airtightness models were developed using the methodology outlined in Chapter 3. The first type of model was the builder-specific model, and the second type of model incorporated handicraft. Three builder specific models were constructed utilising 3 predictor variables, while 4-5 variable models were developed when controlling for handicraft. Most airtightness models used a unique combination of predictors. The diversity in predictor variables echoed differences in dominant leakage path between housing populations. Air leakage around fenestration was significant in some models, while other models were more influenced by ceiling or exposed floors transitions. Custom predictor variables such as Rim Joist Ratio, Ceiling to Wall Ratio, and Fenestration Perimeter to Height Ratio were found to highly predictive of air leakage in select models. Air leakage at the rim joist was found to be an important contribution for most builder-specific models. The respective predictive model strength for Builder A, B, and C were found to be 51% ($p < 0.001$), 34% ($p < 0.001$), and 58% ($p < 0.001$). Window air leakage as expressed by the nondimensional *Fenestration Perimeter to Building Height Ratio* was found to be important in most models. The strongest model in Phase II was found to predict 74% ($p < 0.001$) of whole building airtightness. In summary, all Phase II models were capable of forecasting whole building preconstruction airtightness using conventional construction, independently of building age, and local climate. These preconstruction airtightness models were stronger than postconstruction models found in the literature. Furthermore, the preconstruction models were temporally independent, and climate independent.

7.2.3 Chapter 6 Summary: Predicting Airtightness with Laboratory Tests

Phase III encompassed a laboratory-based design of experiments on air leakage through building details. A 2^3 full factorial experiment and analysis was used to evaluate various approaches, ranging from basic to exemplary, for a detail that was shown to impact air leakage in Phase II.

The research question guiding the investigation was:

- *Can an experimentally based methodology be used to modify estimates of whole building airtightness in new construction at pre-construction phases of development, for low rise, detached, residential, light-framed homes, in a Canadian cold climate?*

A novel testing methodology that incorporated building details airtightness models into whole building airtightness equations was developed. The test procedure replicated air leakage through path identified in builder-specific models developed in Phase II. A set of floor-to-wall details for light-framed homes were tested in random order. Multiple linear regression was performed on the three-factor experimental results. The main effects considered in the floor to wall detail were: chamber pressure, sample length, and exterior air barrier material. All of the factor's interactions were also considered in the modeling. The seven variable model was reduced to two variables; pressure and material. The model equation characterising air leakage at the floor to wall detail was found to be very strong ($R^2 = 0.896$, $p < 0.001$). A weighting function based on the empirically derived results was used to modify a whole building airtightness predictive model from Phase II. Therefore, Phase III showed that builder-specific, non-temporal whole building models can be empirically updated to predict preconstruction airtightness in detached, low-rise, light-framed buildings.

7.3 Strengths and Limitations

The primary objective of this research was to develop an approach to estimate preconstruction airtightness in detached, low-rise, light-framed homes in a Canadian context. A major strength of this research was to combine both reactive and predictive approaches into a single approach. The analysis of post construction airtightness performance (Phase II), together with the modifying effect of laboratory-based air leakage at the building details (Phase III), created a comprehensive methodology. The blower door testing data provided reliable real-world performance for the given testing population. Models derived from these data sets can predict between 58% to 74% of the whole building preconstruction air leakage. Laboratory based design of experiments allow for a controlled environment for the evaluation of novel construction details against conventional details. The factorial design approach allows for testing the influence of multiple effects simultaneously. Thus, the overall framework allows for an understanding of air leakage and both the global scale and micro-scale.

A second strength is that the modeling variables are primarily geometry-based approach that is useable on homogeneous wall construction, homogeneous housing types, and independent of building age. Many of the strongest models in the literature relied upon heterogeneous housing typology, heterogeneous wall typology, year of construction, and an a priori quantification of ABS performance to provide the variance needed for a strong model.

A third strength is the applicability of the research. The approach utilises data sets from a Builder's portfolio. The buildings' post construction air leakage performance is thus directly tied to the designer scope of practice. Therefore, factors unique to the designer such as building massing, material choice, supervision and handicraft form the base equation(s) for the

airtightness models. The weighting function derived from existing and next generation details is also directly relevant to the builder. Furthermore, the sole non-geometric variable *BuilderID* can be extended to other practical discrete variables such as crew management identification (*ManagementID*), or Contractor/Subcontractor identification (*ContractorID*) to compare and quantify the effects of quality control during construction based on different supervision and work crews.

The author acknowledges some limitations in this study. Larger sample sizes for Builders A, B, C and D in Phase II could have proved useful for further modeling and analysis. An increase in sample size would have allowed for the investigation of possible maximum model strength. The occurrence of maximum model strengths based on sample size would help in establishing practical guidelines for designers and builders.

A second limitation was the number of details examined in Phase III. Performing a factorial experiment on a second detail could have further advanced the research. The current results showed that window details and ceiling details were also influential sources of air leakage for select models in Phase II. The test and development of a second weighting factor to the preconstruction airtightness model would further illustrate the applicability of the approach being proposed.

A third limitation was that inside and outside corners were not taken into consideration in the builder specific airtightness models developed in Phase II of this research. This omission was due to the lack of information available for all configurations considered in the modeling exercise.

A fourth limitation was that the whole building air leakage was not explicitly considered for the mechanical systems. Due to the lack of consistent data available for a significant portion of

the housing units under study in Phase I, the heating and air-conditioning systems were not controlled for. To be sure, the heating cooling and air conditioning system penetration of the ABS does have an important effect on whole building air leakage. Thus, predictor variables corresponding to various HVAC treatments could be considered in future population-based regression models.

7.4 Recommendations and Future Work.

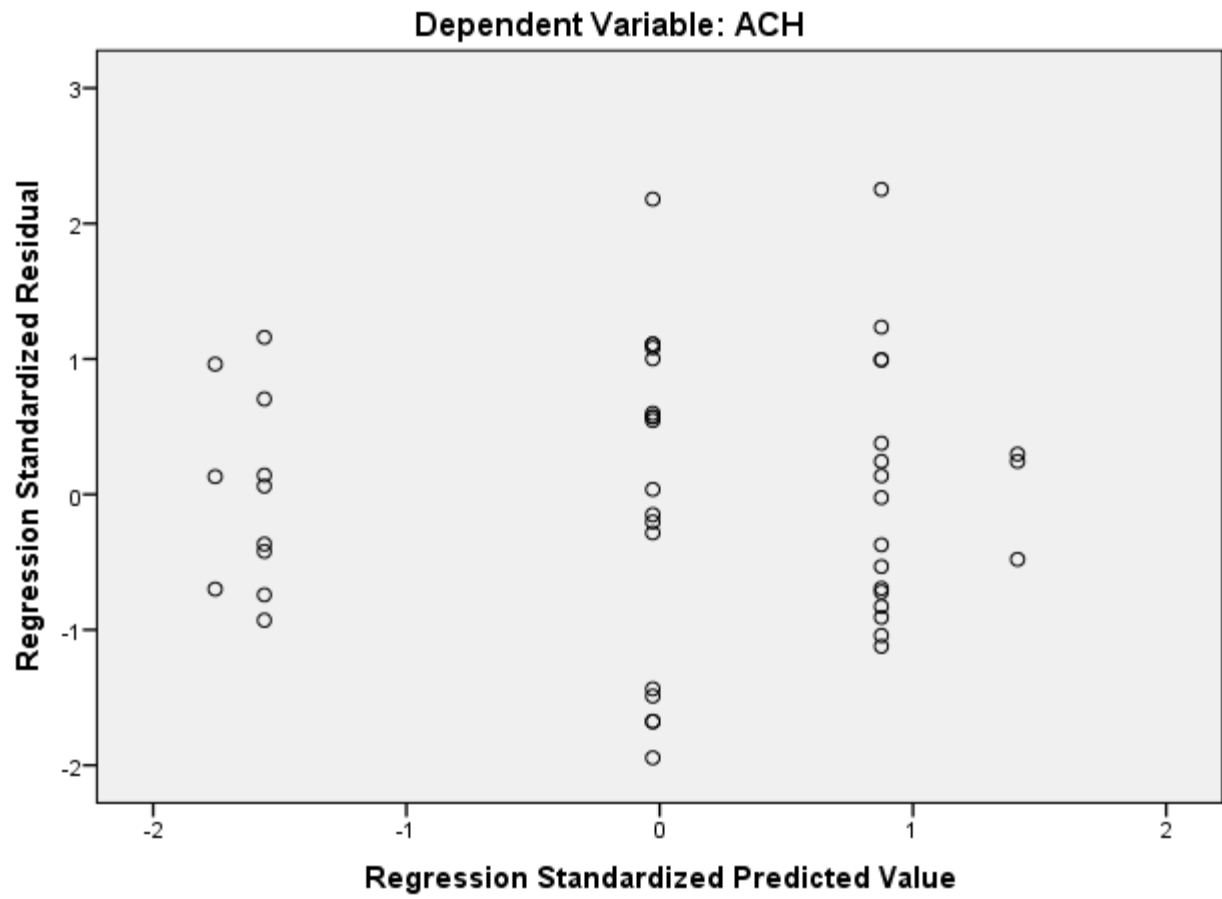
The overall focus of the research was to develop and justify an approach to forecasting preconstruction airtightness in low rise residential buildings. The approach included the examination of both reactive and predictive methods of airtightness estimation. As such, the recommendations will consist of increasing the depth of knowledge in the reactive, predictive, and synthesis the respective approaches.

The first recommendation would be to create length ratio-based predictor variables for ceiling interfaces and opaque wall interfaces such as building corners. The research showed that the significance of ceiling area, and ceiling to wall variables were important, an indication that a more robust predictor could have been used instead. Secondly, the investigation into other building enclosure details could increase the impact on the airtightness predictions models by adding another distinct weighting factor. The author is currently designing a full 2^4 factorial design with two replicants for window to wall detail to address this issue.

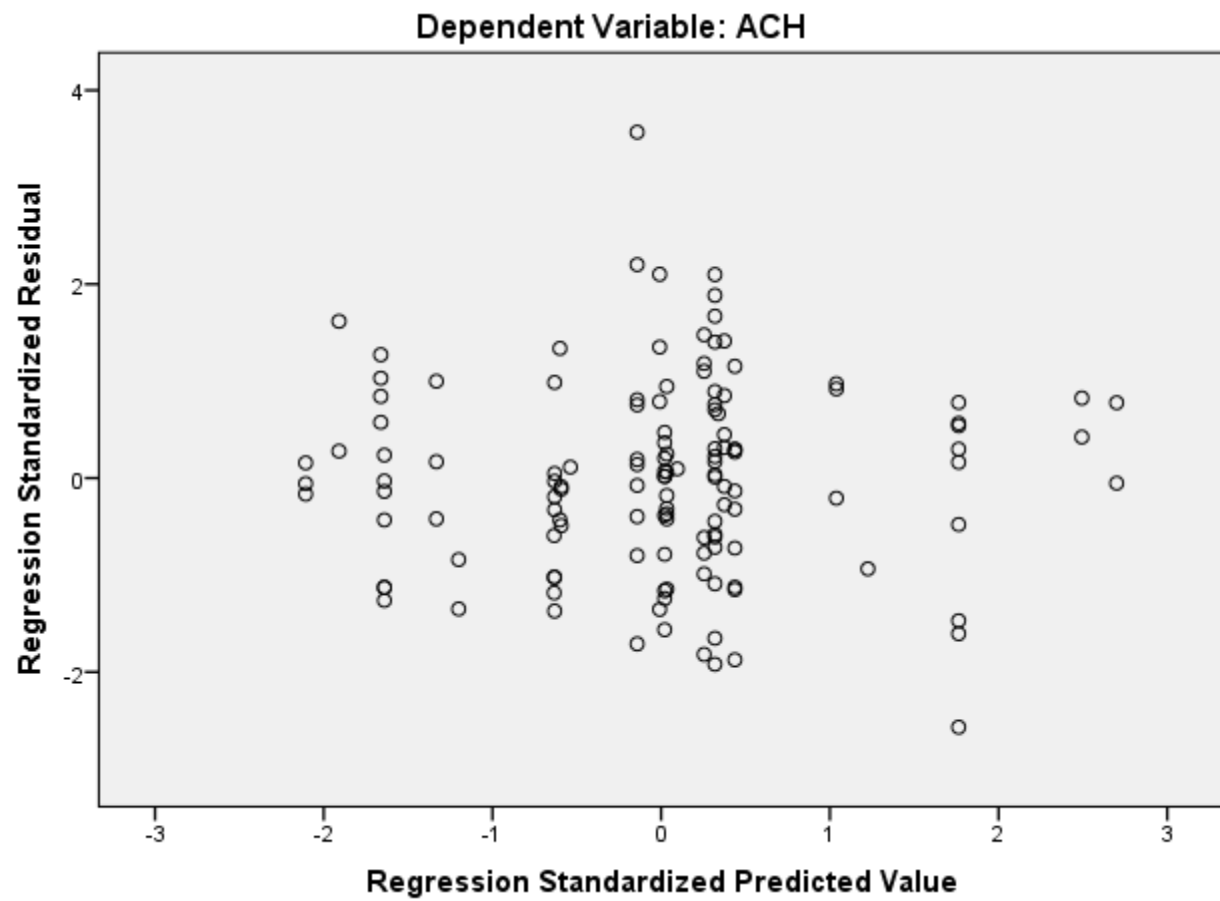
A third recommendation would be to calibrate the methodology with a high-volume builder. Finding a blower door testing population containing a minimum of two sets of construction detail updates details would provide an opportunity to analyse post-construction

homes performance. Performing a factorial design of experiments utilising the two sets of construction details would allow for a comparison of the actual air leakage performance to the reweighted formulation. The author is currently in contact with potential clients who have expressed interest in collaborating in such an endeavor. In addition, it would be highly recommended to perform model validation utilising in situ wall transitions with known detailing. The in-situ airtightness results could be remodeled in the laboratory. The effective air leakage rates between the field measurements and laboratory measurements would then be compared and contrasted. For instance, the airtightness of a standard picture window with a known framing detail could be measured on multiple existing buildings. The same window detail would be tested according to a factorial design approach, where a one laboratory test configuration would correspond to the assembly which conforms to the in-situ test condition previously examined.

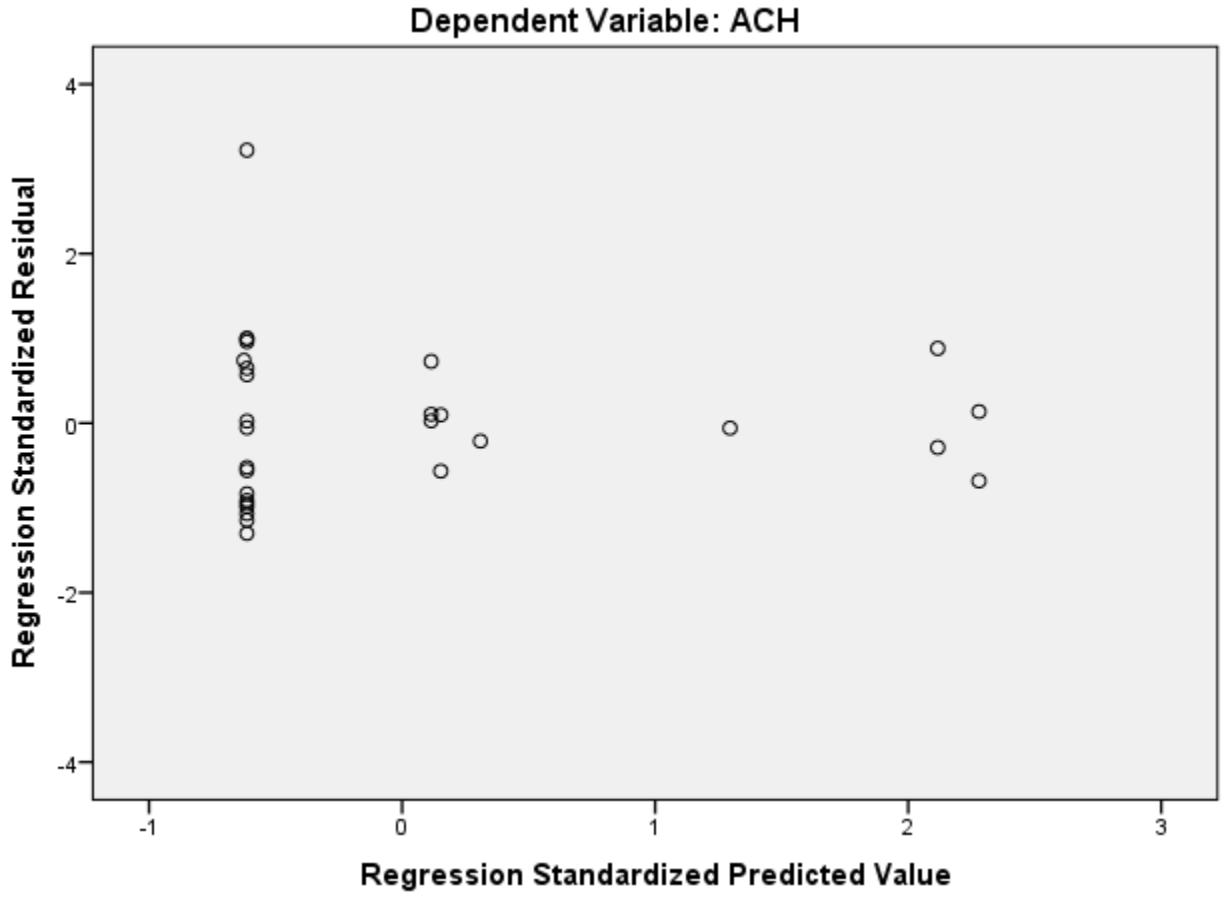
Appendix



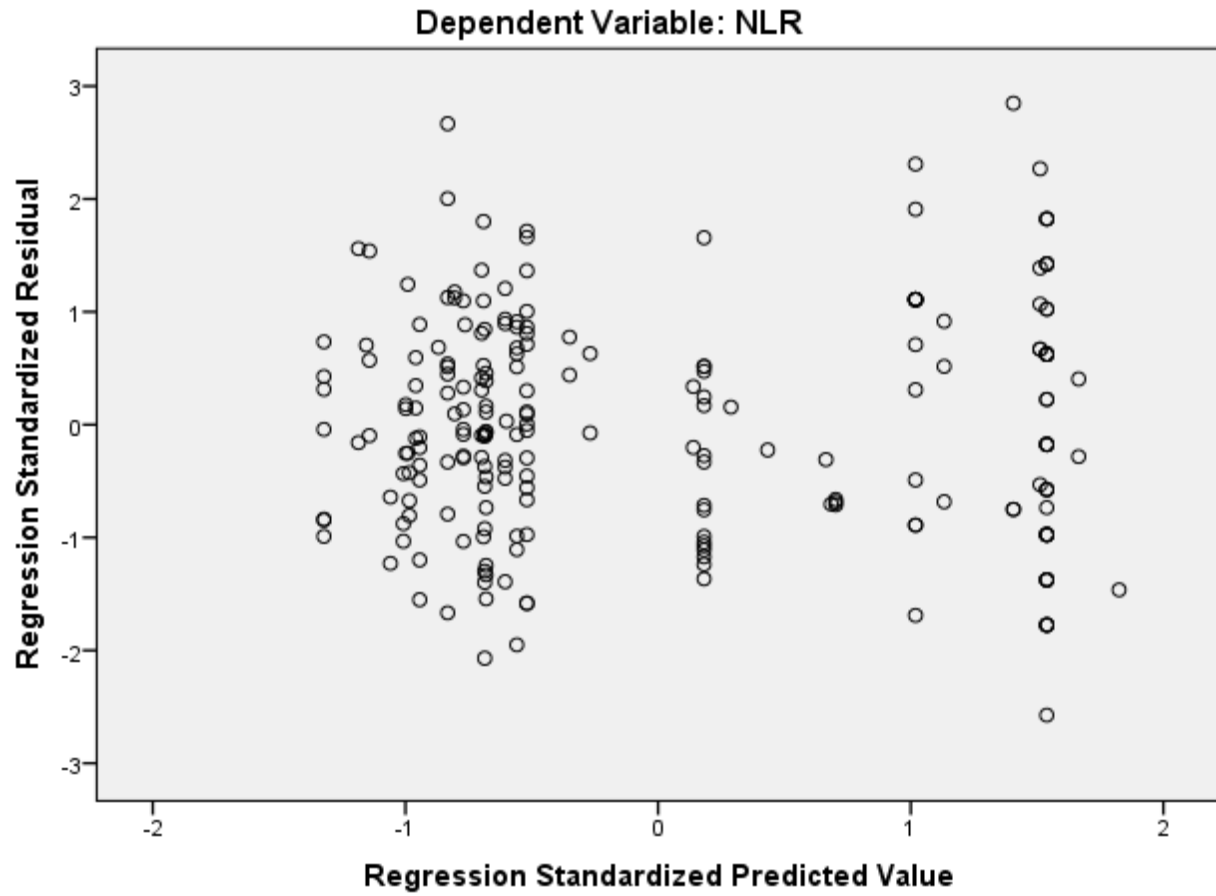
Builder A: Plot of Standardized Residuals vs Standardized Predicted ACH50 Values



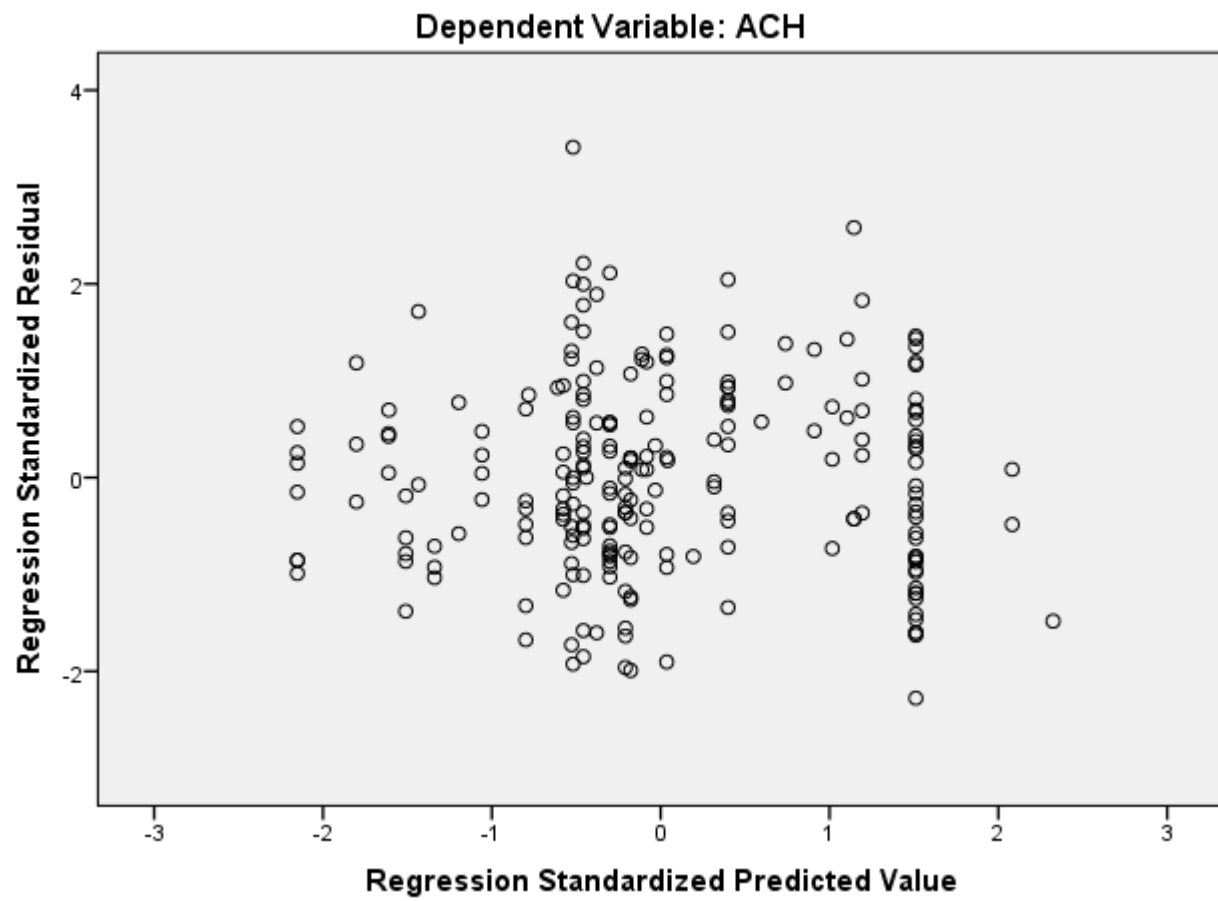
Builder B: Plot of Standardized Residuals vs Standardized Predicted ACH50 Values



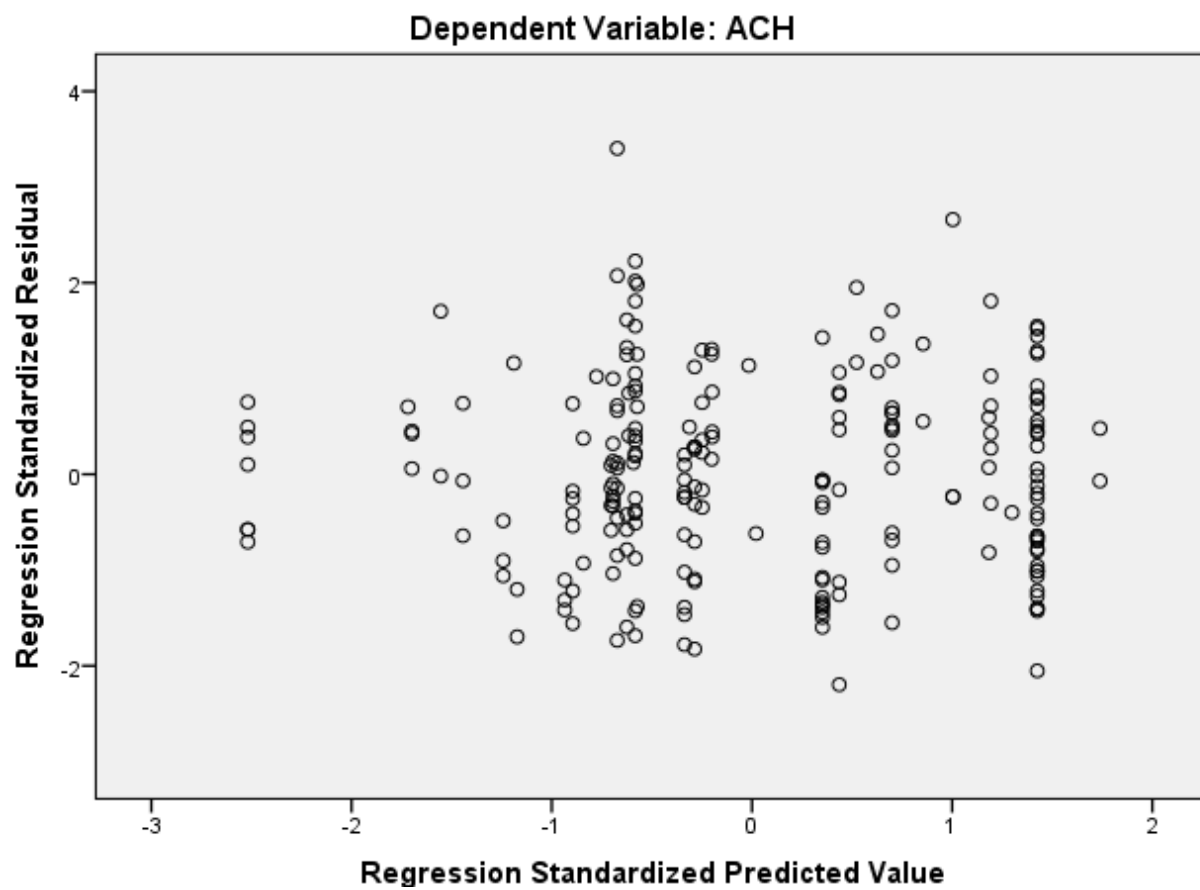
Builder C: Plot of Standardized Residuals vs Standardized Predicted ACH50 Values



NLII: Plot of Standardized Residuals vs Standardized Predicted Normalised Leakage Values



ACH50IIa: Plot of Standardized Residuals vs Standardized Predicted ACH50 Values



ACH50I1b: Plot of Standardized Residuals vs Standardized Predicted ACH50 Values

Works Cited

- Alberta Municipal Affairs. (2014). *Energy efficiency in housing and small buildings – performance path*.
- Almeida, R. M. S. F., Ramos, N. M. M., & Pereira, P. F. (2017). A contribution for the quantification of the influence of windows on the airtightness of Southern European buildings. *Energy and Buildings*, 139, 174–185.
- Antretter, F., Karagiozis, A., TenWolde, A., & Holm, A. (2007). Effects of air leakage of residential buildings in mixed and cold climates. In *Thermal Performance of the Exterior Envelopes of Buildings X Conference Proceedings, Clearwater Beach, FL*.
- ASHRAE. (2013). Fundamentals handbook. Atlanta, GA: American Society of Heating, Refrigerating and Air-Conditioning Engineers, 21.
- ASHRAE, A. H. (2009). Fundamentals (SI edition). Atlanta, GA: American Society of Heating, Refrigerating and Air-Conditioning Engineers.
- ASTM. (2017a). ASTM E741 Standard test method for determining air change in a single zone by means of a tracer gas dilution.
- ASTM. (2017b). *Standard Test Method for Determining Air Change in a Single Zone by Means of a Tracer Gas Dilution E-741*. ASTM International, West Conshohocken, PA.
- ASTM. (2017c). Standard Test Methods for Determining Airtightness of Buildings Using an Orifice Blower Door E-1827. ASTM International, West Conshohocken, PA.
- BC Housing. (2017). *BC Housing Energy Step Code Council 2017 Metrics Research*.
- Bell, M., Wingfield, J., Miles-Shenton, D., & Seavers, J. (2010). Low carbon housing: lessons from Elm Tree Mews.
- Beyea, J., Dutt, G., & Woteki, T. (1977). Critical Significance of Attics and Basements in the Energy Balance of Twin Rivers Townhouses. *Energy and Buildings*, 178, 261–269.
- Box, G. E. P., Hunter, J. S., & Hunter, W. G. (2005). Statistics for experimenters. In *Wiley Series in*

Probability and Statistics. Wiley Hoboken, NJ.

Bramiana, C. N., Entrop, A. G., & Halman, J. I. M. (2016). Relationships between building characteristics and airtightness of Dutch dwellings. *Energy Procedia*, 96, 580–591.

Canada Mortgage Housing Corporation. (2007). *Air Leakage Control Manual for Existing Multi-Unit Residential Buildings*. CMHC, Ottawa, ON.

Chan, W. R., Joh, J., & Sherman, M. H. (2013). Analysis of air leakage measurements of US houses. *Energy and Buildings*, 66, 616–625.

Chan, W. R., Nazaroff, W. W., Price, P. N., Sohn, M. D., & Gadgil, A. J. (2005). Analyzing a database of residential air leakage in the United States. *Atmospheric Environment*, 39(19), 3445–3455.

City of Vancouver. (2015). *Passive House Guidelines for RS-1*.

Cohen, J. (1990). Things I have learned (so far). *American Psychologist*, 45(12), 1304.

Cuce, E. (2017). Role of airtightness in energy loss from windows: Experimental results from in-situ tests. *Energy and Buildings*, 139, 449–455.

d'Ambrosio Alfano, F., Dell'Isola, M., Ficco, G., Palella, B., & Riccio, G. (2016). Experimental air-tightness analysis in mediterranean buildings after windows retrofit. *Sustainability*, 8(10), 991.

Dickerhoff, D. J., Grimsrud, D. T., & Lipschutz, R. D. (1982). *Component leakage testing in residential buildings*.

Djunaedy, E., den Wymelenberg, K., Acker, B., & Thimmana, H. (2011). Oversizing of HVAC system: signatures and penalties. *Energy and Buildings*, 43(2–3), 468–475.

Domhagen, F., & Wahlgren, P. (2017). Consequences of Varying Airtightness in Wooden Buildings. *Energy Procedia*, 132, 873–878.

Environment Accounts and Statistics Division. (2015). *Table 2 Type of main heating fuel used, by province, 2011*. Statistics Canada, Ottawa, ON.

Felts, D., & Bailey, P. (2000). The state of affairs—packaged cooling equipment in California. In

Proceedings of the 2000 ACEEE summer study on energy efficiency in buildings (Vol. 3, pp. 137–147).

Government of Ontario. (2016). *POTENTIAL CHANGES TO ONTARIO'S BUILDING CODE*.

Government of Ontario. (2018). *Supplementary Standard SB-12 Energy Efficiency For Housing*.

Hamlin, T., & Gusdorf, J. (1997). *Airtightness and energy efficiency of new conventional and R-2000 housing in Canada, 1997*.

Harrje, D. T., & Born, G. J. (1982). Cataloguing air leakage components in houses. In *Proceedings of the ACEEE*.

Hutcheon, N. B., & Handegord, G. O. (1983). *Building science for a cold climate*.

Iordache, V., & Catalina, T. (2012). Acoustic approach for building air permeability estimation. *Building and Environment*, 57, 18–27.

James, P. W., Cummings, J., Sonne, J. K., Vieira, R. K., & Klongerbo, J. F. (1997). The effect of residential equipment capacity on energy use, demand, and run-time. *Transactions-American Society Of Heating Refrigerating And Air Conditioning Engineers*, 103, 297–303.

Jokisalo, J., Kurnitski, J., Korpi, M., Kalamees, T., & Vinha, J. (2009). Building leakage, infiltration, and energy performance analyses for Finnish detached houses. *Building and Environment*, 44(2), 377–387.

Kayello, A., Ge, H., Athienitis, A., & Rao, J. (2017). Experimental study of thermal and airtightness performance of structural insulated panel joints in cold climates. *Building and Environment*, 115, 345–357.

Khemet, B., & Richman, R. (2018). A univariate and multiple linear regression analysis on a national fan (de) Pressurization testing database to predict airtightness in houses. *Building and Environment*.

Langmans, J., Klein, R., De Paepe, M., & Roels, S. (2010). Potential of wind barriers to assure airtightness of wood-frame low energy constructions. *Energy and Buildings*, 42(12), 2376–2385.

- Lazure, L. P., & Lavoie, J. (n.d.). Identifying water and moisture infiltration paths in building envelopes.
- Lischkoff, J. K., & Lstiburek, J. W. (1980). *The Airtight House: Using the Airtight Drywall Approach*. Iowa State University Research Foundation.
- Lstiburek, J. W. (2005). Understanding air barriers. *ASHRAE Journal*, 47(7), 24.
- Meiss, A., & Feijó-Muñoz, J. (2015). The energy impact of infiltration: a study on buildings located in north central Spain. *Energy Efficiency*, 8(1), 51–64.
- Montgomery, D. C. (2017). *Design and analysis of experiments*. John Wiley & sons.
- Montgomery, D. C., Peck, E. A., & Vining, G. G. (2012). *Introduction to linear regression analysis* (Vol. 821). John Wiley & Sons.
- Montoya, M. I., Pastor, E., Carrie, F. R., Guyot, G., & Planas, E. (2010). Air leakage in Catalan dwellings: Developing an airtightness model and leakage airflow predictions. *Building and Environment*, 45(6), 1458–1469.
- Muise, B., Seo, D.-C., Blair, E. E., & Applegate, T. (2010). Mold spore penetration through wall service outlets: a pilot study. *Environmental Monitoring and Assessment*, 163(1–4), 95–104.
- Natural Resources Canada. (2012). *R-2000 Standard*. Ottawa: Natural Resources Canada.
- Ng, L. C., Persily, A. K., & Emmerich, S. J. (2015). IAQ and energy impacts of ventilation strategies and building envelope airtightness in a big box retail building. *Building and Environment*, 92, 627–634.
- Office of Energy Efficiency. (n.d.). *L.Lewis, J.Purdy Interviewed by B. Khemet [Electronic Communications] on Jan. 2017, Apr. 2017 \& Nov. 2017*. National Research Council Canada, Ottawa, ON.
- Office of Energy Efficiency. (2018a). *Residential Secondary Energy Use (Final Demand) by Energy Source and End Use*. National Resources Canada, Ottawa, ON.
- Office of Energy Efficiency. (2018b). *Table 11: Residential Housing Stock and Floor Space*. National Resources Canada, Ottawa, ON.
- Office of Energy Efficiency. (2018c). *Table 2: Residential Single Detached Secondary Energy Use by*

- Energy Source and End-Use*. National Resources Canada, Ottawa, ON.
- Office of Energy Efficiency. (2018d). *Table 3: Residential Single Attached Secondary Energy Use by Energy Source and End-Use*. National Resources Canada, Ottawa, ON.
- Office of Energy Efficiency. (2018e). *Table 4: Residential Apartments Secondary Energy Use by Energy Source and End-Use*. National Resources Canada, Ottawa, ON.
- Office of Energy Efficiency. (2018f). *Table 7: Residential Single Detached GHG Emissions by Energy Source and End-Use – Including and Excluding Electricity-Related Emissions*. National Resources Canada, Ottawa, ON.
- Office of Energy Efficiency. (2018g). *Table 8: Residential Single Attached GHG Emissions by Energy Source and End-Use – Including and Excluding Electricity-Related Emissions*. National Resources Canada, Ottawa, ON.
- Office of Energy Efficiency. (2018h). *Table 9: Residential Apartments GHG Emissions by Energy Source and End-Use – Including and Excluding Electricity-Related Emissions*. National Resources Canada, Ottawa, ON.
- Okuyama, H., & Onishi, Y. (2012). Reconsideration of parameter estimation and reliability evaluation methods for building airtightness measurement using fan pressurization. *Building and Environment*, 47, 373–384.
- Pan, W. (2010). Relationships between air-tightness and its influencing factors of post-2006 new-build dwellings in the UK. *Building and Environment*, 45(11), 2387–2399.
- Pollutant Inventories and Reporting Division. (2018). *National Inventory Report 1990–2016: Greenhouse Gas Sources and Sinks in Canada*. Environment and Climate Change, Gatineau QC.
- Prignon, M., & Van Moeseke, G. (2017). Factors influencing airtightness and airtightness predictive models: A literature review. *Energy and Buildings*, 146, 87–97.
- Pritchard, P. J., Mitchell, J. W., & Leylegian, J. C. (2016). *Fox and McDonald's Introduction to Fluid*

Mechanics, Binder Ready Version. John Wiley and Sons.

Proskiw, G., & Eng, P. (1997). Variations in Airtightness of Houses Constructed with Polyethylene and ADA Air Barrier Systems Over a Three-Year Period. *Journal of Thermal Insulation and Building Envelopes*, 20(4), 278–296.

Quirouette, R. L. (1985). The difference between a vapour barrier and an air barrier.

Relander, T.-O., Bauwens, G., Roels, S., Thue, J. V., & Uvsløkk, S. (2011). The influence of structural floors on the airtightness of wood-frame houses. *Energy and Buildings*, 43(2–3), 639–652.

Relander, T.-O., Heiskel, B., & Tyssedal, J. S. (2011). The influence of the joint between the basement wall and the wood-frame wall on the airtightness of wood-frame houses. *Energy and Buildings*, 43(6), 1304–1314.

Relander, T.-O., Kvande, T., & Thue, J. V. (2010). The influence of lightweight aggregate concrete element chimneys on the airtightness of wood-frame houses. *Energy and Buildings*, 42(5), 684–694.

Ren, Z., & Chen, D. (2015). Simulation of air infiltration of Australian housing and its impact on energy consumption. *Energy Procedia*, 78, 2717–2723.

Rousseau, M. Z. (2004). Air barrier materials and systems: What is the difference? Is there a difference. *Ottawa, National Research Council Canada, Institute for Research in Construction*.

Ruya, E., & Augenbroe, G. (2016). The Impacts of HVAC Downsizing on Thermal Comfort Hours and Energy Consumption. *Proceedings of SimBuild*, 6(1).

Saber, H. H., Maref, W., Elmahdy, H., Swinton, M. C., & Glazer, R. (2012). 3D heat and air transport model for predicting the thermal resistances of insulated wall assemblies. *Journal of Building Performance Simulation*, 5(2), 75–91.

Sfakianaki, A., Pavlou, K., Santamouris, M., Livada, I., Assimakopoulos, M.-N., Mantas, P., & Christakopoulos, A. (2008). Air tightness measurements of residential houses in Athens, Greece.

- Building and Environment*, 43(4), 398–405.
- Sherman, M. (1995). The Use of Blower-Door Data 1. *Indoor Air*, 5(3), 215–224.
- Straube, J. (2009). BSD-014 Air Flow Control in Buildings. Retrieved from buildingscience. com.
- Straube, J. F. (2002). Air barriers role in preserving IAQ. *IAQ Applications*, 6–8.
- Sullivan, G. M., & Feinn, R. (2012). Using effect size—or why the P value is not enough. *Journal of Graduate Medical Education*, 4(3), 279–282.
- Van Den Bossche, N., Huyghe, W., Moens, J., Janssens, A., & Depaepe, M. (2012). Airtightness of the window--wall interface in cavity brick walls. *Energy and Buildings*, 45, 32–42.
- Van Wylen, G. J., & Sonntag, R. E. (1985). *Fundamentals of classical thermodynamics*.
- Vancouver, C. of. (2018). *Passive House Relaxations, Guidelines for Larger Projects*.
- Wang, W., Beausoleil-Morrison, I., & Reardon, J. (2009). Evaluation of the Alberta air infiltration model using measurements and inter-model comparisons. *Building and Environment*, 44(2), 309–318.
- Weidt, J. L. (1979). Field air leakage of newly installed residential windows.
- Wolf, D., & Tyler, F. (2013a). Characterization of Air Leakage in Residential Structures—Part 1: Joint Leakage. In *Thermal Performance of the Exterior Envelopes of Whole Buildings XII International Conference- Proceedings of ASHRAE, Clearwater, FL* (Vol. 1).
- Wolf, D., & Tyler, F. (2013b). Characterization of Air Leakage in Residential Structures—Part 2: Whole House Leakage. In *Thermal Performance of the Exterior Envelopes of Whole Buildings XII International Conference- Proceedings of ASHRAE, Clearwater, FL* (Vol. 1).
- Younes, C., & Shdid, C. A. (2013). A methodology for 3-D multiphysics CFD simulation of air leakage in building envelopes. *Energy and Buildings*, 65, 146–158.

